

Half a century of *UBV* photometry at Hvar

I. Overview and emission-line stars and binaries [★]

H. Božić¹, P. Harmanec², J. Horn^{***3}, K. Juza^{***3}, P. Koubský³, S. Kříž^{****3}, P. Mayer^{†2}, P. Hadrava⁴, D. Ruždjak¹,
D. Sudar¹, S. Štefl^{‡3}, M. Wolf², P. Zasche², M. Brož², J. Havelka^{§3}, J. Honsa³, V. Kocourek³, M. Tlamicha³,
F. Žďárský³, A. Harmanec⁵, J. Jonák², A. Oplištilová², I. Piantschitsch^{6,7,8}, I. Skokić¹, J. Švrčková², K. Vitovský²,
D. Vršnak⁹, and M. Zimmer⁵

¹ Hvar Observatory, Faculty of Geodesy, Zagreb University, Kačićeva 26, HR-10000 Zagreb, Croatia

² Astronomical Institute, Faculty of Mathematics and Physics, Charles University, V Holešovičkách 2,
CZ-180 00 Praha 8, Czech Republic

³ Astronomical Institute of the Czech Academy of Sciences, Fričova 298, CZ-251 65 Ondřejov, Czech Republic

⁴ Astronomical Institute of the Czech Academy of Sciences, Boční II 1401/1, CZ-141 00 Praha 4, Czech Republic

⁵ Faculty of Mathematics and Physics, Charles University, Prague, Czech Republic

⁶ Institute of Physics, University of Graz, Universitätsplatz 5, A-8010 Graz, Austria

⁷ Departament de Física, Universitat de les Illes Balears (UIB), E-07122, Spain

⁸ Institute of Applied Computing & Community Code (IAC3), UIB, Spain

⁹ Faculty of Electrical Engineering and Computing, University of Zagreb, Unska 3, HR-10000 Zagreb, Croatia

Received August 29, 2025

ABSTRACT

We present a summary report on 52 years of systematic photoelectric *UBV* observations of early-type emission-line stars **and binaries of all luminosity classes** secured by a number of mainly Croatian and Czech observers at the Hvar Observatory. All these observations were **carefully re-reduced** to the standard *UBV* system defined by the Johnson standard stars through the nonlinear transformation formulae. **These observations represent a very unique set of homogeneous observations, covering also the near ultraviolet parts of the electromagnetic spectrum, where the hot stars emit the maximum of their flux. This is extremely important addition to the modelling of emission-line envelopes since the existing models are usually only based on *V* magnitude observations and/or very broad-band space photometries. Our observations indicate that all emission-line stars of all luminosity classes are light and colour variables, but there is great individuality in the behaviour of each star and often different variability patterns are found in the individual passbands. We tried to classify various types of variability only on the basis of Hvar photometry, complemented by the Hipparcos *H_p* photometry transformed to Johnson *V* passband, since these observations conveniently fill the gap in Hvar observations. We also provide simple statistics of the recognized types of variations and a list of known binaries and multiple systems. Observations of various other types of variables, including accidental discoveries, will be reported in a follow-up paper II.**

Key words. stars: early-type – stars: emission-line (Be) – binaries: eclipsing – binaries: ellipsoidal

1. Introduction

The astronomical observatory at Hvar, Croatia was founded in 1972 as a joint enterprise of several astronomical institutions from former Yugoslavia and Czechoslovakia. **The instrument used for stellar photometry** is a 0.65 m Cassegrain reflector with a single-channel photoelectric photometer operating with the *UBV* filters. The early history was summarised by Mayer (2013) and Harmanec & Božić (2013) and the instrumentation and the original reduction techniques were described in Mayer (1977) and Harmanec et al. (1977a). The first observations were

secured on July 29, 1972 and continued more or less systematically since then, with the only longer gap (caused by the war in the disintegrating Yugoslavia) from February 1991 until September 1993. In 2013, a Cousins *R* filter was installed to the photometer and since then we have been obtaining four-colour observations. For consistency, we report here the results of *UBV* observations only but the archives of four-colour observations will also be made publicly available after the publication of this study – see Sect. 6. **Readers interested in more details on the stellar photometric programs are referred to Appendix A.**¹

2. Investigation of early-type emission-line objects

When our observing program started, little was known about light variability of early-type emission-line stars and the possible causes of the Be phenomenon. We therefore de-

¹ This, and all other appendices are only available on ZENODO – see <https://...>

[★] Based on photometric observations from the Hvar Observatory and ESA Hipparcos Satellite.

^{**} Jiří Horn passed away on Dec. 13, 1994

^{***} Karel Juza passed away on March 13, 1994

^{****} Svatopluk Kříž passed away on Feb. 23, 2018

[†] Pavel Mayer passed away on Nov. 7, 2018

[‡] Stanislav Štefl passed away on June 11, 2014

[§] Josef Havelka passed away on June 19, 2009

cided to monitor many bright stars, including already known binaries, which have exhibited Balmer emission lines during their recorded history, not restricting our program to only those objects, which are now by some investigators called “classical Be stars”, i.e. stars of apparent luminosity classes III to V. We were, and still are of the opinion that hot emission-line objects should be viewed in their complexity. This is supported, for instance, by the recent finding by Oplštilová et al. (2025) that the B0Ia object ϵ Ori is not probably a genuine supergiant but a rapidly rotating and highly flattened object with circumstellar matter. Our main motivation at that time was an attempt to test the binary hypothesis of the origin of the Be phenomenon (Kříž & Harmanec 1975; Harmanec & Kříž 1976). The idea was that if Be stars are indeed mass accreting components of binary system in the stage of large-scale mass transfer, with Roche-lobe filling secondaries, one should find a non-negligible number of eclipsing and ellipsoidal binaries among them. Although we later indeed found several such systems, for instance CX Dra (Koubský et al. 1980; Horn et al. 1992; Koubský et al. 1998), KX And (Harmanec et al. 1977b; Štefl et al. 1990), V360 Lac (Hill et al. 1997; Linnell et al. 2006), BR CMi (Harmanec et al. 2015), or HD 81357 (Koubský et al. 2019), for the majority of the observed Be stars we discovered long-term light and colour changes related to the changes in their circumstellar envelopes (seen in parallel spectroscopy), on a time scale of years; see, for instance, Harmanec et al. (1976); Doazan et al. (1982b,a); Horn et al. (1982) and the three summary reports (Harmanec et al. 1980b; Pavlovski et al. 1997; Harmanec et al. 1997).

The first three selected Be stars, V744 Her = 88 Her, V439 Her = 4 Her, and EW Lac = HD 217050 were observed already in 1972. Our discovery that essentially all Be stars are light and colour variables was quite important. At that time, Be stars were sometimes used as the comparison stars in various observing programs of differential photometry. Perhaps the most interesting is the case of V1294 Aql = HD 184279, which was recommended as the secondary standard of the *UBV* system – see Horn et al. (1982). That prompted us to prepare a list of all at that time known bright Be stars of all luminosity classes having the Bright-Star catalog (HR) numbers and select suitable comparison and check stars for them. We again refer readers for more details to Appendix A.

When it turned out that only a smaller part of hot emission-line objects are in the stage of mass transfer, new suggestions appeared. They sought the agent creating the envelopes in the equatorial outflow of matter, first advocated by Struve (1931) and argued that the outflow is facilitated by stellar non-radial pulsations (NRP) (e.g. Baade 1982; Bolton 1982; Percy 1983).

Pols et al. (1991) argued that the majority of Be stars are products of the previous mass transfer, during which they gained their high rotation (as suggested already by Kříž & Harmanec 1975) but that their current companions are compact hot stars and also advocated the idea that the Be phenomenon is often related to outflow, not accretion. The idea that the majority of Be stars are products of mass-exchange in binaries has then been further developed by, e.g., Boubert & Evans (2018); Nazé et al. (2022); Dufton et al. (2022) or Rubio et al. (2023).

Interpretation of long-term *V/R* changes of the Balmer emission lines in terms of one-armed density waves was suggested by Kato (1983) and developed by Okazaki (1991) and Okazaki (1997). Modelling of emission-line profiles

progressed with the model of viscous decretion disk by Carciofi et al. (2012) and the Bedisk and Bera models by Sigut & Jones (2007); McGill et al. (2011) and Silaj et al. (2014).

Later, the idea that a constructive interference of several pulsational modes can trigger a temporal outflow of material into the disk has been developed (e.g. Rivinius et al. 1998; Carciofi 2011; Baade et al. 2017) or Labadie-Bartz et al. (2025). See also the review by Rivinius et al. (2013) for one widely accepted current interpretation of the Be phenomenon.

At first glance, it might appear that the ground-based *UBV* photometry is no longer interesting at the era of accurate space photometries from instruments like MOST (Walker et al. 2003), CoRoT (Bordé et al. 2003), Kepler (Jenkins et al. 2010), BRITE Constellation (Weiss et al. 2014) or TESS (Ricker et al. 2015). However, the value of the data we are presenting in this study lies in the fact that they represent probably the longest series of homogeneous and well calibrated observations, and especially for the hot stars they provide also the monitoring in the ultraviolet part of the stellar flux, where the radiation of hot stars dominates. It can also be conveniently combined with the spectroscopic monitoring of emission-line stars provided in the Be Star spectra (BeSS) database (Neiner et al. 2011).

3. The observational strategy and the new reduction of all observations since 1972

3.1. Principles of our observational strategy

Since our motivation, especially for the dominant Be-star program, was to ensure a stable and accurate transformation to the standard Johnson system (Johnson & Morgan 1953; Johnson & Harris 1954), we soon realised that a non-linear transformation formulae are required for the conversion of extinction-free instrumental magnitudes to the standard Johnson magnitudes. It is also necessary to derive the coefficients of these transformations from all observations of standard stars in each observing season (Harmanec et al. 1994). The strategy of Hvar observations, developed first for the Be star program but later used for all observing programs, was that we prepared a list of all known bright Be stars north of declination of -30° , which were listed in the Bright Star Catalogue (Hoffleit & Jaschek 1982), and a few fainter ones. For all of them, we selected suitable comparison and check stars. If more Be stars were found close to each other in the sky, we observed them all together, using the same comparison and check stars. Since most of our observations dealt with early-type blue stars, we also selected the so-called red standards for each group, to facilitate good seasonal transformation.

Whenever possible, we have chosen the comparison stars, for which the *UBV* photometry obtained by Johnson and his collaborators was available. Our primary source was the summary publication by Johnson et al. (1966). It was, of course, a “must” for the red standards. This allowed us to save observing time. Comparisons, checks, and red standard stars with known *UBV* magnitudes could be used for both, the monitoring the extinction during observing nights and for seasonal transformation to the standard *UBV* system. However, it turned out that the stars, which have only a few original Johnson observations, suffered from rather large accidental errors. Our task then was to improve the original Johnson values but to preserve the original Johnson

system over the whole range of the Hertzsprung – Russell (HR) diagram.

We used the program suite HEC22/SORTARCH/VYPAR for data reduction from the whole observing seasons, sorting and creating data archives, and for data extraction.² The reduction program HEC22 proceeds as follows. For each star and the time of observation, the zenith distance z is calculated from its equatorial coordinates recalculated for the time of observation and the program derives the accurate air mass after Bemporad (1904):

$$X = \sec z - 0.0018167Q - 0.02875Q^2 - 0.0008083Q^3, \quad (1)$$

where

$$Q \equiv \sec z - 1. \quad (2)$$

Transformation coefficients G_i ($i = 1, 28$) between observed instrumental magnitudes, denoted v , b , u , and r , and extinction-free magnitudes v_0 , b_0 , u_0 , and r_0 , determined (or fixed) separately for each night, include the first-order extinction coefficients and a possibility to model time variations of the linear extinction coefficients during each night through polynomials up to the 5th degree as a function of time t . The corresponding equations read as follows:

$$v = v_0 + G_1 + (G_5 + G_9 t + G_{13} t^2 + G_{17} t^3 + G_{21} t^4 + G_{25} t^5) X, \quad (3)$$

$$b = b_0 + G_2 + (G_6 + G_{10} t + G_{14} t^2 + G_{18} t^3 + G_{22} t^4 + G_{26} t^5) X, \quad (4)$$

$$u = u_0 + G_3 + (G_7 + G_{11} t + G_{15} t^2 + G_{19} t^3 + G_{23} t^4 + G_{27} t^5) X, \quad (5)$$

$$r = r_0 + G_4 + (G_8 + G_{12} t + G_{16} t^2 + G_{20} t^3 + G_{24} t^4 + G_{28} t^5) X. \quad (6)$$

An example of how such fit can improve the model of all-sky magnitudes during long nights is shown in Appendix B.

There is also a possibility to take into account a linear or a quadratic drift of the zero point of the instrument. In that case, the drift is derived via the yellow-magnitude observations and forced upon the data in all other passbands. The corresponding equations then read as

$$v = v_0 + G_1 + G_5 X + G'_9 t + G'_{13} t^2, \quad (7)$$

$$b = b_0 + G_2 + G_6 X + G'_9 t + G'_{13} t^2, \quad (8)$$

$$u = u_0 + G_3 + G_7 X + G'_9 t + G'_{13} t^2, \quad (9)$$

$$r = r_0 + G_4 + G_8 X + G'_9 t + G'_{13} t^2. \quad (10)$$

We applied this drift only in a few cases for the earlier analog high-voltage amplifiers. Naturally, the coefficients G'_9 and G'_{13} are not the same as the similarly denoted coefficients G_9 and G_{13} in Eq. (3). We never tried to combine the time change of the extinction during the night with the zero-point drifts, since there would be a strong correlation between the two and the fit would be unstable.

The colour transformation equations between the Johnson standard value for each magnitude (V, B, U, R) and the

extinction-free instrumental magnitudes are linear in the $U - B$ index, but have the form of a third-degree polynomial in $B - V$. This form is necessary to compensate for the unavoidably non-linear effect of the Balmer jump on the magnitudes of stars from mid-B to F spectral types (see Cousins & Jones 1976). The colour extinction coefficients in the form recommended by Young et al. (1991) are also included among the seasonal transformation coefficients. It is our experience that this form of transformation equations ensures the reproduction of the standard Johnson system within 0^m.01, even in U , for any standard star.

The respective equations are as follows:

$$\begin{aligned} v_0 - V &= H_1(B - V) + H_2(U - B) \\ &+ H_3(B - V)^2 + H_4(B - V)^3 \\ &+ H_5 X B_4(B - V + 0.5 X B_4) + H_6, \end{aligned} \quad (11)$$

$$\begin{aligned} b_0 - B &= H_7(B - V) + H_8(U - B) \\ &+ H_9(B - V)^2 + H_{10}(B - V)^3 \\ &+ H_{11} X B_4(B - V + 0.5 X B_4) + H_{12}, \end{aligned} \quad (12)$$

$$\begin{aligned} u_0 - U &= H_{13}(B - V) + H_{14}(U - B) \\ &+ H_{15}(B - V)^2 + H_{16}(B - V)^3 \\ &+ H_{17} X B_5(U - B + 0.5 X B_5) + H_{18}, \end{aligned} \quad (13)$$

$$\begin{aligned} r_0 - R &= H_{19}(B - V) + H_{20}(U - B) \\ &+ H_{21}(B - V)^2 + H_{22}(B - V)^3 \\ &+ H_{23} X B_5(U - B + 0.5 X B_5) + H_{24}, \end{aligned} \quad (14)$$

where $B_4 \equiv G_6 - G_5$ and $B_5 \equiv G_7 - G_6$ are the linear extinction coefficients in the $B - V$ and $U - B$ colours.

We note that in our formalism, quantities with suffix 0 are not, in fact, really extinction-free instrumental magnitudes, but extinction-free magnitudes uncorrected for the colour extinction, which is only taken into account in the seasonal transformation equations, where they actually belong, since they depend on the colour properties of the photometer, not on the properties of the Earth atmosphere. **The program derives the transformation coefficients iteratively, using all nights of a given season denoted as suitable for that purpose and starting either with the values derived during the previous seasons or with an instrumental system, i.e. choosing all H coefficients equal to zero.**

We **note** that it is necessary to obtain observations of a reasonably large number of standard stars of different colours, luminosity classes, and reddenings to derive reliable non-linear transformation coefficients H_i . Since this is not always possible, e.g., due to bad weather, the latest versions of the program HEC22 also allow the use of bilinear transformation formulae, which contain no terms of the second and third power in $(B - V)$ and converge to reasonable transformation coefficients in these bad-weather conditions. This compromise is, however, at the expense of a slightly worse transformation into the standard system, yet still much better than what would result from the use of the often applied linear transformation formulae.

The possibility to derive and use the linear transformation formulae is also included (non-zero coefficients H_1 & H_6 , H_7 & H_{12} , H_{13} & H_{18} , and H_{19} & H_{24}). This can be justified in situations when the observations only include objects with a limited range of colours, or for passbands covering the flat parts of the stellar energy distributions (R or even V , for instance).

Since the non-linear transformations imply that all three passbands affect the accuracy of the determination of the standard values for each passband, we took care to use different integration times for each star in each passband, usually longest

² The program suite for data reduction, sorting and archiving, several auxiliary programs, manual, test examples, and data files can be downloaded at <https://astro.troja.mff.cuni.cz/projects/hec22/>

for the U passband, to obtain comparable signal-to-noise (S/N) ratios in all of them (usual integration times being between 10 and 25 seconds).

We always inspected individual nights of observations for a given observing season and assigned them one of three possible grades: excellent if the rms of the fit of all-sky magnitudes for the standard stars observed was 0^m010 or lower, good for the rms between 0^m011 and 0^m015 , and poor for the rms exceeding 0^m015 in the UBV passbands. Respective individual observations were then treated with the weights 1.5, 1.0, and 0.5. Besides, we selected nights with enough different standards observed and a large range of air masses, and only for these nights, the all-sky data were archived in the all-sky archive. The remaining nights were only used for the differential photometry and are stored in the archive of differential observations, together with information about the comparison star used. More details can be found in the paper by Harmanec et al. (1994), **where also all relevant references to the development of methods of photoelectric data reduction to a standard system are discussed**, and in the user manual to the program suite.

3.2. Reasons for the complete revision of all observations secured since 1972

Originally, our reduction program HEC22 used **only linear extinction coefficients, which were** assumed to remain constant during each observing night. This is actually almost never so, even at observing stations with good climate conditions such as La Silla or Sutherland. For Hvar Observatory, located on an island at an altitude of only 260 m above the sea level, the variations of linear extinction during the night are usually quite large, especially during the summer seasons. To cope with this problem, we had to split many observing nights into shorter time segments and to derive the extinction for each segment separately. This was not satisfactory because standard stars from many – otherwise good and long observing nights – could not be used for seasonal transformations. Only much later a version of the reduction program was developed, which allows the monitoring of the variable extinction during the observing night. This was one of the reasons why we decided to undertake the tedious task to re-reduce all observing seasons since 1972.

The other was the following: Although we took care during the first revision of our system of standard Johnson UBV values, as described by Harmanec et al. (1994), we realised that we should base our standard system on frequent observations of standard stars recommended by Johnson and his collaborators. Several years ago, we therefore derived robust mean $UBVR$ values for all individual observations of the recommended Johnson primary standards, for which extinction was measured, from Johnson et al. (1966) study and used them in all consecutive observations at Hvar during good nights, suitable for all-sky photometry. Additionally, we did the same for several well-observed stars from the list of 108 recommended Johnson secondary standards (Johnson & Harris 1954). **For convenience of other observers, these robust $UBVR$ values for Johnson standards are provided in Appendix C: in Table C.1 for the primary standards, and in Table C.2 for the selected secondary standards.**

All selected stars were carefully checked for variability with the help of individual Hipparcos satellite H_p photometry (Perryman & ESA 1997) and SIMBAD bibliography³.

As shown already by Harmanec et al. (1994), the usual range of values of individual observations for non-variable stars at

Hvar is within 0^m02 to 0^m03 . This is comparable to the rms errors per one observation for the Johnson standards used; see Tables C.1 and C.2. Accordingly, the use of the selected Johnson standards, even those having possible low-amplitude variations, has no systematic effect on the stability of the Hvar standard photometric system.

The Johnson standards were then systematically observed several times during each good observing night. Care was taken to observe them in high and low air masses to "bracket" observations of all other stars during each observing night. We also carried out dedicated observations of all our comparison, check, and red-standard stars, for which good Johnson values were missing. This effort has continued till today and allowed us to get better standard Johnson values for comparison, check, and red stars used in the early observing seasons.

Subsequently, we repeated the reductions of all seasons since 1972. In the vast majority of cases, this resulted in much better seasonal transformations and a significant decrease in mean standard errors. However, to our satisfaction, the final values of the standard all-sky UBV magnitudes do not differ too much from the values derived during the first homogenisation (Harmanec et al. 1994).

Our improved standard Johnson UBV magnitudes for all the frequently observed comparison, check, and red standard stars, which were later used as our new standards, are in Table C.3. In Table C.4 we also provide our standard Johnson UBV magnitudes for the less frequently observed comparison, check, and red standard stars. We underline that these stars were not used as our transformation standards, since their UBV values are naturally still less accurate.

3.3. Notes on the accuracy of the observations and stability tests of our standard system

First, it is useful to explain what a single observation means. In the early years 1972 - 1978, strip-chart recorders were used. About 10 to 15 s long integrations in the three filters were drawn on the paper, from time to time followed by the sky readings in the same filters and gains of the amplifier. These were graphically averaged and read out with a ruler. It would not be straightforward to estimate their rms errors. The current voltage-frequency converter used is controlled by the program PEHVAR⁴, which records individual one-second integrations into a separate file.

We provide several tests of the stability of our observations.

The general idea about the accuracy of Hvar photometry is well documented by Figure 1, where we show plots of the bottom envelope of diagrams showing the dependence of the rms errors per one observation of unit weight versus the magnitude of the object, both for the all-sky archive, and for the archive of differential observations. This characterises the accuracy for non-variable objects. It is encouraging to see that it is quite comparable for all three passbands, thanks to somewhat longer integration times used for the U filter.

The accuracy of Hvar observations of individual stars can also be estimated with the help of the check stars used for each observed program star. We underline that the check stars were always observed as frequently as the corresponding program stars. The HD numbers of the check stars can be found in Table 1 and their rms errors per one observation can be found in Table C.3. For instance, the check star HR 289 = HD 6114 has the rms errors 0^m009 , 0^m009 , and 0^m010 in V , B , and U , respectively.

³ <http://simbad.u-strasbg.fr/simbad/sim-fid>

⁴ Written by J. Horn and currently developed by P. Zasche

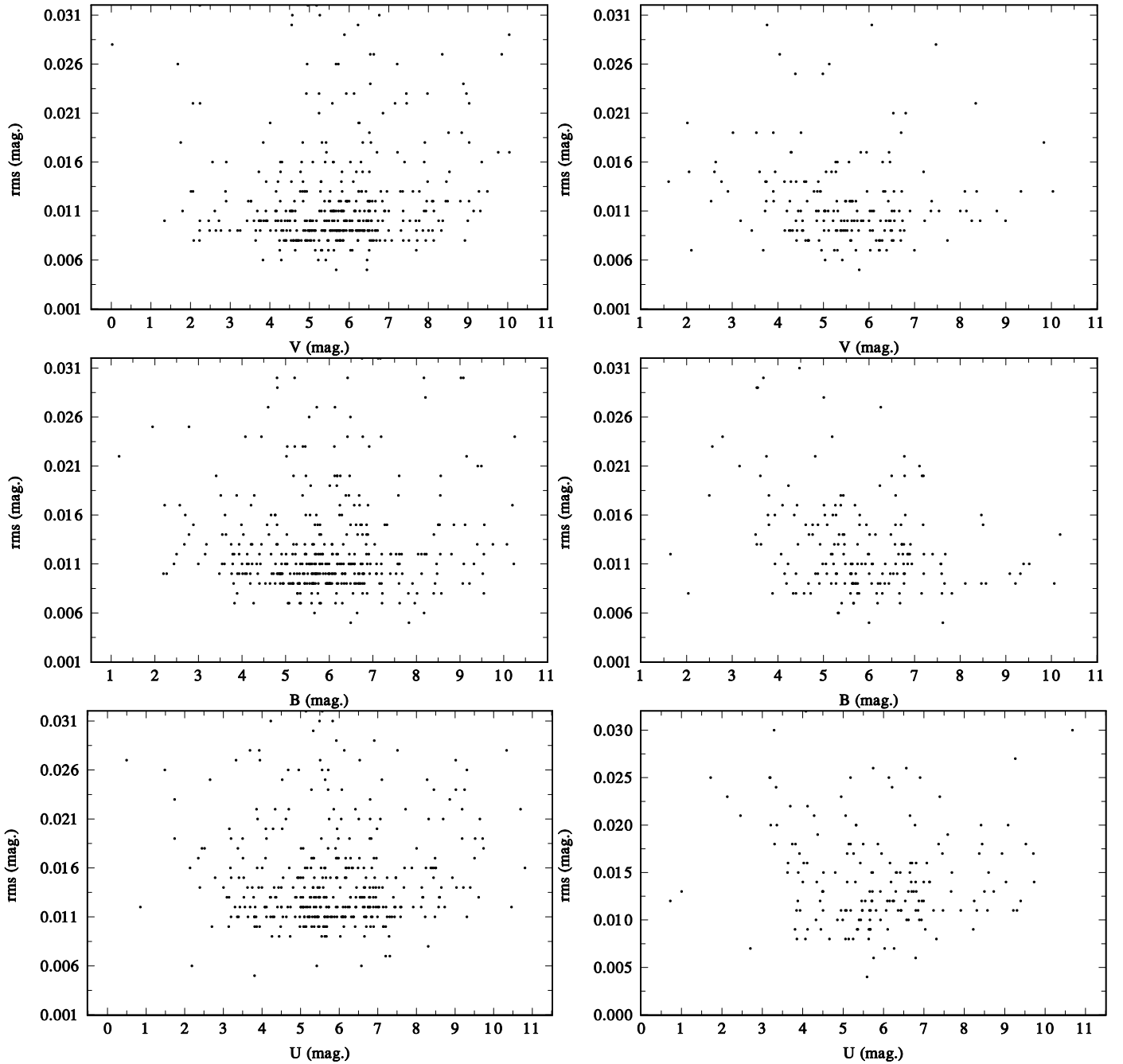


Fig. 1: A plot of rms errors of one observation of unit weight versus magnitude for all three passbands. The left panels are for data from the all-sky archive, the right ones for the data from the archive of differential observations.

Already in some published studies, we have shown that our homogenised magnitudes lead to very good reproduction of observed magnitudes obtained at different observing sites, even from mountain observatories like San Pedro Mártir. This is well illustrated, for instance by Table 2 of the paper by Božić et al. (2007), where the differential *UBV* magnitudes of the check star φ Her derived for different seasons at the Hvar, San Pedro Mártir, and Tubitak stations are compared. The mutual agreement of the values is excellent in all cases.

A very convincing test of the quality of our transformations into the standard Johnson system is the case of the red standard 51 And. This star was alternatively observed as the red standard in two different groups, in both cases relative to blue and much fainter comparisons, 4 Per and HR 189. As Fig. 2 shows, the

individual values relative to both comparisons are stable in time and close to our standard all-sky value for 51 And.

We also plot in Fig. 3 nightly mean values for φ Her = 11 Her = HD 145389. This star was used as the check star in observations of the Be star V839 Her and was observed since 1972. Therefore, it provides a good idea about the accuracy of Hvar observations over time. It is now known to be a 565 d spectroscopic binary seen nearly pole-on, a rotating star with a 3^d708 period and also a low-amplitude pulsating star (see Kochukhov et al. 2021, and references therein). As Fig. 4 in their paper shows, the light variability has a full amplitude lower than 0^m01.

We also investigate the secular stability of the transformation to the standard system on the example of the Johnson primary standard 10 Lac, which was regularly observed in Hvar

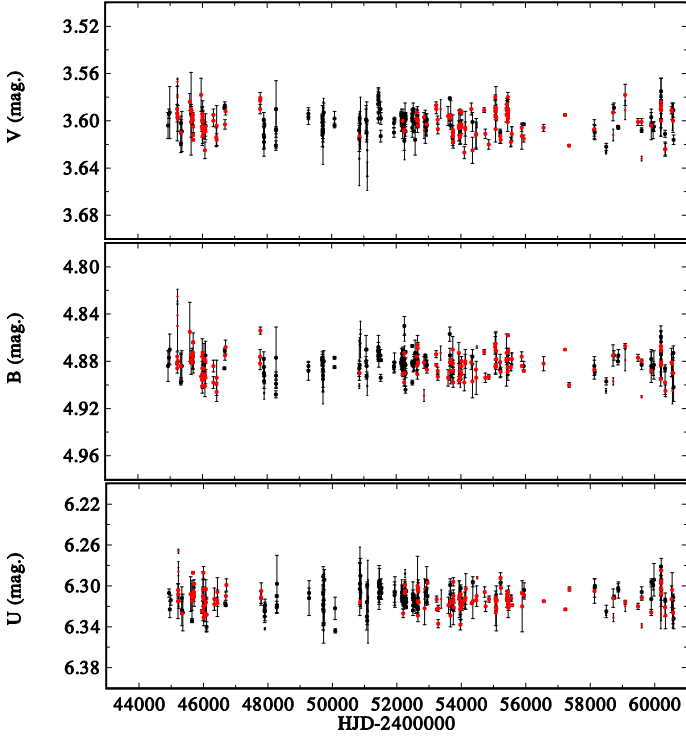


Fig. 2: Individual differential observations *UBV* observations of the red standard 51 And, obtained relative to two different blue comparison stars. Observations relative to 4 Per ($V = 5^m009$, $B - V = -0^m073$, $U - B = -0^m305$) are shown by black circles and those obtained relative to HR 189 ($V = 5^m674$, $B - V = -0^m125$, $U - B = -0^m571$) are shown by red circles. Observations from nights of poor quality are shown by small symbols. Our standard all-sky values for 51 And are $V = 3^m600(10)$, $B = 4^m881(10)$, and $U = 6^m312(11)$.

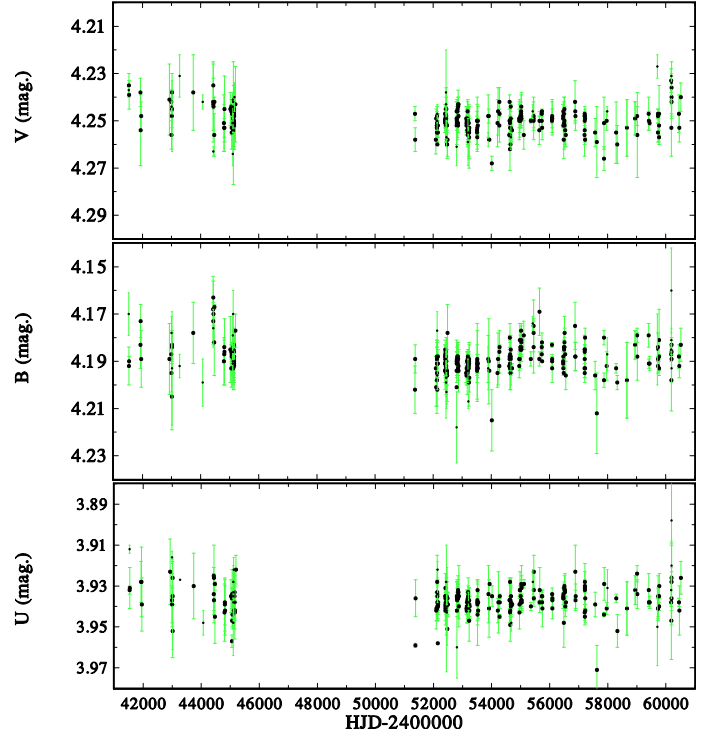


Fig. 3: The *UBV* daily mean *V*, *B*, and *U* differential observations of the check star ϕ Her = HD 145389 relative to ν Her with their rms errors per one observation. Data from the night of dubious quality are shown by smaller symbols.

since 1974. In Fig. 4 we show seasonal mean values with their rms errors. Once again, the secular stability of the values is very satisfactory. Thus, we believe that the standard Hvar *UBV* values for all our standards can be trusted and used in other observing programs elsewhere, **including the CCD observations using Johnson filters.**

380

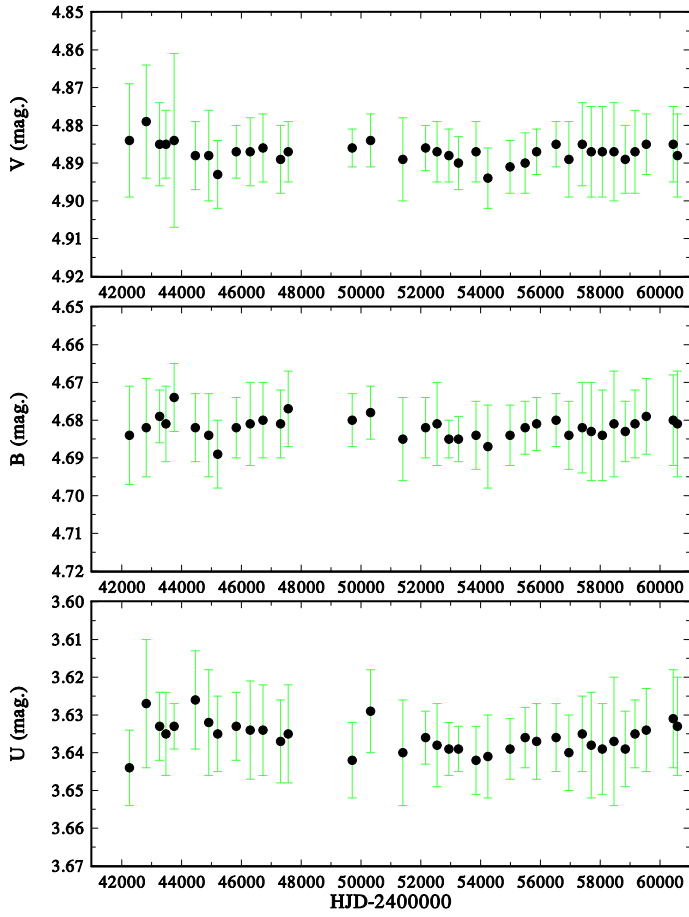


Fig. 4: The *UBV* seasonal mean *V*, *B*, and *U* all-sky normal points with their rms errors per one observation for the Johnson primary standard 10 Lac.

Table 1: A complete list of 106 early-type emission-line stars observed at Hvar Observatory, number of their observations, the comparison and check stars used, and the orbital period and eccentricity if known, with references to sources of binary orbits.

Star name	HD/BD number	No. of obs.	Comp. HD/BD	Check HD	Spectral type	P (days)	e	Ref.
10 Cas	144	18	2626	2011	B9IIIe	-	-	-
V742 Cas	698	6	2626	2011	B5II-IIIe+BVI	55.9233	0.0	33
κ Cas	2905	17	2626	2011	B1Iae	-	-	-
o Cas	4180	895	4142	6114	B5III-IVe	1031.55	0.0	2
γ Cas	5394	137	2626	2011	B0.5IVe	203.52	-	3
V442 And	6226	964	4142	6114	B3.5IIIe	-	-	-
φ And	6811	504	4142	6114	B7e	-	-	-
HD 9709	9709	7	4142	6114	B8Ve	-	-	-
φ Per	10516	678	12303	11291	B0.5IVe+sdOB	126.6731	0.0	7
V777 Cas	11606	11	12303	11291	B2Ve	-	-	-
V780 Cas	12302	9	12303	11291	B1:V:pe+sdOB	-	-	5
HR 654	13854	13	12303	11291	B1Iabe	-	-	-
V554 Per	14818	146	12303	11291	B2Iae	-	-	-
HR 894	18552	118	18411	19736	B7IVe	-	-	-
RX Cas	+67 244	361	18962	19556, 19193	B3e+K1III	32.3301	0.0	6
HR 1051	21551	30	21278	24546	B8Ve	-	-	-
ψ Per	22192	29	21278	24546	B5Ve	126.6982	-	7
HR 1113	22780	41	21856	23193	B7Ve	-	-	-
13 Tau	23016	114	23324	23288	B7Ve	-	-	-
17 Tau	23302	367	23324	23288	B6IIIe	-	-	-
V971 Tau	23480	265	23324	23288	B6IVe	-	-	-
HR 1160	23551	17	21278	24546	B8Ve	-	-	-
η Tau	23630	205	23324	23288	B7IIIe	-	-	-
BU Tau	23862	469	23324	23288	B8Ve	218.34	0.0	8
MX Per	25940	32	21278	24546	B3Ve	-	-	-
HR 1500	29866	30	33641	29722	B8Ve	-	-	-
BV Cam	32343	9	39283	34787	B3Ve	-	-	-
λ Eri	33328	24	32249	33224	B2IIIep	-	-	-
V960 Tau	36576	392	36589	37711, 36819	B2IV-Ve	-	-	-
ζ Tau	37202	1100	36589	37711, 36819	B2IVe	132.987	9	-
ω Ori	37490	90	36591	36351	B3Ve	-	-	-
V731 Tau	37967	107	36589	37711	B4Ve	-	-	-
V696 Mon	41335	318	42690	45546, 43023	B1Ve	80.913	0.0	10
HR 2231	43285	36	44783	43526	B6Ve	-	-	-
AX Mon	45910	40	44783	43526	B2e+K2II	232.499	0.0	6
HR 2370	45995	7	44783	43526	B1.5Vne	103.1	0.0	11
HD 46150	46150	3	44783	43526	O5V((f))z	-	-	-
HR 2418	47054	63	42690	45546, 43023	B8IVe	-	-	-
ψ^9 Aur	50658	29	49949	52860, 50860	B8IIIe	-	-	-
AU Mon	50846	15	50109	50169	B5V+F0	11.113	0.0	12
OT Gem	58050	437	58187	59059	B2Ve	-	-	-
β CMi	58715	168	58187	59059	B8Ve	-	-	-
BR CMi	61273	103	58187	61341	B9.5e+G8III	12.919	0.0	13
UX Mon	65607	152	65199	65005	A5IIIe+G2III	5.9044365	0.0	14
HR 3135	65875	24	63975	71155	B2Ve	-	-	-
HD 81357	81357	93	82861	77692, 81772	B8e	33.77458	0.0	15
κ Dra	109387	429	107193	115612, 104316	B6IIIe	61.5549	0.0	16
ϑ CrB	138749	158	138341	136849	B6Vnne	-	-	-
V839 Her	142926	685	142926	145389, 141930	B7e	46.1921	0.0	17
δ Sco	143275	98	144470	142096	B0.3IVe	3950.8	0.938	18
χ Oph	148184	11	144470	142096	B1.5Ve	34.121	0.26	19
ζ Oph	149757	168	148367	147550	O9.2IVnne	-	-	-
V2315 Oph	161261	5	161677, 169420	—	kA0hB8Ve	-	-	-
V744 Her	162732	1449	158414, 162132	162579	B6IIIe	86.7221	0.16	20
V2048 Oph	164284	164	164432	163641	B2Ve	-	-	-
V974 Her	164447	183	166182	166230	B8IVe	-	-	-
o Her	166014	182	166182	166230	B9.5IIIe	-	-	-
NW Ser	168797	327	170200	169578	B2Vne	-	-	-

Table 1: continued

Star name	HD/BD number	No. of obs.	Comp. HD/BD	Check HD	Spectral type	P (days)	e	Ref.
CX Dra	174237	1167	173664	172883	B3e+F5III	6.696	0.0	21
β Lyr	174638	544	176437	174602, 172044	B8II+B0e::	12.913779	0.0	22
V4024 Sgr	178175	1	177817	182678, 182645	B2Ve	-	-	-
ν Sgr	181616	46	177817	182678, 182645	B2Vpe	137.9343	0.0	1
HD 183261	183261	1	184606	188260	B3IIe	-	-	-
7 Vul	183537	131	188260	184606	B4-5IVe	69.4212	0.113	23
V923 Aql	183656	1620	183227	184663	B6e	214.716	0.0	24
β 2 Cyg	183914	14	188260	184606	B8Ve	-	-	-
V1294 Aql	184279	1709	183227	184663	B0.5IVe	192.91	0.0	25
HR 7482	185859	38	188260	184606	B3I	-	-	-
V1507 Cyg	187399	193	188170	186357	B8III+Be	27.9705	0.389	26
V395 Vul	187811	39	188260	184606	B2.5Ve	-	-	-
V1746 Cyg	189687	209	188892	193369	B3IVe	-	-	-
V1624 Cyg	191610	510	188892	193369	B2.5Ve+sdO	359.98	0.0	27
20 Vul	192044	130	190993	191747	B7Ve	-	-	-
QR Vul	192685	191	190993	191747	B3Ve	-	-	-
P Cyg	193237	122	188892	193369	B1-2Iae	-	-	-
25 Vul	193911	124	190993	191747	B6IVe	-	-	-
V2119 Cyg	194335	140	188892	193369	B2IIIe	63.146	0.0	28
V2120 Cyg	194883	74	194668	197618	B2Ve	-	-	-
HR 7843	195554	161	194668	197618	B8.5Ve	-	-	-
V1661 Cyg	198478	288	203245	199311	B2.5Iae	-	-	-
HR 7983	198625	78	203245	199311	B4Ve	-	-	-
V2140 Cyg	199478	90	203245	199311	B7Iae	-	-	-
V832 Cyg	200120	849	203245	199311	B1.5Ve+sdOB	28.1871	0.144	34
V1931 Cyg	200310	889	203245	199311	B1Ve	147.617	0.20	5
HR 8103	201733	71	203245	199311	B4IVe	-	-	-
ν Cyg	202904	6	202349	204403	B2Ve	-	-	-
HR 8153	203025	8	208218	202214	B2IIIe	-	-	-
V382 Cep	203467	82	208218	202214	B3IVe	-	-	-
HR 8259	205551	21	207330	206259, 207793	B7IIIe	-	-	-
ϵ Cap	205637	2	144206, 213420	—	B3IIIe	128.3	0.0	29
HD 206773	206673	57	208218	202214	B0.5V:pe	-	-	-
EM Cep	208392	10	208218	202214	B1Vne	-	-	-
HR 8375	208682	8	208218	202214	B2Ve	-	-	-
8 Lac A	214168	151	217101	214680	B1Vne	-	-	-
HR 8682	216057	205	218470	219080, 212593	B7Ve	-	-	-
V360 Lac	216200	424	217101	214680	B3e+F9IV	10.0854	0.0	30
EW Lac	217050	1281	218470	219080, 212593	B4IIIpe	-	-	-
V378 And	217543	267	217101	214680	B2.5Vne	-	-	-
ϕ And	217675	1636	217101	214680	B6Ve	2525	0.24	35
KX And	218393	1210	218470	219080, 212593	B0.5e+K1III	33.918	0.0	31
KY And	218674	970	218470	219080, 212593	B4Ve	-	-	-
LQ And	224559	590	223229	222439, 224342	B4Ve	7.41324	0.3	32
V639 Cas	225094	22	2626	2011	B2.9Iabe	-	-	-
MWC 327	227611	6	+35 3955	190919	B1:III/Ve	-	-	-
V1322 Cyg	229221	2	229234	229238	B0.2IIIe	-	-	-

Notes. Column ‘References’: 1...Koubský et al. (2006); 2...Koubský et al. (2010); 3...Nemravová et al. (2012); 4...Božić et al. (1995); 5...Klement et al. (2024); 6...Harmanec (2001); 7...Mourard et al. (2015); 8...Nemravová et al. (2010); 9...Ruždjak et al. (2009); 10...Peters et al. (2016); 11...Nazé et al. (2022); 12...Sahade & Ferrer (1982); 13...Harmanec et al. (2015); 14...Sudar et al. (2011); 15...Koubský et al. (2019); 16...Juza et al. (1991); 17...Koubský et al. (1997); 18...Tycner et al. (2011); 19...Harmanec (1987); 20...Harmanec et al. (1974); 21...Horn et al. (1992); 22...Mourard et al. (2018); 23...Harmanec et al. (2020); 24...Wolf et al. (2021); 25...Harmanec et al. (2022); 26...Hutchings & Redman (1973); 27...Harmanec et al. (2025); 28...Klement et al. (2022b); 29...Rivinius et al. (2006); 30...Linnell et al. (2006); 31...Floquet et al. (1989); 32...Matthews et al. (1991); 33...Rivinius et al. (2025); 34...Peters et al. (2013); 35...Hill et al. (1988)

Table 2: Time intervals covered by Hvar observations of individual Be stars and the total range of their recorded variability.

Star name	JD range -2400000	V range (mag.)	B range (mag.)	U range (mag.)	B – V range (mag.)	U – B range (mag.)
10 Cas	45307.3–56515.6	5.558–5.614	5.534–5.582	5.332–5.385	-0.044 – -0.005	-0.223 – -0.196
V742 Cas	55791.5–55798.5	7.078–7.089	7.263–7.274	6.854–6.870	+0.178 – +0.187	-0.412 – -0.397
κ Cas	45307.3–56515.6	4.115–4.211	4.255–4.363	3.486–3.595	+0.129 – +0.163	-0.786 – -0.756
o Cas	45212.6–60583.5	4.301–4.652	4.291–4.685	3.691–4.012	-0.073 – +0.033	-0.673 – -0.512
γ Cas	45307.3–60362.3	2.084–2.245	1.954–2.153	0.944–1.123	-0.141 – +0.005	-1.078 – -0.984
V442 And	45212.6–60583.5	6.572–6.897	6.592–6.867	5.966–6.327	-0.064 – +0.033	-0.646 – -0.540
φ And	45212.6–60583.5	4.217–4.308	4.163–4.271	3.801–3.932	-0.085 – -0.030	-0.403 – -0.324
HD 9709	53026.3–54356.5	7.085–7.179	7.022–7.155	6.586–6.740	-0.066 – -0.007	-0.436 – -0.414
φ Per	44935.4–60583.5	3.927–4.159	3.795–4.049	2.885–3.171	-0.188 – -0.036	-0.952 – -0.815
V777 Cas	53026.3–53388.3	6.902–7.040	6.976–7.096	6.152–6.286	+0.044 – +0.076	-0.837 – -0.802
V780 Cas	53028.3–53388.3	8.042–8.102	8.322–8.374	7.842–7.936	+0.268 – +0.284	-0.482 – -0.435
HR 654	44985.3–46696.6	6.446–7.383	6.734–7.621	6.094–6.995	+0.234 – +0.292	-0.644 – -0.615
V554 Per	44935.4–50087.2	6.187–6.318	6.486–6.638	5.878–6.054	+0.282 – +0.327	-0.618 – -0.545
HR 894	44860.6–54026.6	6.105–6.181	6.036–6.108	5.642–5.710	-0.096 – -0.024	-0.424 – -0.372
RX Cas	42603.5–60330.3	8.646–9.500	9.777–11.037	9.959–12.169	+0.919 – +1.554	-0.114 – +1.132
HR 1051	45307.4–46689.6	5.828–5.871	5.787–5.814	5.469–5.495	-0.059 – -0.027	-0.327 – -0.302
ψ Per	45307.4–46689.6	4.194–4.247	4.106–4.136	3.508–3.547	-0.135 – -0.073	-0.604 – -0.573
HR 1113	44988.3–50087.5	5.551–5.596	5.491–5.524	5.060–5.104	-0.088 – -0.048	-0.440 – -0.409
13 Tau	44863.6–54015.5	5.668–5.710	5.660–5.703	5.371–5.452	-0.029 – +0.009	-0.302 – -0.220
17 Tau	44863.6–60373.3	3.638–3.764	3.539–3.672	3.149–3.298	-0.152 – -0.073	-0.455 – -0.345
V971 Tau	44863.6–60373.3	4.170–4.235	4.119–4.187	3.679–3.816	-0.090 – -0.027	-0.471 – -0.344
HR 1160	45307.4–46689.6	6.171–6.200	6.236–6.257	5.915–5.938	+0.043 – +0.070	-0.327 – -0.303
η Tau	44863.6–60373.3	2.875–2.962	2.735–2.854	2.385–2.505	-0.158 – -0.062	-0.393 – -0.303
BU Tau	43140.3–60583.5	4.999–5.405	4.919–5.377	4.452–5.241	-0.113 – -0.001	-0.476 – +0.019
MX Per	43136.4–46689.6	3.984–4.075	3.965–4.046	3.408–3.472	-0.106 – +0.014	-0.574 – -0.547
HR 1500	44921.5–52202.6	6.058–6.096	6.126–6.158	5.813–5.871	+0.046 – +0.086	-0.334 – -0.275
BV Cam	45308.6–45697.4	5.139–5.184	5.077–5.099	4.336–4.354	-0.089 – -0.060	-0.748 – -0.737
λ Eri	51445.6–51520.5	4.246–4.298	4.060–4.117	3.172–3.215	-0.217 – -0.137	-0.925 – -0.871
V960 Tau	44902.6–60583.6	5.368–5.718	5.447–5.737	4.690–4.980	-0.016 – +0.136	-0.832 – -0.719
ζ Tau	43135.4–60583.6	2.769–3.200	2.570–2.993	1.757–2.369	-0.278 – -0.087	-0.866 – -0.614
ω Ori	51512.5–59598.4	4.441–4.597	4.371–4.485	3.601–3.726	-0.134 – -0.070	-0.776 – -0.732
V731 Tau	43136.4–46694.6	6.197–6.270	6.141–6.199	5.489–5.583	-0.114 – -0.034	-0.673 – -0.603
V696 Mon	44902.6–59974.4	5.179–5.302	5.117–5.232	4.280–4.396	-0.092 – -0.015	-0.876 – -0.780
HR 2231	44993.4–50865.3	6.058–6.133	5.943–6.037	5.411–5.529	-0.140 – -0.099	-0.532 – -0.479
AX Mon	44993.4–53388.5	6.684–6.810	6.988–7.134	6.344–6.771	+0.282 – +0.380	-0.661 – -0.351
HR 2370	49730.4–49751.4	6.058–6.101	6.000–6.031	5.152–5.195	-0.078 – -0.058	-0.848 – -0.820
HD 46150	53388.5–53388.5	6.716–6.728	6.875–6.868	6.048–6.051	+0.132 – +0.145	-0.817 – -0.807
HR 2418	44902.6–52561.6	5.501–5.554	5.411–5.466	5.022–5.099	-0.107 – -0.055	-0.411 – -0.340
ψ^9 Aur	45014.4–52940.5	5.833–5.893	5.769–5.828	5.325–5.391	-0.096 – -0.054	-0.454 – -0.419
AU Mon	54862.4–55104.6	8.221–9.134	8.275–9.323	7.648–8.804	-0.003 – +0.193	-0.637 – -0.481
OT Gem	44977.4–58924.4	6.061–6.509	5.944–6.346	5.097–5.541	-0.230 – -0.071	-0.922 – -0.760
β CMi	44977.4–58564.4	2.862–2.917	2.755–2.844	2.473–2.593	-0.128 – -0.062	-0.308 – -0.242
BR CMi	55574.5–56015.3	7.089–7.184	7.355–7.433	7.392–7.483	+0.233 – +0.299	+0.005 – +0.076
UX Mon	52655.4–55594.4	8.230–9.343	8.569–10.112	8.341–10.789	+0.286 – +0.957	-0.233 – -0.717
HR 3135	45056.3–53035.5	6.444–6.505	6.348–6.428	5.602–5.653	-0.133 – -0.052	-0.791 – -0.721
HD 81357	55879.6–57116.4	8.295–8.391	8.459–8.553	8.264–8.334	+0.118 – +0.186	-0.251 – -0.172
κ Dra	42237.4–60454.4	3.766–3.978	3.624–3.882	3.071–3.353	-0.218 – +0.049	-0.637 – -0.483
ϑ CrB	44801.4–58637.5	4.128–4.230	3.986–4.138	3.443–3.628	-0.164 – -0.073	-0.570 – -0.449
V839 Her	41528.5–60520.4	5.705–5.803	5.572–5.710	5.158–5.352	-0.162 – -0.058	-0.447 – -0.291
δ Sco	52068.4–60518.4	1.579–2.231	1.630–2.330	0.705–1.208	-0.137 – -0.147	-1.130 – -0.861
χ Oph	54275.4–54290.4	4.328–4.427	4.637–4.737	3.896–3.970	+0.290 – +0.350	-0.781 – -0.732
ζ Oph	52494.3–58682.4	2.510–2.584	2.522–2.615	1.677–1.782	-0.027 – +0.071	-0.886 – -0.803
V2315 Oph	41896.4–42625.4	8.240–8.461	8.275–8.552	8.106–8.398	+0.035 – +0.100	-0.198 – -0.105
V744 Her	41535.4–60580.3	6.662–6.945	6.504–6.858	6.002–6.519	-0.191 – -0.058	-0.557 – -0.265
V2048 Oph	45105.5–60545.4	4.636–4.898	4.616–4.787	3.737–4.056	-0.132 – -0.001	-0.889 – -0.703
V974 Her	45065.6–58395.3	6.405–6.586	6.339–6.508	5.928–6.134	-0.101 – -0.003	-0.419 – -0.321
o Her	45065.6–58395.3	3.784–3.892	3.720–3.921	3.669–3.851	-0.123 – +0.045	-0.142 – +0.033
NW Ser	44433.4–48133.3	6.019–6.191	6.042–6.173	5.381–5.595	-0.041 – +0.035	-0.666 – -0.578
CX Dra	42977.3–56094.4	5.666–6.014	5.658–5.959	4.890–5.252	-0.143 – +0.025	-0.818 – -0.642

Table 2: continued

Star name	JD range -2400000	<i>V</i> range (mag.)	<i>B</i> range (mag.)	<i>U</i> range (mag.)	<i>B</i> – <i>V</i> range (mag.)	<i>U</i> – <i>B</i> range (mag.)
β Lyr	49272.3–57949.5	3.324–4.269	3.303–4.323	2.745–3.803	-0.052 – -0.090	-0.628 – -0.449
V4024 Sgr	53584.4–53584.4	5.309–5.309	5.308–5.308	4.544–4.544	-0.001 – -0.001	-0.764 – -0.764
ν Sgr	53570.4–54297.4	4.510–4.620	4.627–4.769	4.055–4.190	+0.093 – +0.149	-0.597 – -0.555
HD 183261	54275.5–54275.5	6.865–6.865	6.854–6.854	6.167–6.167	-0.011 – -0.011	-0.687 – -0.687
7 Vul	54273.4–59025.5	6.317–6.388	6.219–6.306	5.677–5.771	-0.109 – -0.073	-0.561 – -0.503
V923 Aql	44073.4–60580.3	5.983–6.166	5.966–6.201	5.618–6.018	-0.044 – +0.095	-0.391 – -0.102
β 2 Cyg	46679.4–46695.4	5.140–5.159	5.051–5.069	4.730–4.744	-0.098 – -0.078	-0.327 – -0.315
V1294 Aql	44073.4–60580.4	6.788–7.565	6.807–7.634	5.997–7.587	-0.005 – +0.173	-0.841 – +0.002
HR 7482	46679.4–58682.5	6.481–6.519	6.859–6.913	6.270–6.326	+0.376 – +0.403	-0.613 – -0.577
V1507 Cyg	43024.4–43760.4	6.896–7.088	7.082–7.260	6.680–6.861	+0.103 – +0.263	-0.463 – -0.323
V395 Vul	46679.4–58682.5	4.909–4.957	4.726–4.792	4.067–4.137	-0.183 – -0.141	-0.700 – -0.644
V1746 Cyg	46245.5–60583.3	5.121–5.246	4.990–5.084	4.251–4.409	-0.168 – -0.108	-0.747 – -0.670
V1624 Cyg	42237.5–60583.3	4.888–5.084	4.721–4.943	3.943–4.281	-0.216 – -0.103	-0.850 – -0.639
20 Vul	44432.5–60565.5	5.867–5.945	5.746–5.842	5.285–5.405	-0.135 – -0.089	-0.485 – -0.428
QR Vul	44794.5–60583.3	4.600–4.820	4.453–4.644	3.684–3.925	-0.227 – -0.109	-0.799 – -0.706
P Cyg	46287.4–55451.4	4.715–4.877	5.116–5.275	4.559–4.718	-0.383 – -0.450	-0.581 – -0.513
25 Vul	44817.4–60565.5	5.499–5.563	5.395–5.487	4.958–5.078	-0.120 – -0.073	-0.460 – -0.387
V2119 Cyg	46238.5–47022.4	5.783–5.923	5.616–5.758	4.652–4.836	-0.190 – -0.141	-0.981 – -0.906
V2120 Cyg	45149.5–55068.4	7.163–7.361	7.221–7.345	6.551–6.730	-0.019 – +0.060	-0.672 – -0.609
HR 7843	44431.5–55064.4	5.863–5.942	5.827–5.880	5.574–5.675	-0.095 – -0.009	-0.253 – -0.166
V1661 Cyg	41528.4–53935.5	4.740–4.896	5.112–5.272	4.651–4.835	+0.333 – +0.424	-0.472 – -0.404
HR 7983	46696.4–53592.5	6.323–6.400	6.264–6.342	5.674–5.796	-0.074 – -0.038	-6.616 – -0.546
V2140 Cyg	43024.4–54662.5	5.634–5.724	6.097–6.192	5.787–5.900	+0.424 – +0.486	-0.334 – -0.283
V832 Cyg	46258.6–60583.4	4.451–4.837	4.432–4.782	3.489–3.887	-0.116 – +0.013	-0.984 – -0.860
V1931 Cyg	46281.5–60583.4	5.289–5.503	5.136–5.303	4.152–4.405	-0.251 – -0.122	-1.001 – -0.890
HR 8103	46696.4–52100.5	6.595–6.650	6.454–6.514	5.747–5.890	-0.164 – -0.124	-0.707 – -0.621
ν Cyg	44817.4–44818.5	4.342–4.371	4.256–4.284	3.433–3.460	-0.094 – -0.081	-0.828 – -0.815
HR 8153	48116.6–48123.6	6.378–6.443	6.585–6.666	6.085–6.220	+0.191 – +0.227	-0.507 – -0.446
V382 Cep	45536.4–52282.2	4.924–5.255	4.942–5.222	4.299–4.651	-0.128 – +0.051	-0.694 – -0.527
HR 8259	45155.5–59078.6	6.153–6.202	6.139–6.199	5.875–5.947	-0.026 – +0.001	-0.283 – -0.238
ϵ Cap	41929.5–41940.4	4.582–4.613	4.453–4.534	3.811–3.880	-0.128 – -0.079	-0.654 – -0.642
HD 206773	52142.6–52282.2	6.876–7.053	6.980–7.183	6.169–6.428	+0.087 – +0.143	-0.830 – -0.742
EM Cep	41954.5–54020.3	6.975–7.115	7.224–7.398	6.665–6.851	+0.239 – +0.296	-0.579 – -0.540
HR 8375	48116.6–48123.6	5.896–5.939	5.807–7.873	5.062–5.131	-0.102 – -0.055	-0.747 – -0.715
8 Lac A	43013.6–54026.5	5.640–5.767	5.483–5.662	4.575–4.723	-0.191 – -0.064	-0.950 – -0.853
HR 8682	44432.6–51426.5	6.117–6.199	6.030–6.114	5.528–5.674	-0.125 – -0.043	-0.536 – -0.440
V360 Lac	44473.5–53980.4	5.862–5.994	5.949–6.067	5.442–5.579	+0.041 – +0.112	-0.554 – -0.469
EW Lac	41534.5–60199.5	5.096–5.492	4.958–5.361	4.198–4.955	-0.165 – -0.030	-0.778 – -0.397
V378 And	42261.5–55460.4	6.461–6.615	6.317–6.530	5.630–5.906	-0.180 – -0.061	-0.743 – -0.624
ϕ And	42614.6–60583.4	3.498–3.784	3.395–3.702	2.861–3.256	-0.178 – +0.000	-0.598 – -0.427
KX And	42261.5–57621.5	6.775–7.212	7.092–7.596	6.661–7.478	+0.251 – +0.431	-0.551 – -0.101
KY And	42614.5–57621.5	6.686–6.894	6.679–6.862	6.075–6.317	-0.092 – +0.059	-0.642 – -0.513
LQ And	44433.5–60583.4	6.498–6.598	6.412–6.524	5.793–5.920	-0.125 – -0.035	-0.669 – -0.554
V639 Cas	45307.3–55798.5	6.201–6.273	6.542–6.610	6.011–6.099	+0.326 – +0.347	-0.532 – -0.506
MWC 327	44841.4–46689.4	8.710–8.790	9.074–9.148	8.384–8.435	+0.335 – +0.364	-0.721 – -0.666
V1322 Cyg	44794.5–44843.3	9.333–9.346	10.190–10.223	9.957–10.016	+0.844 – +0.890	-0.233 – -0.207

4. Long-term, phase-locked, and rapid light and colour changes of Be stars observed at Hvar

The list of all Be stars observed at Hvar, together with information about the comparison and check stars used to their differential observations, and MKK spectral types is in Table 1. For known binaries, also the orbital period, eccentricity and type of orbital light variability is listed. In most cases, we give only one reference for the binary orbit, in which previous studies are listed. Information about the time interval covered by their observations and the total range of variations recorded is in Table 2.

The following typical patterns of light and colour changes can be distinguished:

Long-term changes related to the strength and/or extent of the Be envelope (LTEM). These occur on a time scale of years to decades and have two distinct alternatives, depending on the inclination of the Be disk plane with respect to the observer: positive (LTEM_p), when the brightenings are accompanied by the rise of the emission-line strength, and inverse (LTEM_i), when the light decreases are followed by the emission-line rise (Harmanec 1983, 1994, 2000; Sigut & Patel 2013). We note that in cases of intermediate inclination, a given object can exhibit either a positive, or an inverse correlation in various epochs of observations, depending on the extent of the Be envelope (see, e.g. Harmanec et al. 2022).

Long-term cyclic changes (LTCV). They might be related to the long-term cyclic V/R variations of the relative strength of the V and R peaks of the double Balmer emission lines if the monitoring of corresponding spectral variations is available. They occur typically on a time scale of several years and are related to non-axisymmetric geometrical and/or dynamical changes of the structure of the Be disks. In the past, they were interpreted as a gradual revolution of an elongated disk (see, e.g. Ballereau & Chauville 1989). Since the studies by Okazaki (1991) and Okazaki (1997), they are usually understood as global one-armed oscillations of the disks and can also manifest themselves by the corresponding light changes (see the detailed discussion by Mennickent et al. 1997). A recent example of such changes was presented by Wolf et al. (2021). The problem is that the LTCV sometimes occur simultaneously with the LTEM changes and it is not easy to separate both effects (see, for instance Harmanec et al. 2022).

Light and colour variations related to the duplicity of particular Be stars (MTBIN). Such changes are periodic and generally follow the orbital periods of the Be binaries in question, but they are not easy to detect due to the simultaneous presence of variations on other time scales. In addition to clear cases of binary eclipses, they can also manifest themselves as a combination of ellipticity and reflection, or occasional eclipses of the outer parts of the disks. Numerous examples of such changes were discussed, with corresponding references, by Božić et al. (2013a) and are documented by Hvar systematic photometry; see the discussion of individual Be stars below.

Rapid periodic or multiperiodic low amplitude changes (RAV). These brightness variations usually occur on timescales from about 0.1 to 2 d and have been alternatively interpreted as pulsations or rotational modulation. Since the typical observing strategy at Hvar was focused on monitoring variations on longer time scales, Hvar observations are not very suitable for analyses of such rapid changes, with the exception of several dedicated observing campaigns on selected Be stars,

for instance ζ Tau (Božić & Pavlovski 1988), σ And, KX And, KY And, LQ And and EW Lac (Stagg et al. 1988) or ω Ori (Balona et al. 2001).

Secular very long-term brightness decreases or increases during the quiescent stages without strong LTEM changes (VLTV). This very long timescale of changes was probably first noted for ω CMa by Harmanec (1998b) and empirically modeled in terms of the viscous decretion disk model (Lee et al. 1991; Carciofi et al. 2009) by Ghoreyshi et al. (2021, 2023). Several distinct examples of such behaviour were presented by Harmanec et al. (2022). Understanding this type of variability will require further observational and theoretical efforts.

In the following, we discuss selected fifty two stars, which were observed more systematically at Hvar. Because the observations at Hvar were interrupted during 1990-1992, we complemented the Hvar V series in the V magnitude time plots with the Hipparcos H_p photometry, transformed to Johnson V magnitude after Harmanec (1998a). These are shown by red circles in all plots. The following notes on particular observed Be stars are mostly related to LTEM, LTCV, VLTV, and/or MTBIN changes. Here, we present examples of 19 interesting objects, showing different characteristic variability patterns. Brief discussion of the remaining objects can be found in Appendix D.

σ Cas = 22 Cas = HD 4180 This bright Be star is the primary component A of a wide visual system AB WDS J00447+4817. Koubský et al. (2010) confirmed that it is also a spectroscopic binary with a period of 1031^d6 and a rather large RV semi-amplitude of 22 km s⁻¹, which implies a large mass function. They also obtained a visual orbit with an inclination of 115° and since they did not detect any lines of the secondary, they suggested that the secondary is actually a close pair of two A stars. Such stars were indeed detected in the spectra studied by Grundstrom (2007), with a possible period close to 4 days (see also Touhami et al. 2013; Hutter et al. 2021). Thus, it appears that the object is a hierarchical system Aa1, Aa2, and B. Koubský et al. (2010) also found a period of 1^d2578 in the residuals from their RV orbit and showed large-amplitude cyclic light changes, based on the Hvar photometry. Here, we present an extended series of Hvar observations in Fig. 5.

V442 And = HD 6226 This star was originally used as one of the check stars in our Be star observing program and this led to the discovery of its light variability in the form of occasional brightenings, accompanied by reddening in $B-V$ and blueing in the $U-B$ index. This finding was published by Božić & Harmanec (1998), who suggested that the object could be a Be star. This was indeed confirmed by a detailed spectroscopic and photometric study by Božić et al. (2004), who found that V442 And is a pole-on Be star with a positive correlation between brightness and emission-line strength and pronounced line-profile variations, reminiscent of an archetype Be star ω CMa, and varying with a regular 2^d61507 period. Richardson et al. (2021) published a very detailed study, based on numerous spectra and on the KELT and TESS photometries. They estimated the spectral type as B2.5IIIe and confirmed the period of line-profile changes. Analysing the H α and H β equivalent widths, they found regular changes with two periods, 211^d9, and 87^d0. They also argued that the emission-line episodes could be related to the interference of pulsational modes, resulting in formations of transient circumstellar disks. Other published studies are also summarised in their paper. The complete light curve of V442 And secured at Hvar is in Fig. 6.

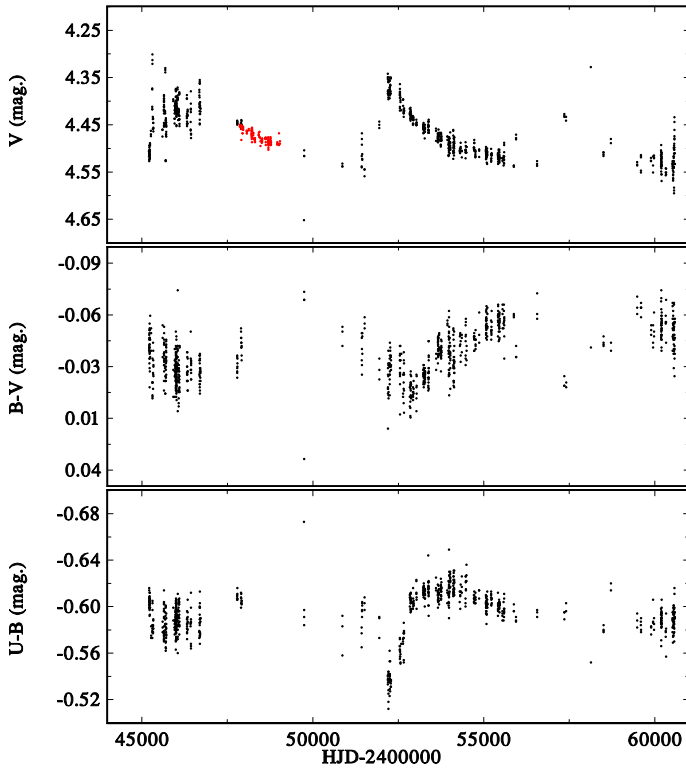


Fig. 5: The *UBV* time variations of *o* Cas. The red dots in this, and in all following time plots for individual objects denote the Hipparcos H_p observations transformed to Johnson *V* magnitude after Harmanec (1998a). As mentioned in Sect. 2, the accuracy of these observations can be judged from the rms errors per one observation of the respective check star, which are provided in Table C.3. For the check star HR 289 observed with *o* Cas, they are 0^m.009, 0^m.009, and 0^m.010 for the *V*, *B*, and *U* passbands, respectively.

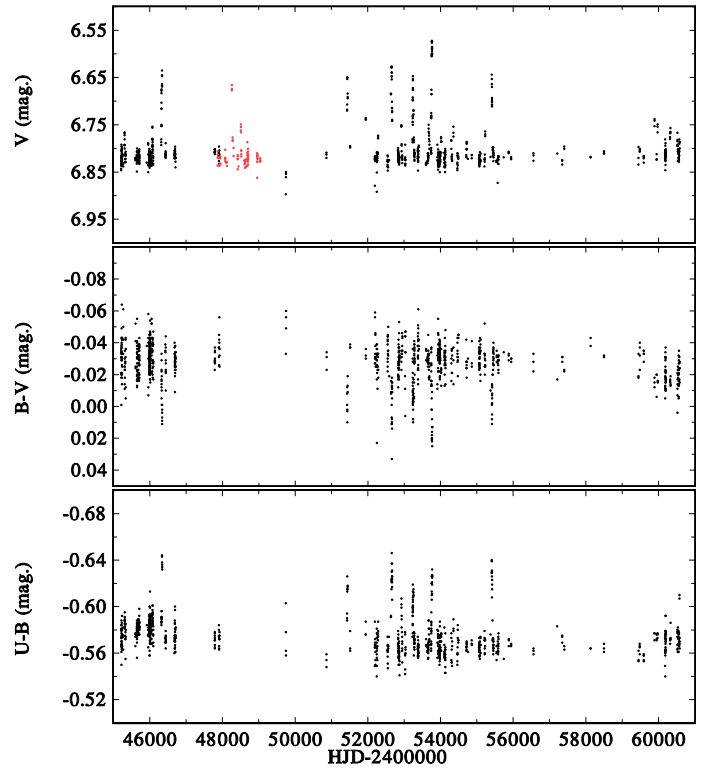


Fig. 6: The *UBV* time variations of V442 And.

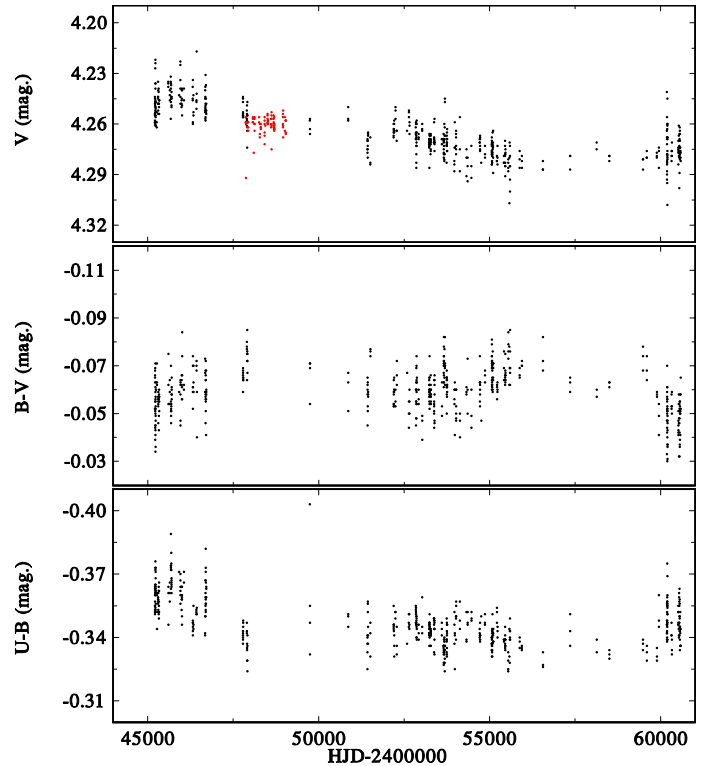
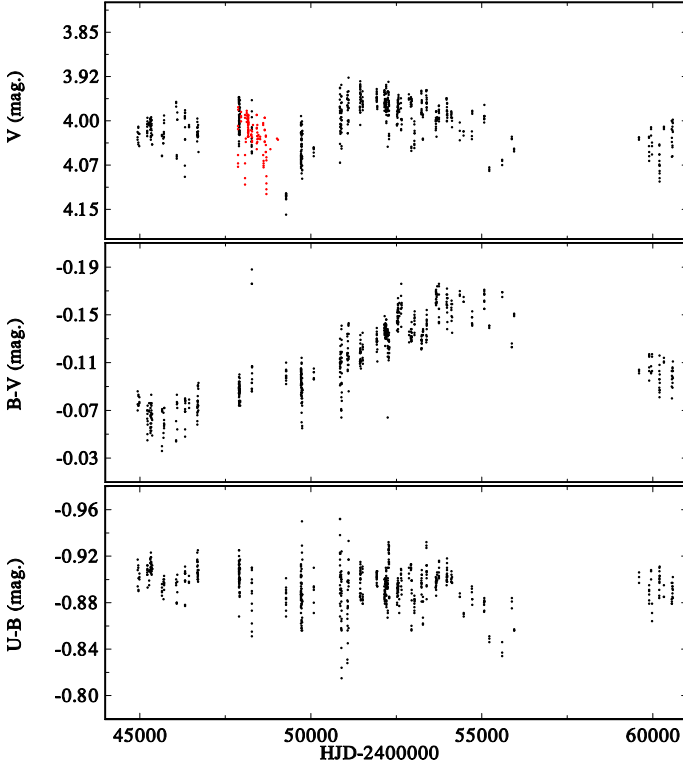
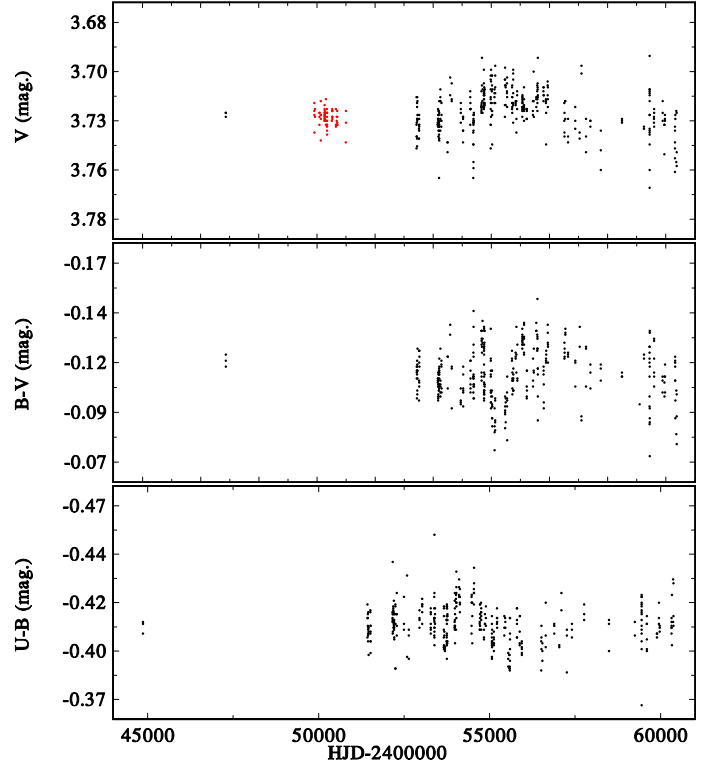


Fig. 7: The *UBV* time variations of φ And.

φ And = 42 And = HD 6811 This Be star is obviously observed pole-on, shows a single-peaked $H\alpha$ emission profile and little light variability, and was alternatively classified as B7Ve and B5IIIe (Jones et al. 2011; Barnsley & Steele 2013). It is also a member of a multiple visual system WDS J01095+4715 and Muterspaugh et al. (2010) published a visual orbit with a period of about 202500 d. Its mild light and colour variability **would probably go unnoticed without** very systematic monitoring and careful reduction; see Fig. 7. It is characterised by a **steady slow light decrease on a very long (LTCV) time scale**, with no known episodes of more rapid brightening or fading.

φ Per = 54 And = HD 10516 This object is a well-known B0.5e+O6 VI binary with a 126^d.7 period (see Poeckert 1981a,b; Gies et al. 1993; Thaller et al. 1995; Božić et al. 1995; Gies et al. 1998, and references therein). Božić et al. (1995) compiled all the photometric and RV observations and summarised the early history of the system. They also derived an improved orbital period of the system. Photometry, including the first part of Hvar observations, shows only mild secular changes. They interpreted the emission seen in He I 6678 Å as a double emission moving with the secondary. However, Štefl et al. (2000) and Hummel & Štefl (2001) argued that this emission actually originates in the part of the disk of the primary, facing the hotter secondary and being illuminated by it. Mourard et al. (2015) resolved the secondary in their optical interferometry and

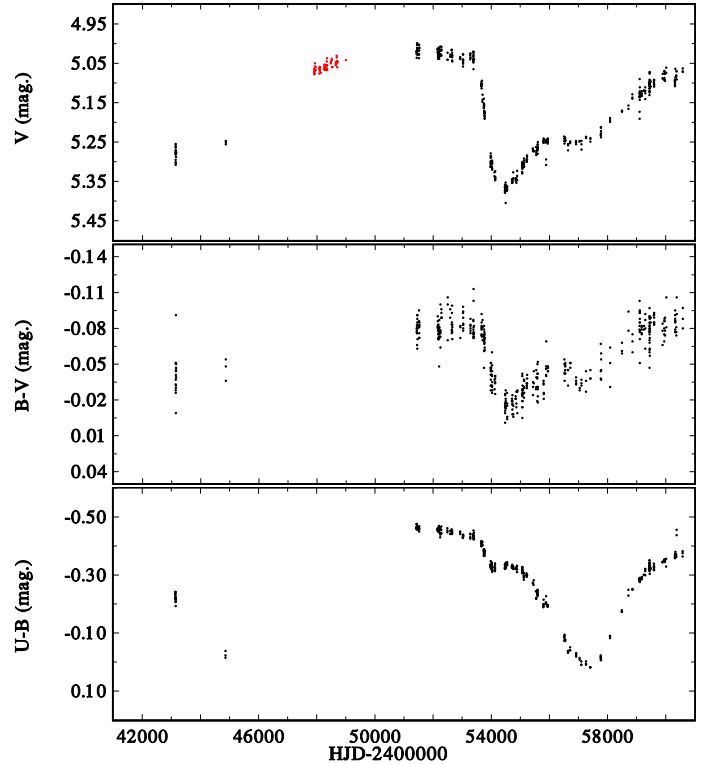
published the most detailed model of the system to date, deriving the component masses of 9.6 and 1.2 M_{\odot} . Božić et al. (2013b) reported small sinusoidal *B* magnitude light variation with the orbital period. The complete Hvar photometry is shown in Fig. 8. It is seen that the light variations are dominated by slow changes

Fig. 8: The *UBV* time variations of ϕ Per.Fig. 9: The *UBV* time variations of 17 Tau.

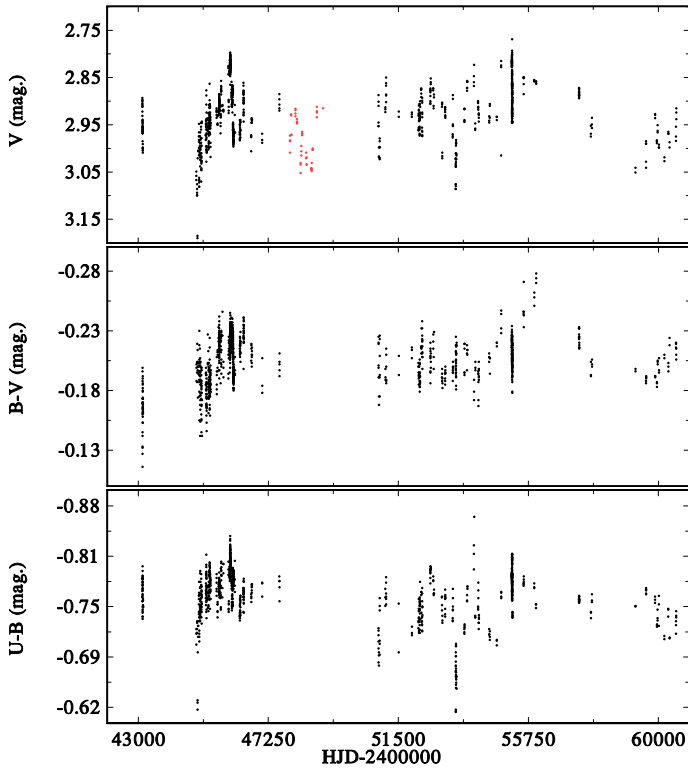
on the **LTCV** time scale. The *V* magnitude varies in a cycle of more than 5000 d, while the *B*–*V* index was gradually brightening over many years but started to get redder recently.

17 Tau = HD 23302 This bright member of the Pleiades cluster, also known as Electra, was reported to be a single-line spectroscopic binary with an orbital period of 100^d.46 by [Abt et al. \(1965\)](#). They claimed that the orbit, based on a limited set of RV measurements, is not well determined. [Pearce & Hill \(1975\)](#) were not able to definitely provide proof that the star was a spectroscopic binary but left the possibility open. [Torres \(2020\)](#) derived accurate RVs over an interval of about 800 days and concluded that there is no evidence of RV changes. [Breger \(1972\)](#) showed that 17 Tau is constant down to 0^m.002–0^m.003. In his search for Maia variables [McNamara \(1985\)](#) used 17 Tau as a comparison star in the photometric search for the Maia candidates, finding it to be constant, and its photometric constancy was also confirmed by [McNamara \(1987\)](#). Also the Hipparcos *H_p* photometry does not show any significant brightness changes. **We note, however, that the star was repeatedly observed with TESS and these observations indicate cyclic variations on a time scale of about 1^d1 with a full amplitude of 0^m.0006 to 0^m.0008.** The Hvar photometry presented in Fig. 9 shows the presence of mild long-term variations in brightness and colours on the level of several hundredths of a magnitude.

BU Tau = 28 Tau = HD 23862 This well-known Be star is one of few for which brightness and colour variations have been recorded systematically for a long time, mainly due to the effort of Sharov and Lyutyj (see [Sharov & Lyutyj 1972](#); [Sharov & Lyutyj 1997](#), and references therein). It is the primary component of a binary with a highly eccentric orbit and an orbital period of 218^d.03 ([Nemravová et al. 2010](#); [Katahira et al. 1996](#)). The orbit was not resolved interferometrically by [Klement et al. \(2024\)](#). The spectroscopic behaviour of

Fig. 10: The *UBV* time variations of BU Tau.

this star is characterised by remarkable changes between the normal Be state to Be-shell and Be phase ([Hirata & Kogure 1976](#); [Hirata 1995](#)). After a long B phase that lasted until 1937, the star passed through 3 cycles of photometric and spectral variation. The photometric variations show long-term cyclic changes

Fig. 11: The *UBV* time variations of ζ Tau.

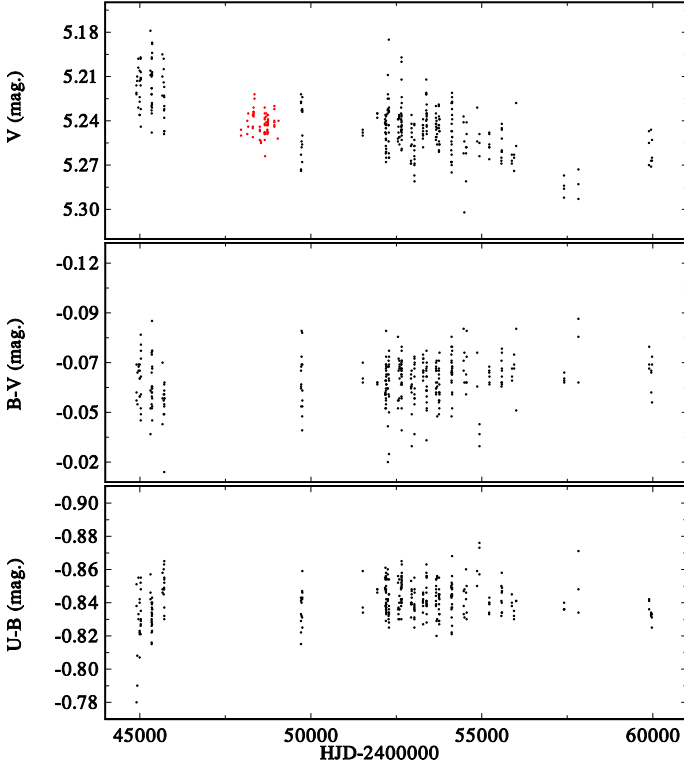
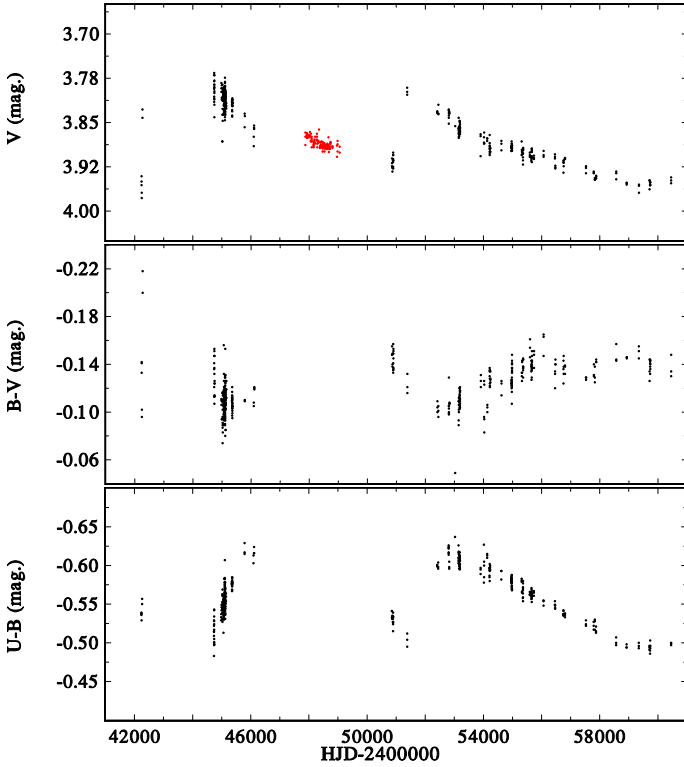
that started with a light decrease that lasted for some two years. After reaching the light minimum, a gradual increase in brightness to the initial level was temporarily replaced by another mild light decrease, related to the development of a metallic shell. The period of the complete cycle lasts 34–36 years (Hirata & Kogure 1976; Harmanec 1982). Using speckle interferometry McAlister et al. (1989) found a third companion at a separation of 0.22 sec. Harmanec (1982) and Gies et al. (1990) (and some others) considered a causal connection between the motion of that distant companion and the occurrence of the shell phases. Roberts et al. (2007) recorded also the fourth companion of BU Tau at a distance of 4.66 sec. Besides a few observations from the season 1976/77, Hvar data cover almost the entire last cycle of photometric changes. A secondary minimum is visible on the ascending part of the curve, the depth of which is the most prominent at shorter wavelengths; see Fig. 10. Iliev & Miroshnichenko (2025) clearly demonstrated that large changes in the strength of the $H\alpha$ profile occur shortly after each periastron passage in the 218^d03 orbit. BU Tau shows the inverse correlation between the brightness and emission-line strength. The behaviour in $U-B/B-V$ is shown in Fig. 26. **A new detailed study of this object is under preparation.**

ζ Tau = 123 Tau = HD 37302 This well-known and for a long time studied Be star is a single-line spectroscopic binary with a 132^d99 orbital period, exhibiting also long-term cyclic RV and V/R changes at certain time intervals (see the detailed studies by Delplace 1970; Harmanec 1984b; Ruždjak et al. 2009; Štefl et al. 2009; Carciofi et al. 2009, where also references to original papers can be found). There is a clear correlation between the long-term RV and V/R changes. However, Ruždjak et al. (2009) have demonstrated that the light and colour behaviour was different in each long cycle, alternating between

positive and inverse correlation. The first part of Hvar photometry has also been discussed in Božić & Pavlovski (1988). In addition to long-term changes, these authors found rapid variations with a 0^d8 period (or a 1^d6 period with a double-wave phase curve). They also detected light decreases reminiscent of atmospheric eclipses in some orbital cycles, which were missing in the others (see also Fig. 1 in Božić et al. 2013b). A complete set of Hvar observations is shown in Fig. 11. The apparent scatter of the data is mainly due to rapid large-amplitude changes.

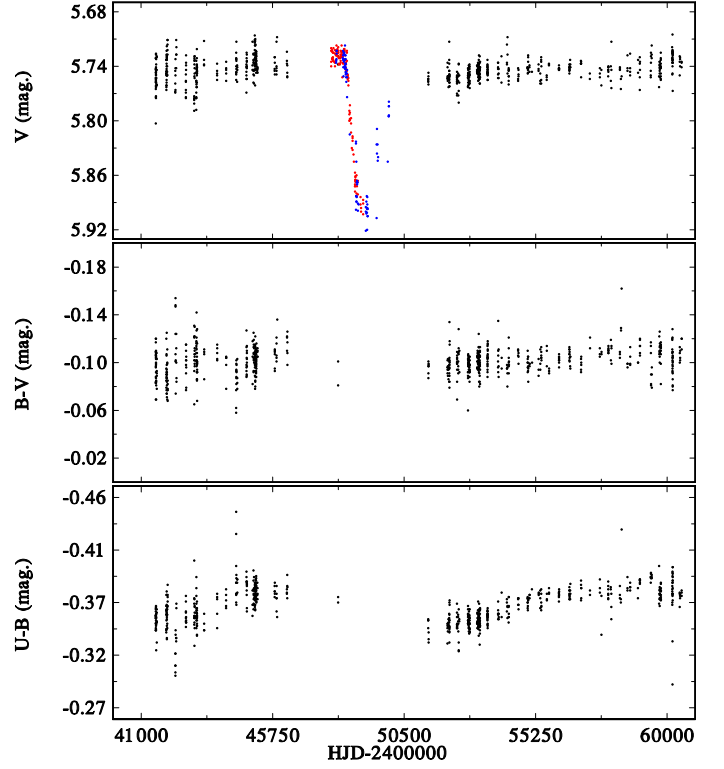
V696 Mon = HR 2142 = HD 41335 This Be star was found to exhibit two consecutive short-lived shell phases periodically every 80^d85 days (Peters 1971, 1972). Later, Peters (1983) found that the object is a single-line spectroscopic binary with an orbital period of 80^d860, derived its radial-velocity curve and argued that the observed shell phases are consequences of mass transfer in a binary system. Peters originally argued that the secondary is a late-type Roche-lobe filling object but no such object has ever been detected and Waters et al. (1991) proposed an alternative model, assuming that the secondary is a small helium star and that the disk around the primary is not an accretion, but an outflowing disk. Peters et al. (2016) indeed detected a weak signal in the IUE spectra corresponding to a hot subdwarf companion, with a mass ratio of 0.07 and T_{eff} around 43000 K. Using numerous optical and IUE spectra, they also revised the orbital period to 80^d913. Sterken (1983) reported a 0^m13 light decrease in the Strömgren b magnitude. Hvar photometry of the object has been secured rather systematically since the end of 1981 and was first used, together with the Kitt Peak and Skalnaté Pleso photometry, to demonstrate that no such light decrease occurred and that also the recurrent shell phases are not accompanied by any light changes (Harmanec et al. 1983). The absence of light changes during a primary shell phase was also reported by Dorren et al. (1984). The time plot of the Hvar photometry, shown in Fig. 12 shows only a very mild secular light decrease on the LTCV time scale and little or no changes in both colour indices. One could suspect some small rapid changes to be present, but we note that the star is always observed at air masses larger than 1.55 at Hvar, which implies somewhat higher scatter of individual observations.

α Dra = 5 Dra = HD 109387 This bright Be star observed in an unusually high northern declination, was found to be a single-line spectroscopic binary with a 61^d55 orbital period and a small RV amplitude by Juza et al. (1991). This was confirmed by subsequent orbital solutions by Saad et al. (2005) and Saad et al. (2021). However, all attempts to detect the spectrum of the secondary failed. The secondary was finally detected from near-IR interferometry by Klement et al. (2022a). They found a mass ratio of 0.117 ± 0.009 , in agreement with the range estimated by Juza et al. (1991). Juza et al. (1994) investigated spectral, polarimetric and photometric observations from the past 100 years, including their own, and argued that all observables varied with a period of 8406 days. Saad et al. (2004) concluded that this variability (which they estimated to 8044 ± 167 days) is probably cyclic, not strictly periodic. This is definitively confirmed by the extended series of Hvar photometry, shown in Fig. 13, which shows a long systematic brightness decrease since about JD 2451000 up to the present time. This nicely correlates with the disappearance of the Balmer emission documented over a similar time interval by Klement et al. (2022a). **A slow secular decrease on the VLTV scale seems to be present.** Balona & Ozuyar (2021) reported rotational modu-

Fig. 12: The *UBV* time variations of V696 Mon.Fig. 13: The *UBV* time variations of κ Dra.

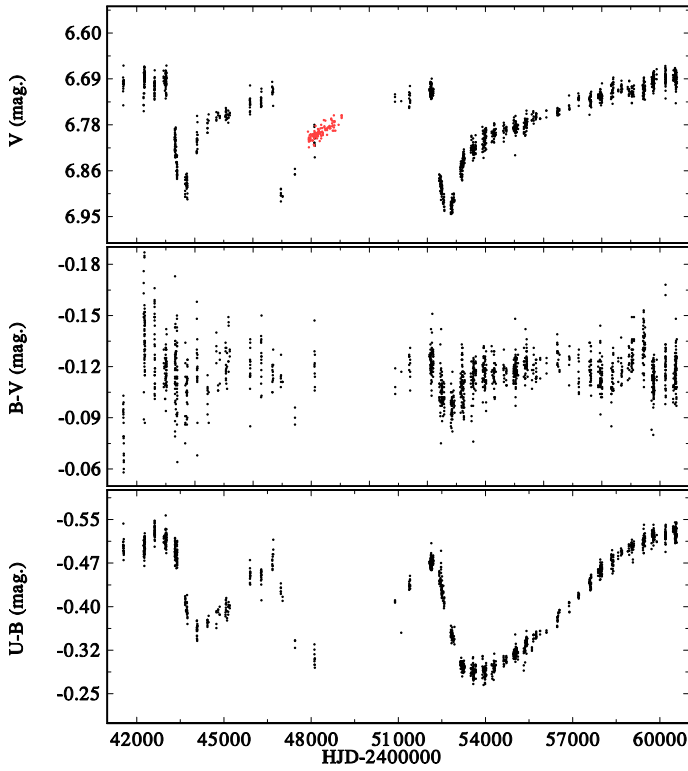
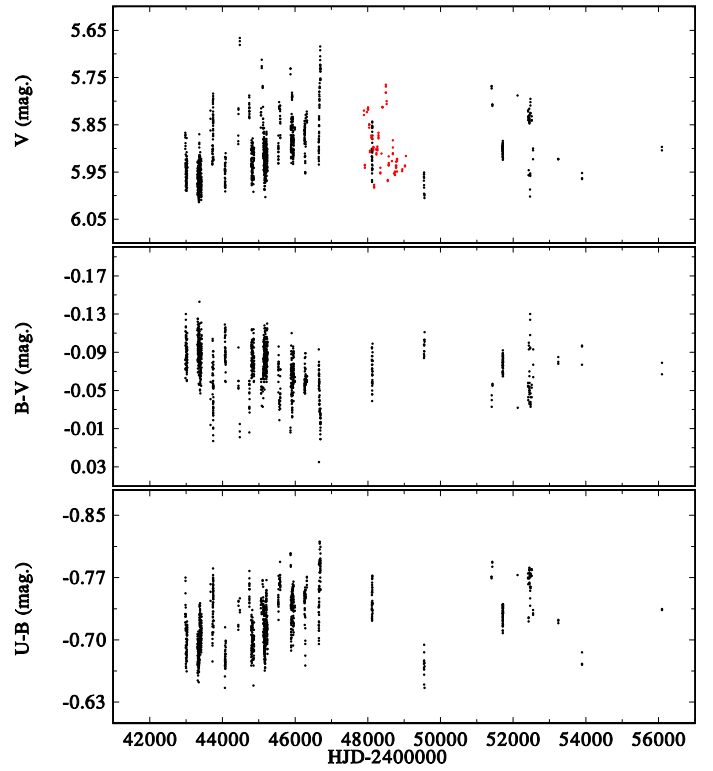
lation with a period of 1^d134 from their analysis of TESS photometry.

V839 Her = 4 Her = HD 142926 This Be star belongs to a few Be stars systematically monitored at Hvar since 1972. It was identified as a single-line spectroscopic binary

Fig. 14: The *UBV* time variations of V839 Her. The blue dots denote observations published by Percy et al. (1997).

with a 46^d2 period (Harmanec et al. 1973b; Heard et al. 1975; Harmanec et al. 1976). Božić et al. (2013a) reported very mild light variations with the orbital period. The time plot of all Hvar and transformed H_p photometric observations is shown in Fig. 14. So far, the only large light decrease, associated with the formation of a new shell phase, was discovered by Percy et al. (1997) and is also recorded in the H_p photometry. Since this is a very interesting case, we made an exception and also included the observations by Percy et al. (1997) in our time plot (shown by blue circles). This identifies V839 Her as an object with the inverse correlation between the light and the emission-line strength (Koubský et al. 1997). This is corroborated by the study of Sigut & Ghafourian (2023). These authors compared the inclination angles of a number of Be stars based alternatively on the effects of gravitational darkening and on the $H\alpha$ emission line profile modelling. They found that V839 Her is seen almost equator-on. In photometry, no secular variations outside the shell phase have been detected in either the V magnitude or $B-V$ index, but are obvious in the $U-B$ index.

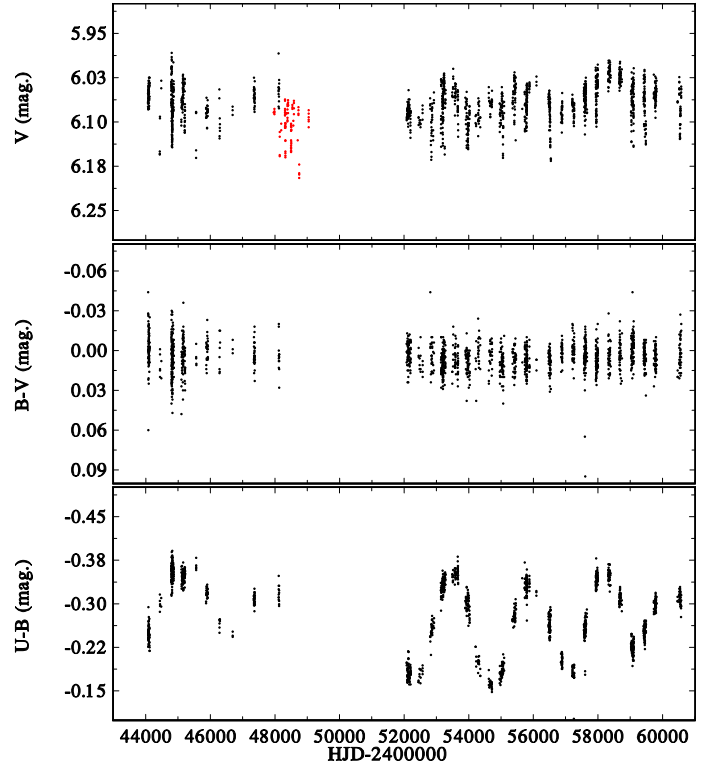
V744 Her = 88 Her = HD 162732 This Be star has also been systematically monitored at Hvar since 1972. It was found to be a single-line spectroscopic binary with an 86^d7 period (Harmanec et al. 1972b,a, 1974; Doazan et al. 1982b,a). Figure 15 shows the light and colour changes of the object over 52 years of Hvar observations. It is seen that the star underwent three episodes of secular light decreases, accompanied by the emission and metallic shell episodes, the first one being discussed in detail by Harmanec et al. (1978). It is a very good example of an inverse correlation between the brightness and emission-line strength (see Fig. 26). It is also seen that there is a slight secular brightness decrease at the light maxima over the whole interval of Hvar observations on the LTCV time scale. There are almost no secular colour changes in $B-V$ but very


Fig. 15: The *UBV* time variations of V744 Her.

Fig. 16: The *UBV* time variations of CX Dra.

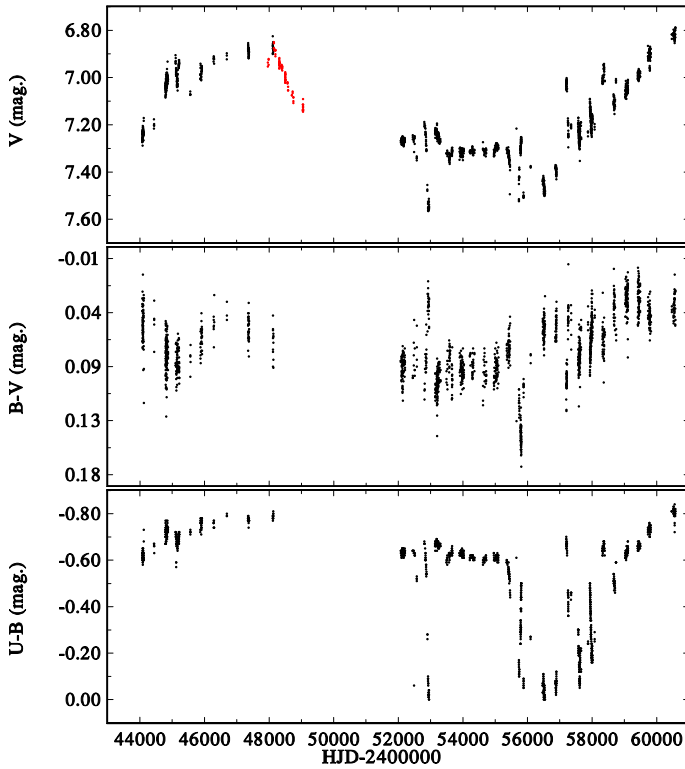
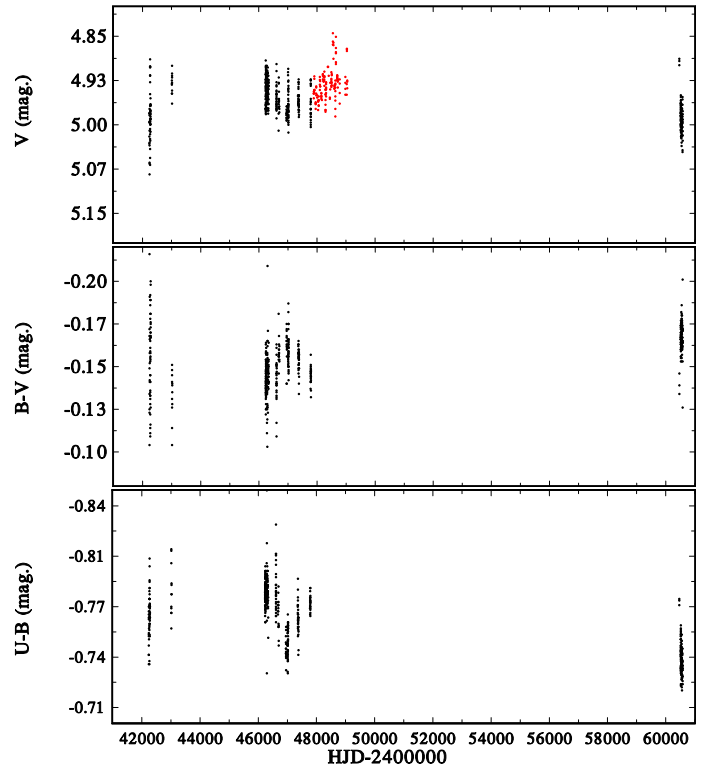
pronounced ones in $U-B$. The secondary star is probably a hot and small object but it has never been directly observed (see, e.g. Wang et al. 2018).

CX Dra = HD 174237 This object is now known as a B2e+F5III semi-detached binary with a 6^d696 period seen under an intermediate inclination of the orbit – see the RV studies by Koubský (1976, 1978); Horn et al. (1992); Richards et al. (2000), and references therein. The light and colour variations show cyclic changes correlated with the variations of the strength of the $H\alpha$ emission on a time scale of several hundred days, showing a positive correlation (Koubský et al. 1980, 1998). In addition to that, there are low-amplitude phase-locked light changes with rather unusual properties – see Fig. 3 in Koubský et al. (1998). The lower envelope of these changes is reminiscent of ellipticity and reflection in the undisturbed state, but frequent brightenings are seen. We show the complete light and colour changes recorded at Hvar in Fig. 16.

V923 Aql = HD 183656 This Be star was found to be the primary component of a 214^d7 binary by Koubský et al. (1989). Its very detailed study, based on all available spectral and photometric observations over many decades was published by Wolf et al. (2021). They documented its long-term, orbital, and rapid variations. The object is a typical example of the inverse correlation between the brightness and emission-line strength. Although it exhibits large-amplitude cyclic RV and V/R variations with cycle lengths between about 1800, and 3000 days in RV, V/R , V magnitude, and $U-B$ index, its $B-V$ index remains secularly stable and close to zero. Rapid changes, if periodic, may follow a 0^d8442 period. In Fig. 17 we show the time plot of Hvar photometry, extended a bit for more recent observations. No evidence of changes on the longest LTCV time scale is seen.


Fig. 17: The *UBV* time variations of V923 Aql.

V1294 Aql = HD 184279 This is one of the Be stars with the largest recorded range of light variations. Its amazing and complicated spectral, light and colour variations were recently described in detail in the study by Harmanec et al. (2022), who discovered that the object is also a spectroscopic binary with a

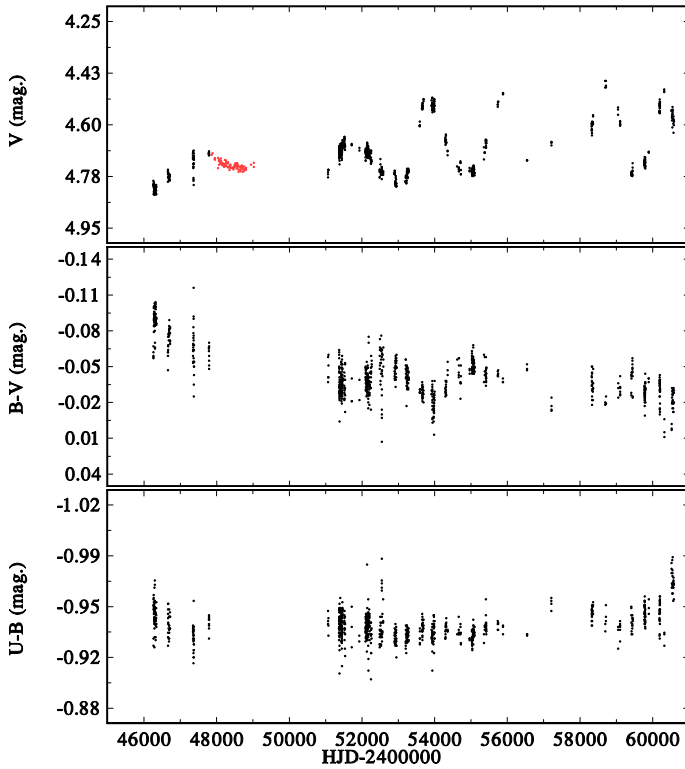
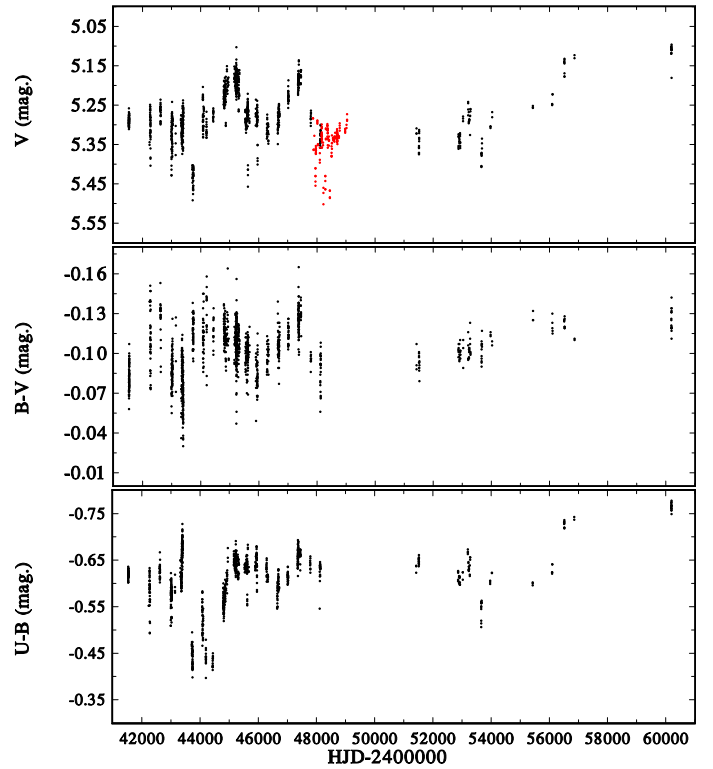
Fig. 18: The *UBV* time variations of V1294 Aql.Fig. 19: The *UBV* time variations of V1624 Cyg.

192^d9 period. The readers are referred to this study. Here we only show the extended series of photometric observations from Hvar in Fig. 18. It is seen that the brightness of the object is still rising and is maximal throughout the recorded history.

V1624 Cyg = 28 Cyg = HD 191610 This Be star is well known for its pronounced rapid photometric variations (Percy & Lane 1977; Mills et al. 1979; Pavlovski & Ružić 1990; Pavlovski et al. 1997, for instance). Baade et al. (2018) analyzed long strings of photometry from the BRITe and SMEI satellites in relation to the long-term variations of the strength of the H α emission. They identified a number of rapid periods ranging from 0^d318 to 0^d759, some of them being combinations of others, and also a period of 19^d634 with the largest amplitude, seen in both, SMEI and BRITe data. They advocated the hypothesis that the coupled non-radial pulsations are connected to mass transfer from the stellar photosphere to the Be star disk. Wang et al. (2018) tried to detect new hot subdwarf companions to Be stars in the IUE spectra. For V1624 Cyg they tabulated RVs for 25 spectra. Wang et al. (2021) investigated far-UV spectra from the Imaging Spectrograph of the Hubble Space Telescope (HST/STIS) and were unable to find any lines of the secondary. Klement et al. (2022b) observed the object interferometrically with the CHARA array and tentatively suggested an orbit with a 246 d period. Later, Klement et al. (2024) concluded from extended interferometry covering about half of the orbital period that the binary has a circular orbit with a 359^d260 period and orbital inclination of 119° (i.e. 61°). Using RVs from Wang et al. (2018) and Wang et al. (2021) papers and the probable distance to the system, they estimated the masses of both stars. Sigut & Ghafourian (2023) obtained the inclination of the Be disk from H α emission profile fitting as 40° ± 5°, and 69° ± 17° from the gravity darkening. It is therefore possible that the disk lies in the orbital plane of the binary. Harmanec et al. (2025) confirmed the orbital period of 359^d26 from the analysis of RVs de-

rived from historical and new electronic spectra and documented the long-term changes, showing that the object never lost the Balmer emission during its recorded history. Hvar photometry is shown in Fig. 19. The variations are dominated by rapid changes. There are obviously also changes on longer time scales, but our limited set of observations does not allow us to draw any firm conclusions about their character.

V832 Cyg = 59 Cyg = HD 200120 This object is the brightest component A of the multiple visual system ADS 14526, with rather distant fainter components B, C, D, and E. Already Harmanec (1982) speculated that – at that time already known – spectral variations and appearance of shell phases of V832 Cyg could be related to the presence of as yet unknown close visual companion. McAlister et al. (1984) indeed discovered such a companion Ab and its orbital variations have been monitored since then. Mason published a preliminary orbit of the Aa-Ab pair with an orbital period of 161.5 yr and eccentricity of 0.261 in Information Circular 175 of the IAU Comm. 26, but no details were given. Tarasov & Tuominen (1987) discovered radial-velocity (RV) and V/R variations of the H α emission with a 29^d14 period, which they interpreted as evidence that the object is a spectroscopic binary. Harmanec et al. (2002) carried out a detailed study of this Be star, based on spectral and photometric observations from several observatories. They indeed confirmed that V832 Cyg is a spectroscopic binary with a 28^d1971 period and argued that the true orbital RV amplitude is best defined by the RVs measured on the steep emission wings of the H α line profile. This was nicely confirmed by the study of Peters et al. (2013), who derived the RV curves of both binary components from the far-UV spectra and proved that the secondary is a hot O type subdwarf. Harmanec et al. (2002) also documented long-term light and colour changes with a positive correlation between the light and emission-line strength combined with changes


Fig. 20: The *UBV* time variations of V832 Cyg.

Fig. 21: The *UBV* time variations of EW Lac.

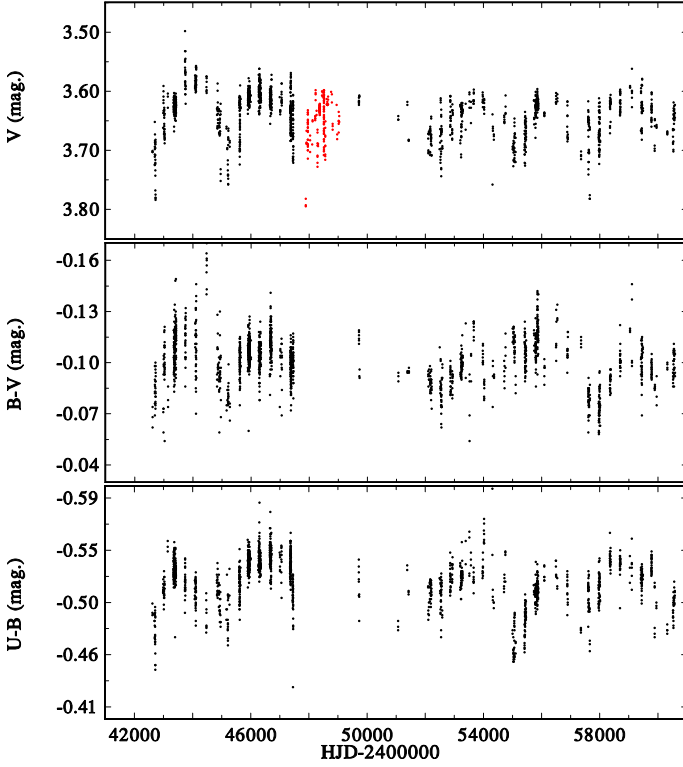
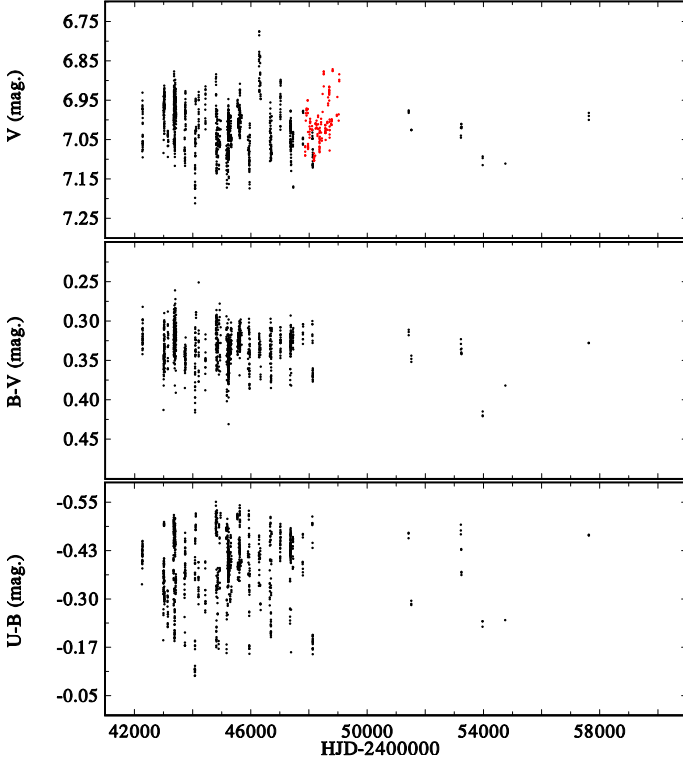
probably attributable to one-arm disk oscillation. Prewhitening photometry for these long-term changes, they found mild, but well-defined sinusoidal light changes phase-locked with the orbital period. The long-term brightness and colour variations of V832 Cyg extended to the present time are shown in Fig. 20. One can see a steady increase in brightness throughout the time interval covered by the *UBV* observations, attributable to the variability on the **LTCV** time scale.

EW Lac = HD 217050 This is a very active Be star, worth of a detailed and complex study. It has been studied for about 100 years. Its Balmer emission was variable until 1926. Then a strong emission with sharp shell lines visible over the whole Balmer series has developed and remained stable until 1977, when the star became active again (see, e.g. Harmanec et al. 1979). These authors also showed that the star is a classical example of the positive correlation between the brightness and emission-line strength. Stagg et al. (1988) summarised the history of its photometric studies and suggested a period of 0^d72, close to timescales detected in previous studies, but with a light curve variable with time. The spectra from the BeSS database (Neiner et al. 2011) show that the emission gradually weakened and is virtually missing since 2022. Complete Hvar photometry shown in Fig. 21 indicates that the star is an example of variability on the **LTCV** time scale, with secular brightness increase. This is even better documented in Fig. 13 of Harmanec et al. (2022), where also earlier photometry prior to start of Hvar observations is included. It is also seen that the amplitude of rapid variations has decreased as the star was gradually losing the Balmer emission.

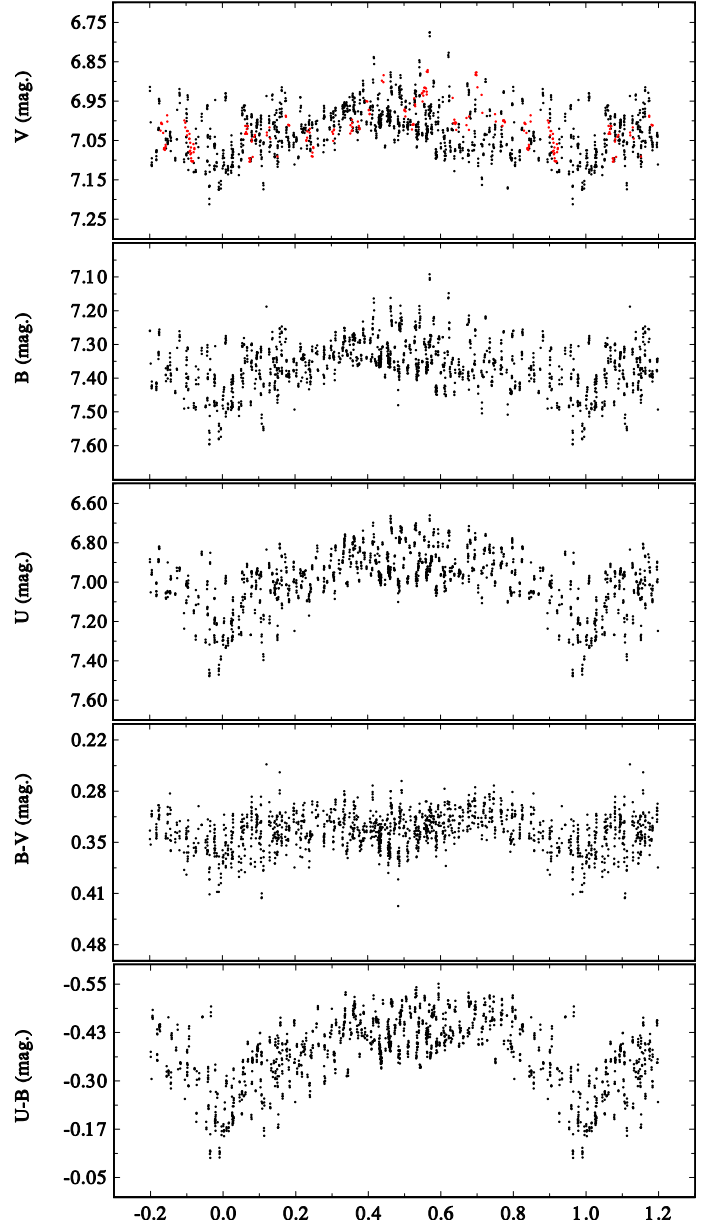
o And = HD 217675 = HR 8762 This is a remarkable Be star, for which rapid photometric variability was discovered already during World War I, based on photoelectric observations published by Guthnick & Prager (1918). Later, Guthnick (1941)

reported a 1^d5765 period of light variations and the star was long considered to be a close contact binary (see Harmanec 1983, for the whole early history of the search for the true period of its changes). Later, it was found that *o* And is a multiple system, containing a double-lined spectroscopic binary with a 33^d085 period, moving in a wide orbit with the Be star, which dominates the optical spectrum (Hill et al. 1988; Harmanec et al. 1987a). In addition to, the object has two speckle-interferometric companions. So far very uncertain closer orbit has a possible period of 5.6 yr, defined by only five observations, and the outer AB orbit has a period of 118.0 yr (Zhuchkov et al. 2010; Mitrofanova et al. 2021). The object exhibits rapid light variations with a period of 1^d571272 and a variable shape of the light curve (Harmanec 1984a; Harmanec et al. 1987b; Stagg et al. 1988) and superimposed cyclic variation with a regular cycle length over 2500 d (8.5 yr). Harmanec (1984a) suggested it could be related to a visual binary discovered by Wilson (1950) and causing recurrent shell phases. Hvar photometry plotted in Fig. 22 shows regular cyclic changes with a possible period of 2525 d.

KX And = HD 218393 The light variability of this object was discovered from Hvar photometry (Harmanec et al. 1977b). A large spectroscopic and photometric study, based also on Hvar photometry, was published by Štefl et al. (1990). These authors found periodic RV, light and colour variations with a 38^d919 period and suggested tentatively that the object could be an interacting binary. Floquet et al. (1995) and Tarasov et al. (1998) obtained a clear circular-orbit period based on the sharp lines of G8II secondary component, with a semiamplitude of 86 km s⁻¹, proving thus definitively the binary nature of the object. Stagg et al. (1988) and Pavlovski & Ružić (1989), who used also Hvar photometry, reported possible short periods of 0^d476 and 0^d353, respectively, after the removal of orbital changes.

Fig. 22: The *UBV* time variations of *o* And.Fig. 23: The *UBV* time variations of KX And.

Such a removal is not straightforward, however, since there are cycle-to-cycle changes in the orbital light curve. Complete Hvar photometry is in Fig. 23. No secular changes are seen. The orbital light curves are in Fig. 24.

Fig. 24: The 38^d919 orbital light curve of KX And based on Hvar (black) and transformed Hipparcos H_p (red) observations.

5. Discussion

Our systematic observational effort and monitoring of a representative sample of fifty nine bright early-type emission-line stars from the Northern Hemisphere (down to declinations of about -20°) helped to realize that virtually all Be stars are light and colour variables and to the recognition of their characteristic timescales. With the exception of several dedicated observational campaigns, our photometry is more suited to the detection of changes on long time scales.

The cases of objects like β Lyr or V1507 Cyg show how the duplicity or multiplicity of individual emission-line objects can lead to a large variety of observational effects. In particular, the Roche-lobe filling brighter but usually less massive secondaries in the binaries with large-scale mass transfer can have spectra, which closely mimic the supergiant or bright giant spectral classification but have masses significantly lower than $10 M_\odot$.

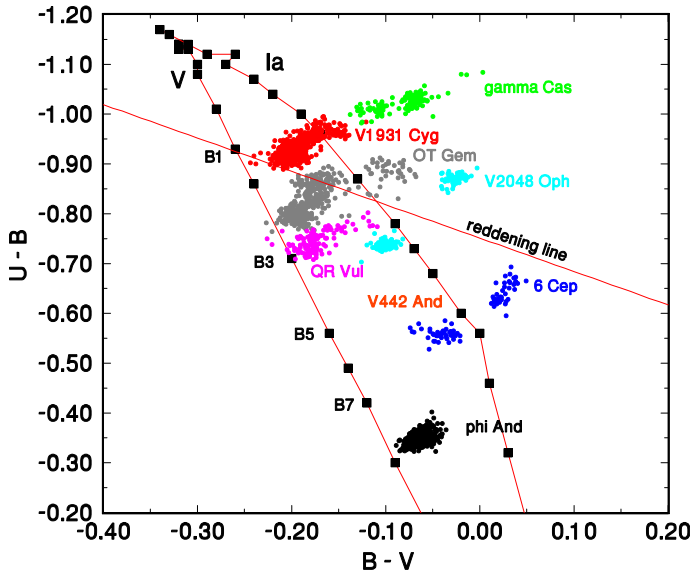


Fig. 25: The $U-B$ versus $B-V$ diagram for several Be stars with a positive correlation between the brightness and emission-line strength. Also shown are the reddening line and the photometric sequences corresponding to the main sequence stars (V) and to bright supergiants (Ia) (adopted from Golay 1974).

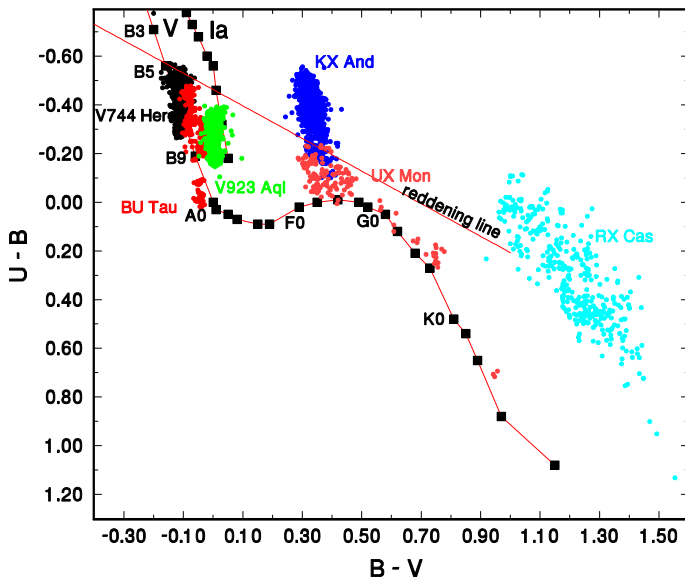


Fig. 26: The $U-B$ versus $B-V$ diagram for several Be stars with an inverse correlation between the brightness and emission-line strength. The same notation as in Fig. 25 is used.

In Table 1 binary stars with known orbits are identified by their orbital period, eccentricity and source of the binary orbit. We note that the confirmed binaries represent only about one third of the whole sample of 106 objects. It is also notable that the vast majority of known binaries with the Be primary has circular orbits. This seems to indicate that these systems have undergone large scale mass transfer sometimes in their evolution, which helped to circularize their orbits. For V1507 Cyg, which has an eccentric orbit, Davidge (2023) argued that the eccentricity was caused by a third body in the system. This could also be the case of BU Tau, a member of the Pleiades cluster, where the encounter with another body

seems quite probable. Also the two other objects with probably eccentric orbits, V832 Cyg, and V1931 Cyg, are member of a relatively close visual systems WDS J20598+4731, and WDS J21012+4609, respectively.

Our sample indicates that the least variable Be stars are found among objects with spectral types later than B5. Shokry et al. (2018) – who studied a different sample of Be stars – arrived at a similar conclusion. However, this is not a general rule. Objects like V839 Her, V744 Her or BU Tau actually show large secular changes. That might be related to the fact that all of them are known binaries.

In Table 3, the variability patterns found for more frequently observed hot emission-line objects are summarised. Although rich, our sample is not numerous enough for truly statistical evaluation. However, some preliminary conclusions can be drawn.

First, it is seen that rapid variability is observed for the vast majority of cases. There are, however, notable exceptions, such as 17 Tau, which was found to be constant on shorter time scales on the level of accuracy of good ground-based photometries. Yet, even this object seems to be variable on sub-millimag level provided by TESS space photometry.

The existence of variations on the very long LTCV time scale was probably detected in twelve cases. In eight cases a slow secular decrease of brightness is found, while the slow increase is seen in only four cases. The existence of this type of variability implies that it might not be reliable to estimate the true stellar radius from the dereddened V magnitude, bolometric correction and measured parallax since even the observed V magnitude outside the emission-line episodes varies with time and probably refers to the remaining stellar pseudo-photosphere.

We note that in some cases of secular changes, the amplitude of variations in the $B-V$ index is larger than that in $U-B$, while in other objects it is just the opposite.

We also want to point out that the models of Be star disks should not be based only on satellite photometries with their very broad passbands. Cases of stars like V744 Her, V1294 Aql or BU Tau show that the variations in the yellow, blue, and ultraviolet parts of the stellar spectrum can be quite different, and these differences are inevitably affecting the variability patterns recorded with the very broad passbands of the MOST (Walker et al. 2003), TESS (Ricker et al. 2015), and largely also BRITe (Weiss et al. 2014) satellites.

LTEM variability was detected in about a half of all monitored objects. From these, about 34 % cent showed the positive correlation between the brightness and emission-line strength, and only 10 % showed the inverse correlation. In two cases, alternation between the two types of correlation was found.

In Figures 25 and 26 we show examples of positive and inverse correlations between brightness and Balmer-line emission strength as defined in Sect. 3. We note that besides the basic type, the inverse correlation is also observed on the time scale of binary orbital motion for binaries observed not far from the equator-on configuration. This is obviously due to varying projection effects of circumstellar matter as these binaries revolve around each other. This is the case of KX And, UX Mon or RX Cas in Fig. 26.

6. Data availability

As soon as this paper will be published, we shall make the complete all-sky and differential archives publicly available, together with lists of all stars observed at Hvar and the

Table 3: Types of variations, as defined in Sect. 3, of 59 hot emission-line objects more frequently observed at Hvar

Star	HD/BD	No.	LTEM	LTCV	MTBIN	VLTV	RAV
<i>o</i> Cas	4180	895	p	?	EL	no	yes
γ Cas	5394	137	p	yes	?	inc	yes
V442 And	6226	964	p	no	no	no	yes
φ And	6811	504	no	no?	no	dec	?
φ Per	10516	678	p	yes	yes	dec	yes
V554 Per	14818	146	no	yes	no	no	yes
HR 894	18552	118	no	no	no	no	yes?
RX Cas	+67 244	361	no	no	EB	no	no?
13 Tau	23016	114	no	no	no	no	no?
17 Tau	23302	367	no	yes	no	no	no
V971 Tau	23480	265	no	yes	no	no	yes
η Tau	23630	205	no	yes	no	no?	no
BU Tau	23862	469	i	no	no	no	no
V960 Tau	36576	392	p	yes	no	no	yes
ζ Tau	37202	1100	p+i	yes	yes	no	yes
ω Ori	37490	90	p	no	no	no	yes
V731 Tau	37967	107	no	no	no	no	yes
V696 Mon	41335	318	no	no	no	dec	no?
HR 2418	47054	63	no	no	no	dec?	yes
OT Gem	58050	437	p	no	no	no	yes
β CMi	58715	168	no	no	no	no	yes
BR CMi	61273	103	no	no	EL	no	no
UX Mon	65607	152	no	no	EB	no	yes
HD 81357	81357	93	no	no	EL	no	no
κ Dra	109387	429	p	no	no	dec	yes
θ CrB	138749	158	no	no	no	no	yes
V839 Her	142926	685	i	no	yes	no	no
δ Sco	143275	98	p	no	no	inc?	no?
ζ Oph	149757	168	p	no	no	no	yes
V744 Her	162732	1449	i	no	no	dec	no
V2048 Oph	164284	164	p	no	no	dec	yes
V974 Her	164447	183	p	no	no	no	no?
<i>o</i> Her	166014	182	no	no	no	no	yes
NW Ser	168797	327	no	no	no	no	yes
CX Dra	174237	1167	p	no	yes	no	yes
β Lyr	174638	544	no	yes	EB	no	yes
7 Vul	183537	131	p	no	no	no	yes
V923 Aql	183656	1620	i	yes	no	no	yes
V1294 Aql	184279	1709	p+i	yes	yes	dec	yes
V1507 Cyg	187399	193	no	no	yes	no	no
V1746 Cyg	189687	209	i?	no	no	no	yes
V1624 Cyg	191610	510	p	no	?	no	yes
20 Vul	192044	130	no	no	no	no	yes?
QR Vul	192685	191	p	no	no	no	yes
P Cyg	193237	122	no	no	no	no	yes
25 Vul	193911	124	?	no	no	no	yes
V2119 Cyg	194335	140	?	no	no	no	yes
HR 7843	195554	161	i?	no	no	no	yes
V1661 Cyg	198478	288	no	no	no	no	yes
V832 Cyg	200120	849	p	yes	yes	inc	no?
V1931 Cyg	200310	889	p	no	no	no	yes
8 Lac A	214168	151	no	no	no	no	yes
V360 Lac	216200	424	no	yes	EL	no	yes
EW Lac	217050	1281	p	no	no	inc	yes
V378 And	217543	267	p	no	no	no	yes
<i>o</i> And	217675	1636	no	yes	no	no	yes
KX And	218393	1210	no	no	yes	no	yes
KY And	218674	970	no	no	no	no	yes
LQ And	224559	590	no	no	no	no	yes

Notes. Column LTEM: p = positive correlation between the brightness and emission-line strength, i = inverse correlation between the brightness and emission-line strength; column MTBIN: EB = eclipsing binary, EL = ellipsoidal variations, yes denotes either mild sinusoidal variation with the known orbital period or some peculiar orbital changes; column VLTV: dec = slow secular decrease of brightness during phases of quiescence, inc = slow secular increase of brightness during phases of quiescence.

instructions how to extract the individual observations or suitably chosen normals points for individual stars at <https://astro.troja.mff.cuni.cz/projects/hvar50/>. A mirror image will also be provided on a server of the Faculty of Geodesy of Zagreb University.

The potential users of these revised Hvar observations should credit this paper in their future publications.

Acknowledgements. H. Božić acknowledges financial support from Croatian Science Foundation under the project 6212 “Solar and Stellar Variability”. P. Harmanec, M. Wolf, M. Brož, A. Oplištilová, J. Jonák, and K. Vitovský were supported by grant GA19-01995S of the Czech Science Foundation. Research

of P. Hadrava was supported by project RVO 67985815. Our colleagues J. Grygar and K. Pavlovski were associated with the whole program and carried out a number of observations. Moreover, K. Pavlovski helped us to check and correct some of his observations. A large number of observations have also been secured by J. Nemravová-Benešová. These three colleagues informed us that they do not want to be listed among the co-authors, which we have to respect. We credit them for their significant contributions. Our thanks go to our colleagues and students A. Arena, J. Arsenijević, R. Brajša, R. Brož, P. Chadima, D. Čikotić, E. Frlež, K. Hoňková, Z. Ivanović, Ž. Ivezić, J. Janík, J. Juryšek, B. Jovanović, G. Lazin, M. Malarić, A. Mulić, M. Muminović, M. Netopil, D. Ondřích, D. Plačko-Vršnak, P. Polechová, Ž. Ružić, I. Vince, B. Vršnak, and M. Zejda who obtained some Hvar observations reported here and are not included among the co-authors. Our special thanks go to J. Vacek for his design, maintenance and regular servicing of the Hvar photoelectric photometer. J.R. Percy kindly put the archive of his *UBV* observations of bright Be stars at our disposal. **Detailed comments of the referee, Dietrich Baade, helped us to re-think and restructure different parts of this study.** The following internet-based resources were consulted: the SIMBAD database and the VizieR service operated at CDS, Strasbourg, France; and the NASA's Astrophysics Data System Bibliographic Services.

References

- Abt, H. A., Barnes, R. C., Biggs, E. S., & Osmer, P. S. 1965, *ApJ*, 142, 1604
- Ak, H., Chadima, P., Harmanec, P., et al. 2007, *A&A*, 463, 233
- Alvarez, M. & Schuster, W. J. 1981, *Rev. Mexicana Astron. Astrofis.*, 6, 163
- Andersen, J., Pavlovski, K., & Pirola, V. 1989, *A&A*, 215, 272
- Baade, D. 1982, *A&A*, 105, 65
- Baade, D., Pigulski, A., Rivinius, T., et al. 2018, *A&A*, 610, A70
- Baade, D., Rivinius, T., Pigulski, A., Carciofi, A., & BRITE Executive Science Team. 2017, in *IAU Symposium*, Vol. 329, *The Lives and Death-Throes of Massive Stars*, ed. J. J. Eldridge, J. C. Bray, L. A. S. McClelland, & L. Xiao, 384–384
- Ballereau, D. & Chauville, J. 1989, *A&A*, 214, 285
- Balona, L. A., Aerts, C., Božić, H., et al. 2001, *MNRAS*, 327, 1288
- Balona, L. A. & Engelbrecht, C. A. 1986, *MNRAS*, 219, 131
- Balona, L. A. & Ozuyar, D. 2021, *ApJ*, 921, 5
- Barnsley, R. M. & Steele, I. A. 2013, *A&A*, 556, A81
- Bedding, T. R. 1993, *AJ*, 106, 768
- Bemporad, A. 1904, *Mitteil. Grossherzog. Sternwarte Heidelberg*, 4, 1
- Bergin, E. A., Burns, J. F., Guinan, E. F., & McCook, G. P. 1989, *Information Bulletin on Variable Stars*, 3358, 1
- Bolton, C. T. 1982, in *IAU Symposium*, Vol. 98, *Be Stars*, ed. M. Jасhek & H. G. Groth, 181–184
- Bordé, P., Rouan, D., & Léger, A. 2003, *A&A*, 405, 1137
- Borre, C. C., Baade, D., Pigulski, A., et al. 2020, *A&A*, 635, A140
- Boubert, D. & Evans, N. W. 2018, *MNRAS*, 477, 5261
- Božić, H., Ruždjak, D., & Sudar, D. 1999, *A&A*, 350, 566
- Božić, H. & Harmanec, P. 1998, *A&A*, 330, 222
- Božić, H., Harmanec, P., Horn, J., et al. 1995, *A&A*, 304, 235
- Božić, H., Harmanec, P., & Koubský, P. 2013a, *Central European Astrophysical Bulletin*, 37, 9
- Božić, H., Harmanec, P., & Koubský, P. 2013b, *Central European Astrophysical Bulletin*, 37, 9
- Božić, H., Harmanec, P., Yang, S., et al. 2004, *A&A*, 416, 669
- Božić, H., Muminović, M., Pavlovski, K., et al. 1982, *Information Bulletin on Variable Stars*, 2123, 1
- Božić, H. & Pavlovski, K. 1988, *Hvar Observatory Bulletin*, 12, 15
- Breger, H., Wolf, M., Harmanec, P., et al. 2007, *A&A*, 464, 263
- Breger, M. 1972, *ApJ*, 176, 367
- Brož, M., Mourard, D., Budaj, J., et al. 2021, *A&A*, 645, A51
- Burki, G., Rufener, F., Burnet, M., et al. 1995, *A&AS*, 112, 383
- Carciofi, A. C. 2011, in *IAU Symposium*, Vol. 272, *Active OB Stars: Structure, Evolution, Mass Loss, and Critical Limits*, ed. C. Neiner, G. Wade, G. Meynet, & G. Peters, 325–336
- Carciofi, A. C., Bjorkman, J. E., Otero, S. A., et al. 2012, *ApJ*, 744, L15
- Carciofi, A. C., Okazaki, A. T., Le Bouquin, J. B., et al. 2009, *A&A*, 504, 915
- Chadima, P., Harmanec, P., Bennett, P. D., et al. 2011, *A&A*, 530, A146
- Copeland, J. A. & Heard, J. F. 1963, *Publications of the David Dunlap Observatory*, 2, 317
- Cote, J. & van Kerkwijk, M. H. 1993, *A&A*, 274, 870
- Cousins, A. W. J. & Jones, D. H. P. 1976, *MmRAS*, 81, 1
- Davidge, T. J. 2023, *AJ*, 166, 188
- Delplace, A. M. 1970, *A&A*, 7, 68
- Doazan, V., Harmanec, P., Koubský, P., Krpata, J., & Žďárský, F. 1982a, *A&A*, 115, 138
- Doazan, V., Harmanec, P., Koubský, P., Krpata, J., & Žďárský, F. 1982b, *A&AS*, 50, 481
- Dorren, J. D., Fu, H. H., & Wu, H. H. 1984, *Information Bulletin on Variable Stars*, 2521, 1
- Dufton, P. L., Lennon, D. J., Villaseñor, J. I., et al. 2022, *MNRAS*, 512, 3331
- Dulaney, N. A., Richardson, N. D., Gerhartz, C. J., et al. 2017, *ApJ*, 836, 112
- Ebbets, D. 1981, *PASP*, 93, 119
- Elliott, A., Richardson, N. D., Pablo, H., et al. 2022, *MNRAS*, 509, 4246
- Floquet, M., Hubert, A. M., Hubert, H., Ballereau, D., & Chauville, J. 1995, *A&A*, 294, 227
- Floquet, M., Hubert, A. M., Maillard, J. P., Chauville, J., & Chatzichristou, H. 1989, *A&A*, 214, 295
- Gaposchkin, S. 1944, *ApJ*, 100, 230
- Ghoreyshi, M. R., Carciofi, A. C., Jones, C. E., et al. 2021, *ApJ*, 909, 149
- Ghoreyshi, M. R., Jones, C. E., & Granada, A. 2023, *MNRAS*, 518, 30
- Gies, D. R., Bagnuolo, William G., J., Ferrara, E. C., et al. 1998, *ApJ*, 493, 440
- Gies, D. R., McKibben, W. P., Kelton, P. W., Opal, C. B., & Sawyer, S. 1990, *AJ*, 100, 1601
- Gies, D. R., Wang, L., & Klement, R. 2023, *ApJ*, 942, L6
- Gies, D. R., Willis, C. Y., Penny, L. R., & McDavid, D. 1993, *PASP*, 105, 281
- Golay, M. 1974, in *Astrophysics and Space Science Library*, Dordrecht: Reidel, Vol. 41, *Introduction to astronomical photometry*
- Grundstrom, E. D. 2007, PhD thesis, Georgia State University
- Guinan, E. F. & Hayes, D. P. 1984, *ApJ*, 287, L39
- Guthnick, P. 1941, *Vierteljahrsschrift Astron. Gesell.*, 76
- Guthnick, P. & Prager, R. 1918, *Veröff. Berlin Babelsberg*, 2, 113
- Harmanec, P. 1980, *Be Star Newsletter*, 1, 2
- Harmanec, P. 1982, in *Be Stars*, ed. M. Jасhek & H. G. Groth, Vol. 98, 279–297
- Harmanec, P. 1983, *Hvar Observatory Bulletin*, 7, 55
- Harmanec, P. 1984a, *Information Bulletin on Variable Stars*, 2506, 1
- Harmanec, P. 1984b, *Bulletin of the Astronomical Institutes of Czechoslovakia*, 35, 193
- Harmanec, P. 1987, *Bulletin of the Astronomical Institutes of Czechoslovakia*, 38, 283
- Harmanec, P. 1989, *Bulletin of the Astronomical Institutes of Czechoslovakia*, 40, 201
- Harmanec, P. 1994, in *NATO Advanced Study Institute (ASI) Series C*, Vol. 436, *The Impact of Long-Term Monitoring on Variable Star Research: Astrophysics*, ed. C. Sterken & M. de Groot, 55
- Harmanec, P. 1998a, *A&A*, 335, 173
- Harmanec, P. 1998b, *A&A*, 334, 558
- Harmanec, P. 1999, *A&A*, 341, 867
- Harmanec, P. 2000, in *Astronomical Society of the Pacific Conference Series*, Vol. 214, *IAU Colloq. 175: The Be Phenomenon in Early-Type Stars*, ed. M. A. Smith, H. F. Henrichs, & J. Fabregat, 13
- Harmanec, P. 2001, *Publications of the Astronomical Institute of the Czechoslovak Academy of Sciences*, 89, 9
- Harmanec, P. 2002, *Astronomische Nachrichten*, 323, 87
- Harmanec, P. & Božić, H. 2013, *Central European Astrophysical Bulletin*, 37, 3
- Harmanec, P., Božić, H., Koubský, P., et al. 2022, *A&A*, 666, A136
- Harmanec, P., Božić, H., Percy, J. R., et al. 2002, *A&A*, 387, 580
- Harmanec, P., Grygar, J., Horn, J., et al. 1977a, *Bulletin of the Astronomical Institutes of Czechoslovakia*, 28, 133
- Harmanec, P., Habuda, P., Štefl, S., et al. 2000, *A&A*, 364, L85
- Harmanec, P., Hill, G. M., Walker, G. A. H., Dinshaw, N., & Yang, S. 1987a, *Publications of the Astronomical Institute of the Czechoslovak Academy of Sciences*, 5, 115
- Harmanec, P., Horn, J., & Juza, K. 1994, *A&AS*, 104, 121
- Harmanec, P., Horn, J., & Koubský, P. 1980a, *Be Star Newsletter*, 2, 3
- Harmanec, P., Horn, J., & Koubský, P. 1982, in *Be Stars*, ed. M. Jасhek & H. G. Groth, Vol. 98, 269
- Harmanec, P., Horn, J., Koubský, P., et al. 1977b, *Information Bulletin on Variable Stars*, 1324, 1
- Harmanec, P., Horn, J., Koubský, P., et al. 1978, *Bulletin of the Astronomical Institutes of Czechoslovakia*, 29, 278
- Harmanec, P., Horn, J., Koubský, P., et al. 1979, *Information Bulletin on Variable Stars*, 1555, 1
- Harmanec, P., Horn, J., Koubský, P., et al. 1980b, *Bulletin of the Astronomical Institutes of Czechoslovakia*, 31, 144
- Harmanec, P., Horn, J., Koubský, P., et al. 1983, *Information Bulletin on Variable Stars*, 2447, 1
- Harmanec, P., Koubský, P., Horn, J., & Havelka, J. 1973a, *Bulletin of the Astronomical Institutes of Czechoslovakia*, 24, 311
- Harmanec, P., Koubský, P., & Krpata, J. 1972a, *Bulletin of the Astronomical Institutes of Czechoslovakia*, 23, 218
- Harmanec, P., Koubský, P., & Krpata, J. 1972b, *Astrophys. Lett.*, 11, 119
- Harmanec, P., Koubský, P., & Krpata, J. 1973b, *A&A*, 22, 337
- Harmanec, P., Koubský, P., & Krpata, J. 1974, *A&A*, 33, 117
- Harmanec, P., Koubský, P., Krpata, J., & Žďárský, F. 1976, *Bulletin of the Astronomical Institutes of Czechoslovakia*, 27, 47
- Harmanec, P., Koubský, P., Nemravová, J. A., et al. 2015, *A&A*, 573, A107

- Harmanec, P. & Kříž, S. 1976, in *Be and Shell Stars*, ed. A. Slettebak, Vol. 70, 385
- 1140 Harmanec, P., Lipták, J., Koubský, P., et al. 2020, *A&A*, 639, A32
- Harmanec, P., Matthews, J. M., Božić, H., et al. 1991, *Bulletin of the Astronomical Institutes of Czechoslovakia*, 42, 1
- Harmanec, P., Morand, F., Bonneau, D., et al. 1996, *A&A*, 312, 879
- Harmanec, P., Olah, K., Božić, H., et al. 1987b, in *IAU Colloq. 92: Physics of Be Stars*, ed. A. Slettebak & T. P. Snow, 456
- Harmanec, P., Pavlovski, K., Božić, H., et al. 1997, *Journal of Astronomical Data*, 3, 5
- Harmanec, P., Švanda, M., Korčáková, D., et al. 2019, *ApJ*, 875, 13
- Harmanec, P., Yang, S., Koubský, P., et al. 2025, *A&A*, 699, A321
- 1150 Heard, J. F., Hurkens, R., Harmanec, P., Koubský, P., & Krpata, J. 1975, *A&A*, 42, 47
- Hill, G., Harmanec, P., Pavlovski, K., et al. 1997, *A&A*, 324, 965
- Hill, G., Hilditch, R. W., & Pfannenschmidt, E. L. 1976, *Publications of the Dominion Astrophysical Observatory Victoria*, 15, 1
- Hill, G. M., Walker, G. A. H., Dinshaw, N., Yang, S., & Harmanec, P. 1988, *PASP*, 100, 243
- Hirata, R. 1995, *PASJ*, 47, 195
- Hirata, R. & Kogure, T. 1976, *PASJ*, 28, 509
- Hoffleit, D. & Jaschek, C. 1982, *The Bright Star Catalogue*. Fourth revised edition. (Containing data compiled through 1979).
- 1160 Horn, J., Harmanec, P., Koubský, P., et al. 1982, *Bulletin of the Astronomical Institutes of Czechoslovakia*, 33, 308
- Horn, J., Hubert, A. M., Hubert, H., Koubský, P., & Bailloux, N. 1992, *A&A*, 259, L5
- Hummel, W. & Štefl, S. 2001, *A&A*, 368, 471
- Hutchings, J. B. & Redman, R. O. 1973, *MNRAS*, 163, 209
- Hutter, D. J., Tycner, C., Zavala, R. T., et al. 2021, *ApJS*, 257, 69
- Iliev, L. & Miroshnichenko, A. 2025, *Contributions of the Astronomical Observatory Skalnaté Pleso*, 55, 470
- 1170 Jenkins, J. M., Caldwell, D. A., Chandrasekaran, H., et al. 2010, *ApJ*, 713, L87
- Johnson, H. L. & Harris, D. L. 1954, *ApJ*, 120, 196
- Johnson, H. L., Mitchell, R. I., Iriarte, B., & Wisniewski, W. Z. 1966, *Communications of the Lunar and Planetary Laboratory*, 4, 99
- Johnson, H. L. & Morgan, W. W. 1953, *ApJ*, 117, 313
- Jones, C. E., Tycner, C., & Smith, A. D. 2011, *AJ*, 141, 150
- Jones, C. E., Wiegert, P. A., Tycner, C., et al. 2013, *AJ*, 145, 142
- Juza, K., Harmanec, P., Božić, H., et al. 1994, *A&AS*, 107, 403
- Juza, K., Harmanec, P., Hill, G. M., Tarasov, A. E., & Matthews, J. M. 1991, *Bulletin of the Astronomical Institutes of Czechoslovakia*, 42, 39
- 1180 Katahira, J.-I., Hirata, R., Ito, M., et al. 1996, *PASJ*, 48, 317
- Kato, S. 1983, *PASJ*, 35, 249
- Kazarovets, E. V., Samus, N. N., Durlevich, O. V., et al. 1999, *Information Bulletin on Variable Stars*, 4659, 1
- Klement, R., Baade, D., Rivinius, T., et al. 2022a, *ApJ*, 940, 86
- Klement, R., Rivinius, T., Gies, D. R., et al. 2024, *ApJ*, 962, 70
- Klement, R., Schaefer, G. H., Gies, D. R., et al. 2022b, *ApJ*, 926, 213
- Kochukhov, O., Khalack, V., Kobzar, O., et al. 2021, *MNRAS*, 506, 5328
- Koenigsberger, G. & Estrella-Trujillo, D. 2024, *A&A*, 685, A145
- Koubský, P. 1976, *Information Bulletin on Variable Stars*, 1188, 1
- 1190 Koubský, P. 1978, *Bulletin of the Astronomical Institutes of Czechoslovakia*, 29, 288
- Koubský, P., Harmanec, P., Božić, H., et al. 1998, *Hvar Observatory Bulletin*, 22, 17
- Koubský, P., Harmanec, P., Brož, M., et al. 2019, *A&A*, 629, A105
- Koubský, P., Harmanec, P., Gulliver, A. F., Ballereau, D., & Chauville, J. 1989, *Bulletin of the Astronomical Institutes of Czechoslovakia*, 40, 31
- Koubský, P., Harmanec, P., Horn, J., et al. 1980, *Bulletin of the Astronomical Institutes of Czechoslovakia*, 31, 75
- Koubský, P., Harmanec, P., Hubert, A. M., et al. 2000, *A&A*, 356, 913
- 1200 Koubský, P., Harmanec, P., Kubát, J., et al. 1997, *A&A*, 328, 551
- Koubský, P., Harmanec, P., Yang, S., et al. 2006, *A&A*, 459, 849
- Koubský, P., Hummel, C. A., Harmanec, P., et al. 2010, *A&A*, 517, A24
- Koubský, P. & Pavlovski, K. 1982, *Hvar Observatory Bulletin*, 6, 1
- Krajčeva, Z. T. & Koubský, P. 1983, *Information Bulletin on Variable Stars*, 2313, 1
- Kraus, M., Haucke, M., Cidale, L. S., et al. 2015, *A&A*, 581, A75
- Królowski, J., Strobel, A., Galazutdinov, G. A., Bondar, A., & Valyavin, G. 2019, *MNRAS*, 486, 112
- 1210 Kříž, S., Arsenijević, J., Grygar, J., et al. 1980, *Bulletin of the Astronomical Institutes of Czechoslovakia*, 31, 284
- Kříž, S. & Harmanec, P. 1975, *Bulletin of the Astronomical Institutes of Czechoslovakia*, 26, 65
- Labadie-Bartz, J., Carciofi, A. C., Henrique de Amorim, T., et al. 2022, *AJ*, 163, 226
- Labadie-Bartz, J., Carciofi, A. C., Rubio, A. C., et al. 2025, *A&A*, 699, A82
- Lee, U., Saio, H., & Osaki, Y. 1991, *MNRAS*, 250, 432
- Linnell, A. P., Harmanec, P., Koubský, P., et al. 2006, *A&A*, 455, 1037
- Lockwood, G. W. & Thompson, D. T. 1986, *AJ*, 92, 976
- Matthews, J. M., Harmanec, P., Walker, G. A. H., Yang, S., & Wehlau, W. H. 1991, *MNRAS*, 248, 787
- 1220 Mayer, P. 1976, *Bulletin of the Astronomical Institutes of Czechoslovakia*, 27, 308
- Mayer, P. 1977, *Hvar Observatory Bulletin*, 1, 5
- Mayer, P. 2013, *Central European Astrophysical Bulletin*, 37, 1
- McAlister, H. A., Hartkopf, W. I., Gaston, B. J., Hendry, E. M., & Fekel, F. C. 1984, *ApJS*, 54, 251
- McAlister, H. A., Hartkopf, W. I., Sowell, J. R., Dombrowski, E. G., & Franz, O. G. 1989, *AJ*, 97, 510
- McGill, M. A., Sigut, T. A. A., & Jones, C. E. 2011, *ApJ*, 743, 111
- McNamara, B. J. 1985, *ApJ*, 289, 213
- 1230 McNamara, B. J. 1987, *ApJ*, 312, 778
- Mennickent, R. E., Djurašević, G., Petrović, J., et al. 2022, *A&A*, 666, A51
- Mennickent, R. E., Otero, S., & Kołaczowski, Z. 2016, *MNRAS*, 455, 1728
- Mennickent, R. E., Sterken, C., & Vogt, N. 1997, *A&A*, 326, 1167
- Merrill, P. W. 1949, *ApJ*, 110, 59
- Mikulášek, Z., Harmanec, P., Grygar, J., & Žďárský, F. 1978, *Bulletin of the Astronomical Institutes of Czechoslovakia*, 29, 44
- Mills, J. J., Snedden, S. A., & Spear, G. G. 1979, *PASP*, 91, 614
- Mitrofanova, A., Dyachenko, V., Beskakotov, A., et al. 2021, *AJ*, 162, 156
- Mourard, D., Brož, M., Nemravová, J. A., et al. 2018, *A&A*, 618, A112
- 1240 Mourard, D., Monnier, J. D., Meilland, A., et al. 2015, *A&A*, 577, A51
- Muterspaugh, M. W., Hartkopf, W. I., Lane, B. F., et al. 2010, *AJ*, 140, 1623
- Nazé, Y., Rauw, G., Smith, M. A., & Motch, C. 2022, *MNRAS*, 516, 3366
- Neiner, C., de Batz, B., Cochard, F., et al. 2011, *AJ*, 142, 149
- Nemravová, J., Harmanec, P., Koubský, P., et al. 2012, *A&A*, 537, A59
- Nemravová, J., Harmanec, P., Kubát, J., et al. 2010, *A&A*, 516, A80
- Okazaki, A. T. 1991, *PASJ*, 43, 75
- Okazaki, A. T. 1997, *A&A*, 318, 548
- Oplištilová, A., Brož, M., Hummel, C. A., Harmanec, P., & Barlow, B. 2025, *arXiv e-prints*, arXiv:2507.02276
- 1250 Pavlovski, K. 1979, *A&A*, 76, 362
- Pavlovski, K. & Božić, H. 1982, *Hvar Observatory Bulletin*, 6, 45
- Pavlovski, K., Božić, H., Harmanec, P., Horn, J., & Koubský, P. 1983, *Information Bulletin on Variable Stars*, 2431, 1
- Pavlovski, K., Harmanec, P., Božić, H., et al. 1997, *A&AS*, 125, 75
- Pavlovski, K., Harmanec, P., Horn, J., et al. 1979, *Information Bulletin on Variable Stars*, 1689, 1
- Pavlovski, K. & Ružić, Z. 1988, *A&AS*, 76, 137
- Pavlovski, K. & Ružić, Z. 1989, *Ap&SS*, 152, 35
- Pavlovski, K. & Ružić, Z. 1990, *A&A*, 236, 393
- 1260 Pearce, J. A. & Hill, G. 1975, *Publications of the Dominion Astrophysical Observatory Victoria*, 14, 319
- Percy, J. R. 1982, in *Bulletin of the American Astronomical Society*, Vol. 14, 879
- Percy, J. R. 1983, *AJ*, 88, 427
- Percy, J. R., Harlow, J., Hayhoe, K. A. W., et al. 1997, *PASP*, 109, 1215
- Percy, J. R. & Lane, M. C. 1977, *AJ*, 82, 353
- Percy, J. R., Marinova, M. M., Božić, H., & Harmanec, P. 1999, *A&A*, 348, 553
- Percy, J. R., Napke, A. E., Richer, M. G., et al. 1988, *A&A*, 191, 248
- 1270 Perry, C. L., Olsen, E. H., & Crawford, D. L. 1987, *PASP*, 99, 1184
- Perryman, M. A. C. & ESA. 1997, *The HIPPARCOS and TYCHO catalogues (Astrometric and photometric star catalogues derived from the ESA Hipparcos Space Astrometry Mission. Publisher: Noordwijk, Netherlands: ESA Publications Division, 1997, Series: ESA SP Series 1200)*
- Peters, G. J. 1971, *ApJ*, 163, L107
- Peters, G. J. 1972, *PASP*, 84, 334
- Peters, G. J. 1983, *PASP*, 95, 311
- Peters, G. J., Pewett, T. D., Gies, D. R., Touhami, Y. N., & Grundstrom, E. D. 2013, *ApJ*, 765, 2
- 1280 Peters, G. J., Wang, L., Gies, D. R., & Grundstrom, E. D. 2016, *ApJ*, 828, 47
- Poeckert, R. 1981a, *PASP*, 93, 297
- Poeckert, R. 1981b, *PASP*, 93, 535
- Polidan, R. S. 1976, in *Be and Shell Stars*, ed. A. Slettebak, Vol. 70, 401
- Polis, O. R., Cote, J., Waters, L. B. F. M., & Heise, J. 1991, *A&A*, 241, 419
- Rast, R. G., Jones, C. E., Carciofi, A. C., et al. 2024, *ApJ*, 968, 30
- Reimann, H. G., Ossenkopf, V., & Beyersdorfer, S. 1992, *A&A*, 265, 360
- Richards, M. T., Koubský, P., Simon, V., et al. 2000, *ApJ*, 531, 1003
- Richardson, N. D., Thizy, O., Bjorkman, J. E., et al. 2021, *MNRAS*, 508, 2002
- 1290 Ricker, G. R., Winn, J. N., Vanderspek, R., et al. 2015, *Journal of Astronomical Telescopes, Instruments, and Systems*, 1, 014003
- Rivinius, T., Baade, D., Štefl, S., et al. 1998, *Be Star Newsletter*, 33, 15
- Rivinius, T., Carciofi, A. C., & Martayan, C. 2013, *A&A Rev.*, 21, 69
- Rivinius, T., Klement, R., Chojnowski, S. D., et al. 2025, *A&A*, 694, A172
- Rivinius, T., Štefl, S., & Baade, D. 2006, *A&A*, 459, 137
- Roberts, Lewis C. J., Turner, N. H., & ten Brummelaar, T. A. 2007, *AJ*, 133, 545

- Rubio, A. C., Carciofi, A. C., & Bjorkman, J. E. 2023, in *Two in a Million - The Interplay Between Binaries and Star Clusters*, 42
- Rufener, F. 1986, *A&A*, 165, 275
- 1300 Ruždjak, D., Božić, H., Harmanec, P., et al. 2009, *A&A*, 506, 1319
- Saad, S. M., Kubát, J., Hadrava, P., et al. 2005, *Ap&SS*, 296, 173
- Saad, S. M., Kubát, J., Koubský, P., et al. 2004, *A&A*, 419, 607
- Saad, S. M., Nouh, M. I., Shokry, A., & Zead, I. 2021, *Rev. Mexicana Astron. Astrofis.*, 57, 91
- Sahade, J. & Ferrer, O. E. 1982, *PASP*, 94, 113
- Saio, H., Cameron, C., Kuschnig, R., et al. 2007, *ApJ*, 654, 544
- Sharov, A. S. & Lyutyi, V. M. 1997, *Astronomy Letters*, 23, 93
- Sharov, A. S. & Lyutyj, V. M. 1972, *Peremennye Zvezdy*, 18, 377
- Shokry, A., Rivinius, T., Mehner, A., et al. 2018, *A&A*, 609, A108
- 1310 Sigut, T. A. A. & Ghafourian, N. R. 2023, *ApJ*, 948, 34
- Sigut, T. A. A. & Jones, C. E. 2007, *ApJ*, 668, 481
- Sigut, T. A. A. & Patel, P. 2013, *ApJ*, 765, 41
- Silaj, J., Jones, C. E., Sigut, T. A. A., & Tycner, C. 2014, *ApJ*, 795, 82
- Smith, M. A. & Henry, G. W. 2021, *ApJ*, 915, 13
- Stagg, C. R., Božić, H., Fullerton, A. W., et al. 1988, *MNRAS*, 234, 1021
- Stagg, C. R., Božić, H., Fullerton, A. W., et al. 1985, *JRASC*, 79, 243
- Štefl, S., Harmanec, P., Horn, J., et al. 1990, *BAiCz*, 41, 29
- Sterken, C. 1983, *The Messenger*, 33, 10
- Struve, O. 1931, *ApJ*, 73, 94
- 1320 Struve, O. 1944, *ApJ*, 99, 295
- Sudar, D., Harmanec, P., Lehmann, H., et al. 2011, *A&A*, 528, A146
- Tarasov, A. E., Berdyugina, S. V., & Berdyugin, A. V. 1998, *Astronomy Letters*, 24, 316
- Tarasov, A. E. & Tuominen, I. 1987, *Publications of the Astronomical Institute of the Czechoslovak Academy of Sciences*, 5, 127
- Thaller, M. L., Bagnuolo, William G., J., Gies, D. R., & Penny, L. R. 1995, *ApJ*, 448, 878
- Torres, G. 2020, *ApJ*, 901, 91
- Touhami, Y., Gies, D. R., Schaefer, G. H., et al. 2013, *ApJ*, 768, 128
- 1330 Tycner, C., Ames, A., Zavala, R. T., et al. 2011, *ApJ*, 729, L5
- Štefl, S., Hummel, W., & Rivinius, T. 2000, *A&A*, 358, 208
- Štefl, S., Rivinius, T., Carciofi, A. C., et al. 2009, *A&A*, 504, 929
- Walker, G., Matthews, J., Kuschnig, R., et al. 2003, *PASP*, 115, 1023
- Walker, G. A. H., Kuschnig, R., Matthews, J. M., et al. 2005, *ApJ*, 623, L145
- Walker, G. A. H., Yang, S., & Fahlman, G. G. 1979, *ApJ*, 233, 199
- Wang, L., Gies, D. R., & Peters, G. J. 2018, *ApJ*, 853, 156
- Wang, L., Gies, D. R., Peters, G. J., et al. 2021, *AJ*, 161, 248
- Waters, L. B. F. M., Cote, J., & Pols, O. R. 1991, *A&A*, 250, 437
- Weiss, W. W., Rucinski, S. M., Moffat, A. F. J., et al. 2014, *PASP*, 126, 573
- 1340 Weßmayer, D., Przybilla, N., & Butler, K. 2022, *A&A*, 668, A92
- White, T. R., Pope, B. J. S., Antoci, V., et al. 2017, *MNRAS*, 471, 2882
- Wilson, R. H., J. 1950, *AJ*, 55, 153
- Wolf, M., Harmanec, P., Božić, H., et al. 2021, *A&A*, 647, A97
- Young, A. T., Genet, R. M., Boyd, L. J., et al. 1991, *PASP*, 103, 221
- Zhuchkov, R. Y., Malogolovets, E. V., Kiyeva, O. V., et al. 2010, *Astronomy Reports*, 54, 1134

Appendix A: Details on the history of the photometric program at Hvar

Over the years, there were essentially three principal observing programs: (i) systematic monitoring of bright emission-line (Be) stars, (ii) studies of selected chemically peculiar (CP) stars (e.g. Mikulášek et al. 1978; Pavlovski 1979), and (iii) studies of various interesting binaries (for instance Mayer 1976; Božić et al. 2007; Chadima et al. 2011). In this paper, we present the results of the first program, while the report on the remaining two programs will be the subject of another study.

During the first observing season, we primarily tried to cover a complete light curve of the short-periodic eclipsing binary BR Cyg to demonstrate the good performance of the new instrument, and this result was soon published (Harmanec et al. 1973a). In January 1973, Pavel Mayer obtained a nearly complete light curve of another eclipsing binary, IU Aur, and confirmed his 1971 discovery that the depths of the light-curve minima of this system are secularly changing due to the precession of the binary orbit caused by the presence of a third body in the system (Mayer 1976).

From 1980 to 1986 we were coordinating an international observing campaign, mainly via the Be Star Newsletter, created and for a long time run by M. Jaschek (Harmanec 1980; Harmanec et al. 1980a, 1982). We provided the list of Be stars with the recommended comparisons to interested observers and reported their observations in the issues of the Be Star Newsletters.

Around 1980, the first studies appeared, in which low-amplitude periodic or even multiperiodic light variations of some Be stars were detected (Bolton 1982; Percy 1982, 1983; Harmanec 1984b; Balona & Engelbrecht 1986). Since the typical timescales of such variations were from about 0.3 to 2 d, observations secured at any single observing station suffered from strong aliasing problems. This led us to organise a collaborative observing campaign with the participation of several observers located in very different geographic longitudes all over the globe. The campaign was carried out in 1983 and was quite successful. The preliminary results were reported by Stagg et al. (1985) and the final report was published three years later (Stagg et al. 1988).

Gradually, we have started producing detailed studies of individual, well-observed Be stars of all luminosity classes, which were based not only on Hvar observations but also on the collection of all available homogenised photometric and spectroscopic data from various sources. Such studies were usually carried out in a broad international collaboration. In recent years, we have also profited from the collaboration with the colleagues operating large optical interferometers and from comparisons with theoretical models. This is, for instance, the case of papers like Harmanec et al. (1996); Koubský et al. (1997); Harmanec et al. (2002); Božić et al. (2004); Linnell et al. (2006); Ruždjak et al. (2009); Koubský et al. (2010); Harmanec et al. (2015); Koubský et al. (2019); Wolf et al. (2021); Mourard et al. (2018); Brož et al. (2021) or Harmanec et al. (2022), which are discussed in more detail later, during the discussion of individual well-observed objects.

For curiosity, a complete list of observers who participated in some observations at Hvar and the number of usable differential observations they obtained is given in Table A.1.

Table A.1: A complete list of Hvar observers and the number of usable individual differential observations per observer, which they secured at the Hvar Observatory over the years 1972 – 2024

Name of observer	No. of observations
Hrvoje Božić	46237
Petr Harmanec	9530
Krešimir Pavlovski	8674
Domagoj Ruždjak	5636
Davor Sudar	5259
Jana Nemravová	3945
Václav Kocourek	3876
Miloslav Tlamicha	3715
Petr Hadrava	3485
Alžběta Oplištilová	2859
František Žďárský	2752
Kristian Vitovský	2064
Jiří Horn	1927
Pavel Koubský	1924
Jaroslav Honsa	1902
Petr Zasche	1849
Miroslav Brož	1837
Svatopluk Kříž	1805
Marek Wolf	1722
Josef Havelka	1607
Jana Švrčková	1552
Michal Zummer	1474
Damir Čikotić	1449
Donik Vršnak	1436
Rostislav Brož	1250
Juraj Jonák	1036
Jiří Grygar	988
Stanislav Štefl	964
Karel Juza	626
Adam Harmanec	606
Isabelle Piantschitsch	582
Ivica Skokić	515
Jakub Juryšek	417
Mirjana Malarić	373
Pavla Polechová	347
Miloš Zejda	334
Jan Janík	334
Pavel Chadima	327
Zoran Ivanović	315
David Ondřích	302
Željko Ružić	269
Dunja Plačko-Vršnak	218
Ištván Vince	209
Pavel Mayer	177
Kateřina Hoňková	166
Gordana Lazin	137
Jiří Vacek	136
Muhamed Muminović	136
Martin Netopil	121
Emil Frlež	99
Jelisaveta Arsenijević	83
Amir Mulić	68
Boro Jovanović	43
Roman Brajša	24
Aldo Arena	24
Bojan Vršnak	17
Željko Ivezić	6

Appendix B: Monitoring the atmospheric extinction at Hvar

Determination of linear extinction coefficients for every night of observations, in which the observed standard stars span a sufficient range of air masses (at least 0.2), was a natural part of the data reduction. We found that the all-sky magnitude residuals during longer observing nights exhibited small cyclic variations, obviously caused by the variable linear extinction during the course of the night. The effect for the low altitude observatory like Hvar is quite pronounced in some nights but we actually found similar, although smaller-amplitude effects even at superb mountain observatories like Sutherland or LaSilla. New versions of HEC22 program allow removal of these changes with polynomials up to fifth degree. Figure B.1 shows an example of such action for one Hvar observing night from the 2013 season.

It was also deemed useful to present an overview of seasonal variations in the extinction, relevant to air pollution at Hvar. Their value exceeds the astronomical interest and can be valuable for broader community, ecology studies in particular.

The seasonal variations, plotted in Fig B.2 and already noted by Koubský & Pavlovski (1982), are clearly seen. During the winter seasons, atmospheric extinction is usually lower as the sea does not evaporate too much. During the summer seasons, the values of the extinction coefficients exhibit a large scatter due to local weather changes but on an average they are much higher than in the winter. Another thing worth noting is that the minimum values of the seasonal changes do not show any annual modulation. Such a behavior has also been found at some other sites, for instance at La Silla (Rufener 1986) or Grossschwabhausen observing station (Reimann et al. 1992)). We note that in Fig B.2 there are some values of extinction coefficients lying below the general slope of the minimum extinction, especially for the *U* band. These extinction coefficients were usually determined on poor photometric nights or the nights where only few extinction standard stars had been measured. Of course, such nights were never used for all-sky photometry.

In Figure B.3 we present a time plot of all extinction coefficients in *U*, *B* and *V* passbands, recorded at Hvar Observatory over the past fifty years. The scatter of the values is mainly caused by seasonal changes discussed above. Nevertheless, a mild growth of the extinction can be seen in 1975 and 1982. Such increases are often related to large volcanic eruptions anywhere in the world. The first maximum, seen in 1975 may be due to eruption of the El Fuego volcano in Guatemala (October 1974). We warn, however, that during the first observing seasons at Hvar, only a limited number of nights and standard stars suitable for accurate determination of the extinction were available.

The next increase of the extinction appeared at the time of eruption of the El Chiichon volcano (March 1982). The growth of extinction coefficients after this eruption was also recorded at other observatories like La Silla (Rufener 1986; Burki et al. 1995), Jena University Observatory (Reimann et al. 1992), or Lowell Observatory (Lockwood & Thompson 1986). However, the effect of the powerful eruption of the St. Helens volcano (March 1980) was not obviously felt at extinction at Hvar. Needless to say, a very small number of observations was made at that time, however. Also the La Silla observations (Rufener 1986) and observations at the Jena University Observatory (Reimann et al. 1992) did not detect this eruption while at the Lowell Observatory (Lockwood & Thompson 1986), the effect was only marginal. The strong Pinatubo eruption (April 1991) was not covered by Hvar observations because of the intermission due to war in Yugoslavia.

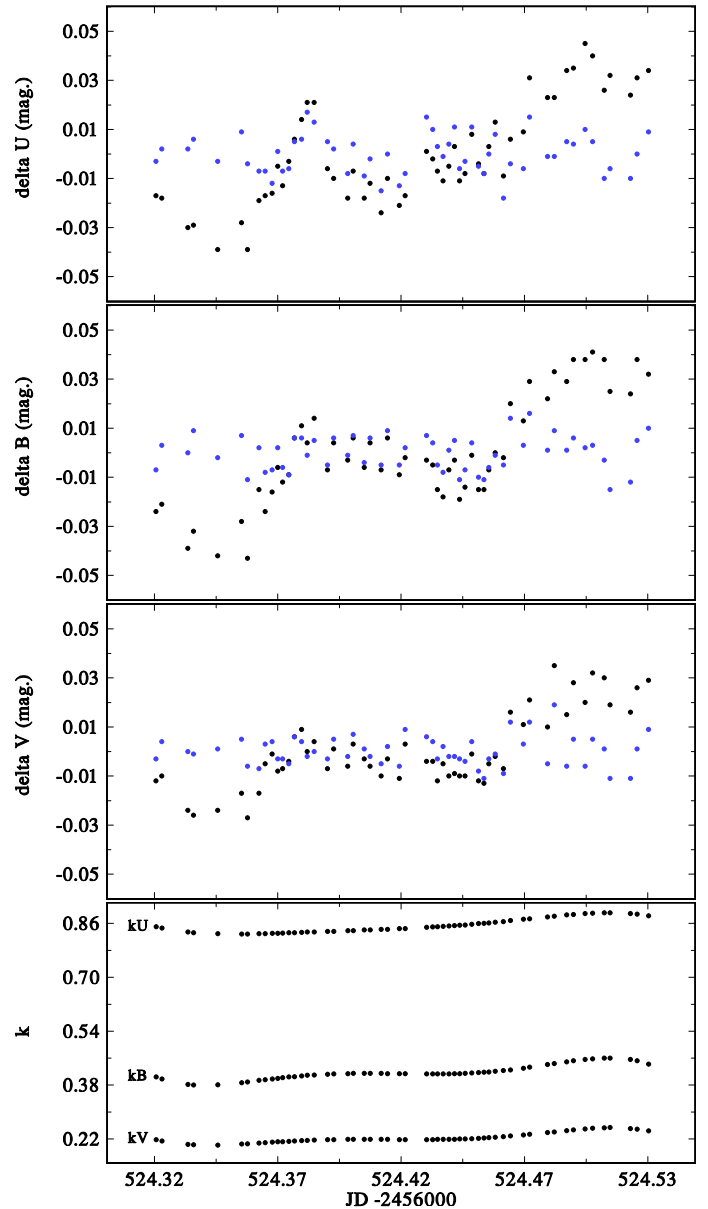


Fig. B.1: An example of the fit of the residuals of the all-sky magnitudes during one long summer night by a polynomial of fifth degree in all three passbands. Original residuals are shown by black dots, those after the polynomial fit by blue dots. The bottom panel shows the instantaneous values of the linear extinction coefficients during the course of the night.

A more detailed analysis of the extinction variations at Hvar and their nature will be published elsewhere. Here we only note that already Pavlovski et al. (1979) pointed out that the influence of the molecular absorption (mainly by O_3) is of little effect in the *UBV* region. The Rayleigh scattering on air molecules that depends on wavelength and the air pressure shows a small range of variability. The most variable component of the extinction is scattering by aerosols. The Hvar Observatory is a low-altitude station and in the vicinity of the sea and is a subject to significant weather changes even within one night. Obviously the sea spray plays a major role in the large variations of extinction during the summer seasons. Also occasional forest fires, quite frequent on the Adriatic coast, may have significant influence on the measured extinction.

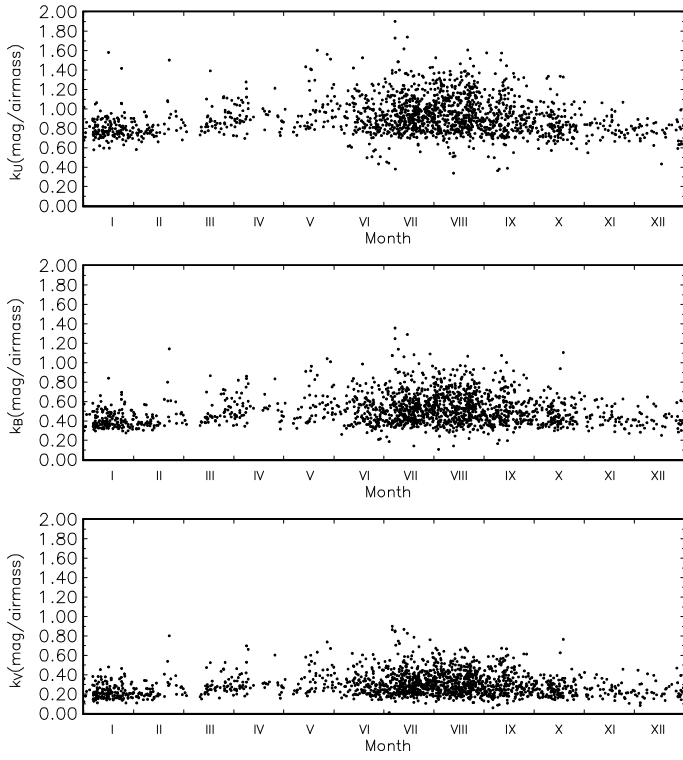


Fig. B.2: The seasonal variations of the extinction coefficients at Hvar Observatory.

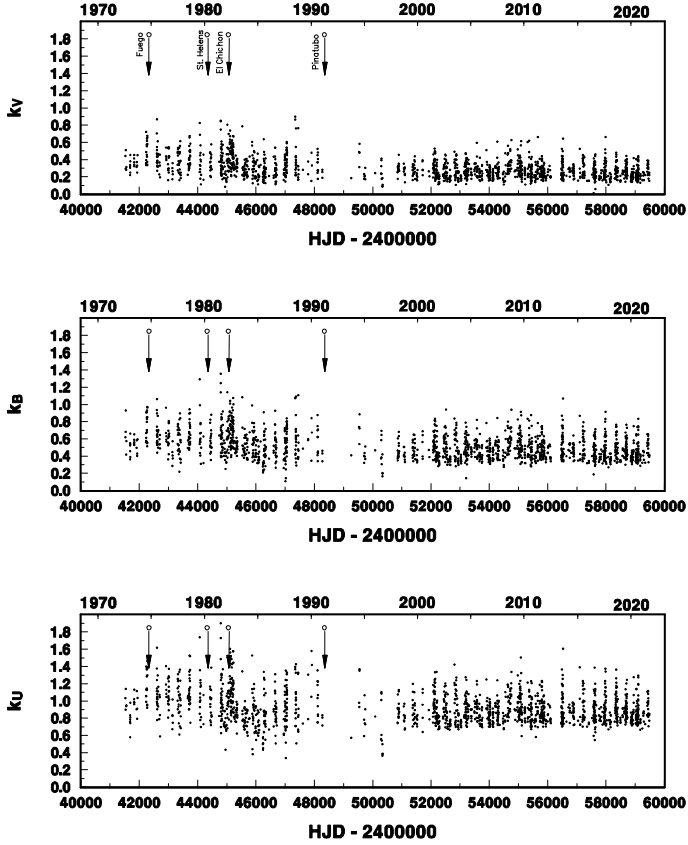


Fig. B.3: The long-time behaviour of the extinction coefficients at Hvar Observatory over the past fifty years.

Table C.1: The robust mean values of the *V* magnitude and the *B* – *V*, *U* – *B* and *V* – *R* indices for the ten primary Johnson standards derived from *N* individual observations published by Johnson et al. (1966). The rms errors are the rms errors of the mean values.

Name	HD	<i>V</i>	rms	<i>N</i>	<i>B</i> – <i>V</i>	rms	<i>N</i>	<i>U</i> – <i>B</i>	rms	<i>N</i>	<i>V</i> – <i>R</i>	rms	<i>N</i>
α Ari	12929	2.0060	0.0033	191	1.1509	0.0012	192	1.1260	0.0018	189	0.8432	0.0039	169
HR 875	18331	4.2836	0.0020	77	-0.0551	0.0018	78	-0.1165	0.0021	63	0.0160	0.0029	63
β Cnc	60267	3.5231	0.0019	223	1.4830	0.0067	225	1.7699	0.0020	224	1.1155	0.0021	197
η Hya	74280	4.2985	0.0012	186	-0.1941	0.0011	186	-0.7446	0.0014	182	-0.0634	0.0021	157
β Lib	135742	2.6072	0.0017	143	-0.1073	0.0015	143	-0.3614	0.0017	143	-0.0384	0.0040	128
α Ser	140573	2.6355	0.0014	135	1.1704	0.0014	137	1.2509	0.0021	137	0.8109	0.0048	123
ϵ CrB	143107	4.1527	0.0032	127	1.2324	0.0012	126	1.2751	0.0025	126	0.9012	0.0036	114
τ Her	147394	3.9052	0.0020	102	-0.1522	0.0019	106	-0.5621	0.0018	103	-0.0822	0.0034	88
10 Lac	214680	4.8845	0.0014	204	-0.2045	0.0012	204	-1.0464	0.0014	203	-0.0751	0.0018	187
HR 8832	219134	5.5738	0.0019	158	0.9966	0.0014	158	0.8861	0.0018	158	0.8346	0.0023	144

Notes. Of the ten primary Johnson standards, two are reported as variables. η Hya is classified as the β Cep pulsator and τ Her as a long-period pulsating star. α Ari, β Cnc, β Lib, α Ser, 10 Lac, and HR 8832 are listed as suspected variables.

Table C.2: The robust mean values of the *V* magnitude and *B* – *V*, *U* – *B* and *V* – *R* indices derived from *N* individual observations of seven selected secondary standards (Johnson & Harris 1954), with the data taken from Johnson et al. (1966). The rms errors are rms errors of the mean values.

Name	HD	<i>V</i>	rms	<i>N</i>	<i>B</i> – <i>V</i>	rms	<i>N</i>	<i>U</i> – <i>B</i>	rms	<i>N</i>	<i>V</i> – <i>R</i>	rms	<i>N</i>
73 Cet	15318	4.2836	0.0020	77	-0.0551	0.0018	78	-0.1165	0.0021	77	0.0160	0.0029	63
HR 753	16160	5.8164	0.0077	10	0.9633	0.0039	10	0.8074	0.0078	10	0.8177	0.0095	7
ν Ori	36512	4.6215	0.0014	273	-0.2618	0.0099	276	-1.0626	0.0012	274	-0.1217	0.0015	246
90 Leo	100600	5.9495	0.0014	170	-0.1547	0.0011	170	-0.6572	0.0013	168	-0.0589	0.0026	129
HR 4550	103095	6.4411	0.0017	167	0.7511	0.0012	169	0.1708	0.0016	167	0.6637	0.0020	131
β Oph	161096	2.7619	0.0023	105	1.1689	0.0018	107	1.2408	0.0018	106	0.8138	0.0033	88
γ Oph	161868	3.7471	0.0024	110	0.0380	0.0015	111	0.0348	0.0021	110	0.0457	0.0042	91

Notes. Of the seven selected secondary standards, β Oph is listed as a suspected variable. HR 4550 got a variable-star name CF UMa. It seems that on some rare occasions (one being recorded in Hipparcos H_p photometry) it becomes much fainter than usual. However, we did not detect such a decrease during our observations and used it along with the other standards.

Appendix C: Improved *UBV* values of the Johnson standards and our comparison, check, and red standard stars

Here we provide our compilation of robust mean *UBVR* values of Johnson standards derived as robust mean values of individual all-sky observations from night, when extinction was measured, from the paper by Johnson et al. (1966). Values for the primary standards are in Table C.1, those for selected secondary standards in Table C.2. Additionally, we also provide our new *UBV* standard values for all comparison, check, and red standard stars used in our observing programs. These can be used by other photometric observers as usable standards in their future photoelectric or CCD observations, intended to be transformed to the standard Johnson system. For standards observed in at least two different seasons and having at least 20 good individual observations, their *UBV* values are listed in Table C.3. For less frequently observed standards, their *UBV* values are provided in Table C.4.

Table C.3: Standard Johnson *UBV* magnitudes of all comparison, check and red standard stars used at Hvar, which have at least 20 observations secured in two or more seasons. The time interval of their observations is also given.

Star name	HD or BD number	JDmin - JDmax -2400000	No. of obs.	<i>V</i> (mag.)	<i>B</i> (mag.)	<i>U</i> (mag.)	<i>B</i> – <i>V</i> (mag.)	<i>U</i> – <i>B</i> (mag.)
12 Cas	2011	45307.3–60362.4	117	5.385±0.009	5.397±0.010	5.246±0.012	0.012	-0.151
HR 96	2054	57627.5–58887.3	29	5.746±0.009	5.683±0.009	5.370±0.011	-0.063	-0.313
HR 113	2626	45216.5–60362.3	161	5.940±0.010	5.953±0.011	5.603±0.013	0.013	-0.350
HR 189	4142	45212.6–60583.5	847	5.674±0.008	5.549±0.009	4.978±0.011	-0.125	-0.571
ν 1 Cas	5234	45216.5–59172.4	94	4.842±0.012	6.057±0.010	7.307±0.011	1.215	1.249
HR 285	5848	56639.2–57957.5	62	4.261±0.012	5.481±0.011	6.798±0.012	1.219	1.317

Table C.3: continued

Star name	HD or BD number	JDmin - JDmax -2400000	No. of obs.	<i>V</i> (mag.)	<i>B</i> (mag.)	<i>U</i> (mag.)	<i>B</i> - <i>V</i> (mag.)	<i>U</i> - <i>B</i> (mag.)
HR 286	5914	54015.4–58385.4	124	6.488±0.010	6.578±0.011	6.652±0.013	0.090	0.074
HR 289	6114	45648.2–60583.5	615	6.472±0.009	6.721±0.009	6.814±0.010	0.248	0.093
HR 333	6798	54015.4–57656.5	35	5.619±0.011	5.641±0.010	5.661±0.013	0.022	0.020
51 And	9927	44956.2–60583.5	925	3.600±0.010	4.881±0.010	6.312±0.011	1.281	1.432
HR 488	10362	54719.5–57779.4	326	6.337±0.009	6.367±0.010	5.942±0.011	0.030	-0.425
2 Per	11291	44956.2–60583.5	754	5.713±0.008	5.646±0.009	5.369±0.011	-0.067	-0.277
HR 561	11875	54719.5–57779.4	257	6.026±0.009	5.996±0.009	5.588±0.010	-0.030	-0.408
47 Cas	12230	55645.4–57615.5	21	5.294±0.014	5.617±0.013	5.658±0.015	0.323	0.041
4 Per	12303	44956.2–60583.5	853	5.009±0.008	4.936±0.009	4.631±0.011	-0.073	-0.305
HR 753	16160	46324.6–59275.3	172	5.815±0.011	6.792±0.010	7.585±0.012	0.977	0.793
HD 16578	16578	52584.3–55068.6	245	9.029±0.022	9.113±0.015	9.186±0.022	0.084	0.073
24 Per	18449	44865.6–59179.4	48	4.959±0.009	6.191±0.011	7.465±0.015	1.232	1.274
HD 18962	18962	42607.5–60323.3	163	7.939±0.011	8.547±0.012	8.644±0.014	0.607	0.098
HD 18992	18992	52584.3–55068.6	190	8.456±0.014	8.545±0.018	8.005±0.018	0.089	-0.540
HD 19193	19193	42607.6–58002.6	109	8.140±0.011	9.396±0.013	10.696±0.022	1.256	1.300
HD 19556	19556	55795.5–60323.3	92	8.441±0.012	9.086±0.011	9.215±0.014	0.645	0.129
ω Per	19656	44861.6–59106.5	169	4.636±0.010	5.748±0.010	6.792±0.014	1.112	1.044
HR 950	19736	44861.6–59097.5	142	6.160±0.011	6.060±0.009	5.486±0.014	-0.099	-0.574
HR 1034	21278	45307.4–59176.4	58	4.999±0.009	4.908±0.012	4.366±0.013	-0.092	-0.541
4 Tau	21686	54116.2–60323.4	390	5.150±0.009	5.105±0.010	5.012±0.012	-0.045	-0.093
HR 1074	21856	44988.3–59179.4	102	5.902±0.010	5.836±0.011	5.005±0.015	-0.066	-0.831
6 Tau	21933	54116.2–60323.4	331	5.774±0.009	5.698±0.010	5.398±0.012	-0.076	-0.300
HR 1133	23193	44988.3–59106.5	49	5.615±0.012	5.675±0.013	5.772±0.016	0.060	0.096
16 Tau	23288	44863.6–60583.5	437	5.476±0.008	5.438±0.009	5.097±0.011	-0.038	-0.341
18 Tau	23324	43140.3–60583.5	621	5.674±0.009	5.601±0.010	5.231±0.011	-0.073	-0.370
43 Per	24546	45307.4–59176.4	30	5.287±0.014	5.704±0.016	5.713±0.018	0.417	0.009
HR 1229	24982	47444.4–59179.4	44	6.506±0.007	6.613±0.009	6.700±0.010	0.107	0.087
HR 1243	25339	56523.6–60583.5	223	5.670±0.011	5.689±0.011	5.267±0.013	0.019	-0.422
ν Tau	25490	41691.2–59248.3	22	3.906±0.014	3.934±0.013	3.999±0.014	0.028	0.064
37 Tau	25604	44863.6–59598.3	240	4.381±0.010	5.440±0.009	6.411±0.010	1.058	0.971
λ Per	25642	48273.3–58888.4	78	4.289±0.006	4.266±0.007	4.258±0.009	-0.023	-0.008
HR 1284	26171	56523.6–60583.5	175	5.954±0.012	5.994±0.011	5.917±0.012	0.040	-0.077
α 2 Eri	26965	41691.2–59275.3	20	4.426±0.009	5.237±0.011	5.679±0.011	0.812	0.442
HR 1482	29526	48273.3–58888.3	75	5.674±0.005	5.661±0.006	5.630±0.009	-0.013	-0.030
59 Per	29722	44926.5–58889.4	37	5.308±0.009	5.324±0.007	5.351±0.010	0.016	0.027
HD 31894	31894	55574.3–58864.4	49	8.484±0.012	8.529±0.015	7.883±0.016	0.045	-0.645
HR 1644	32655	45307.5–59103.5	205	6.222±0.008	6.667±0.009	7.003±0.012	0.445	0.336
μ Aur	33641	44926.5–58889.4	48	4.826±0.013	5.018±0.022	5.119±0.041	0.192	0.101
HR 1725	34332	55858.6–59179.6	32	6.233±0.010	7.610±0.011	9.247±0.024	1.376	1.638
λ Aur	34411	45307.5–59103.5	260	4.708±0.008	5.317±0.009	5.463±0.011	0.609	0.146
HR 1738	34557	55858.6–59179.6	24	5.478±0.007	5.593±0.007	5.682±0.010	0.115	0.088
ρ Aur	34759	55858.6–59179.6	24	5.223±0.006	5.079±0.007	4.485±0.010	-0.144	-0.594
HD 35619	35619	41691.2–59248.4	37	8.533±0.015	8.802±0.012	8.140±0.014	0.269	-0.662
HD 35653	35653	41691.2–59248.4	36	7.451±0.022	7.586±0.018	6.883±0.013	0.135	-0.703
33 Ori	36351	51512.5–60362.4	249	5.458±0.008	5.274±0.008	4.446±0.009	-0.184	-0.828
HR 1860	36589	43136.4–60583.6	892	6.203±0.009	6.176±0.009	5.779±0.011	-0.028	-0.397
HR 1861	36591	53744.4–60362.4	198	5.341±0.009	5.150±0.009	4.223±0.011	-0.190	-0.927
HR 1871	36741	51512.5–54021.6	65	6.584±0.009	6.398±0.009	5.607±0.010	-0.186	-0.791
121 Tau	36819	44902.6–60583.6	170	5.380±0.010	5.300±0.009	4.668±0.012	-0.080	-0.632
126 Tau	37711	43136.4–60574.6	704	4.847±0.009	4.723±0.010	4.075±0.012	-0.125	-0.648
51 Ori	37984	51512.5–60362.3	126	4.930±0.010	6.078±0.010	7.139±0.012	1.147	1.062
χ 1 Ori	39587	43136.4–60575.6	467	4.406±0.011	4.992±0.011	5.060±0.013	0.586	0.069
HR 2154	41692	44902.6–52561.6	72	5.379±0.012	5.252±0.013	4.707±0.016	-0.127	-0.545
HR 2205	42690	44902.6–59974.4	369	5.055±0.009	4.860±0.010	4.077±0.012	-0.196	-0.783
HR 2218	43023	44902.7–59974.4	201	5.860±0.009	6.764±0.010	7.401±0.013	0.904	0.636
HR 2248	43526	44993.4–58892.4	67	6.565±0.010	6.450±0.011	5.946±0.015	-0.114	-0.504
HR 2300	44783	44993.4–58892.5	75	6.268±0.011	6.193±0.012	5.904±0.018	-0.076	-0.289
10 Mon	45546	44902.6–59974.4	271	5.055±0.009	4.876±0.009	4.118±0.011	-0.179	-0.758
ψ 4 Aur	47914	45023.4–58925.4	31	5.039±0.010	6.530±0.011	8.372±0.016	1.491	1.842
18 Mon	49293	44993.4–58892.5	54	4.506±0.010	5.605±0.011	6.637±0.016	1.099	1.031

Table C.3: continued

Star name	HD or BD number	JDmin - JDmax -2400000	No. of obs.	<i>V</i> (mag.)	<i>B</i> (mag.)	<i>U</i> (mag.)	<i>B</i> - <i>V</i> (mag.)	<i>U</i> - <i>B</i> (mag.)
HR 2532	49949	45023.4–58925.4	46	6.263±0.010	6.486±0.009	6.614±0.013	0.223	0.128
16 Lyn	50973	45023.4–58925.4	24	4.919±0.008	4.948±0.009	5.004±0.013	0.030	0.055
HR 2645	52860	45023.4–58925.4	26	6.381±0.009	6.342±0.009	6.091±0.011	-0.038	-0.251
1 CMi	58187	44984.4–59300.4	515	5.383±0.009	5.488±0.009	5.620±0.011	0.104	0.132
ε CMi	58367	44984.4–59300.4	273	5.016±0.010	6.013±0.009	6.791±0.012	0.997	0.777
HR 2858	59059	44984.4–59300.4	367	6.247±0.009	6.202±0.009	6.102±0.011	-0.045	-0.100
HD 61341	61341	55586.5–57792.5	31	7.980±0.014	8.175±0.006	8.276±0.025	0.195	0.101
ζ CMi	63975	45056.3–58929.4	47	5.134±0.009	5.016±0.011	4.539±0.011	-0.118	-0.477
HD 65005	65005	52655.4–58946.3	63	8.003±0.009	8.115±0.012	8.247±0.016	0.111	0.133
HD 65199	65199	52655.4–58946.3	81	7.682±0.010	7.600±0.009	7.214±0.012	-0.082	-0.385
HR 3145	66141	53026.5–58929.4	26	4.414±0.008	5.662±0.011	6.949±0.014	1.247	1.287
30 Mon	71155	43143.5–58929.4	45	3.903±0.010	3.887±0.008	3.862±0.010	-0.016	-0.024
39 Cnc	73665	41691.6–59276.4	21	6.427±0.013	7.400±0.010	8.225±0.011	0.973	0.825
42 Cnc	73785	41691.6–59276.4	25	6.840±0.012	7.042±0.013	7.203±0.010	0.202	0.161
HR 3608	77692	55879.6–58946.4	32	6.454±0.006	6.491±0.005	6.573±0.006	0.037	0.081
HD 81772	81772	55879.6–58946.4	43	8.256±0.010	8.570±0.008	8.732±0.012	0.314	0.162
HD 82861	82861	55879.6–58946.4	61	7.074±0.008	7.218±0.008	7.312±0.007	0.144	0.094
ο Leo	83808	46095.5–58946.3	74	3.523±0.012	4.001±0.011	4.211±0.013	0.478	0.210
ν Leo	86360	46095.5–58946.3	61	5.275±0.013	5.222±0.012	5.101±0.014	-0.053	-0.121
λ UMa	89021	43143.6–50902.5	75	3.456±0.012	3.479±0.010	3.558±0.012	0.022	0.079
43 Leo	89962	46095.5–58892.6	39	6.105±0.014	7.204±0.010	8.317±0.021	1.099	1.112
49 UMa	95310	50854.4–50902.5	71	5.082±0.016	5.317±0.010	5.500±0.013	0.236	0.182
51 UMa	95934	50854.4–50902.5	80	6.031±0.016	6.187±0.011	6.288±0.013	0.156	0.101
55 UMa	98353	50854.4–50902.5	63	4.774±0.015	4.881±0.010	4.919±0.015	0.107	0.038
HD 104316	104316	45357.6–58924.5	77	6.775±0.008	6.867±0.008	6.947±0.013	0.092	0.080
HR 4609	104985	44984.7–59733.4	212	5.825±0.013	6.847±0.013	7.693±0.016	1.022	0.846
HR 4687	107193	44984.7–59733.4	359	5.492±0.010	5.534±0.011	5.611±0.013	0.042	0.077
HR 5018	115612	45357.6–59733.4	165	6.220±0.008	6.165±0.008	6.028±0.009	-0.055	-0.137
81 UMa	118214	41828.4–59025.4	30	5.637±0.009	5.608±0.010	5.544±0.009	-0.029	-0.064
HR 5162	119476	52444.4–52445.5	25	5.845±0.009	5.916±0.010	5.983±0.017	0.071	0.067
HD 119581	119581	52444.4–52445.5	23	6.614±0.008	6.738±0.011	6.845±0.016	0.124	0.107
HR 5216	120874	41828.4–59025.4	45	6.490±0.011	6.578±0.012	6.641±0.014	0.089	0.063
50 Boo	136849	45916.3–59032.4	76	5.393±0.009	5.334±0.008	5.143±0.010	-0.059	-0.191
HR 5760	138341	45916.3–59032.4	97	6.469±0.010	6.667±0.010	6.795±0.013	0.199	0.128
BD+64 1078	139549	53491.4–59344.4	178	9.141±0.011	9.546±0.012	9.503±0.017	0.406	-0.044
BD+64 1079	139703	53491.4–59344.4	141	9.312±0.011	10.233±0.011	10.812±0.016	0.921	0.578
HD 141930	141930	45121.4–58564.6	76	7.716±0.008	7.815±0.008	7.916±0.012	0.099	0.102
λ Lib	142096	52068.4–60518.4	100	5.026±0.010	5.035±0.011	4.430±0.014	0.009	-0.605
χ Her	142373	42994.3–60467.4	472	4.606±0.008	5.176±0.009	5.185±0.011	0.569	0.009
λ CrB	142908	44432.3–59032.4	129	5.436±0.010	5.781±0.011	5.816±0.011	0.345	0.036
ν Her	144206	41528.5–60467.4	720	4.736±0.008	4.642±0.009	4.315±0.011	-0.094	-0.327
ω1 Sco	144470	42241.4–60518.4	121	3.935±0.010	3.932±0.012	3.092±0.013	-0.003	-0.841
φ Her	145389	41536.4–60467.4	544	4.249±0.007	4.189±0.009	3.937±0.010	-0.061	-0.251
HR 6096	147550	52494.3–54296.4	80	6.243±0.013	6.301±0.010	6.293±0.013	0.058	-0.009
ρ Oph	147933	52494.3–56094.4	21	4.567±0.031	4.802±0.030	4.227±0.031	0.235	-0.575
ν Oph	148357	52494.3–56094.4	135	4.636±0.010	4.814±0.013	4.888±0.013	0.178	0.074
16 Oph	151133	52494.3–54280.5	50	6.037±0.007	6.017±0.009	5.878±0.011	-0.020	-0.139
HR 6278	152585	52494.3–53192.4	32	6.584±0.012	6.715±0.015	6.829±0.019	0.130	0.114
ε Her	153808	52068.3–55120.3	95	3.918±0.010	3.895±0.010	3.804±0.011	-0.023	-0.091
HR 6353	154445	54275.4–58002.3	90	5.623±0.010	5.795±0.012	5.171±0.016	0.172	-0.623
HR 6361	154660	54275.4–58006.3	363	6.360±0.010	6.572±0.011	6.667±0.014	0.212	0.095
HR 6367	154895	54275.4–58002.3	275	6.061±0.009	6.140±0.010	6.159±0.011	0.078	0.019
72 Her	157214	52068.3–55120.3	95	5.385±0.011	6.005±0.010	6.090±0.011	0.620	0.085
77 Her	158414	43313.4–60574.3	814	5.851±0.008	5.979±0.009	6.118±0.010	0.128	0.139
30 Dra	162579	41536.4–60574.3	710	5.040±0.008	5.073±0.009	5.080±0.010	0.033	0.007
ξ Dra	163588	42241.4–60574.3	626	3.745±0.010	4.925±0.010	6.150±0.011	1.180	1.225
HR 6689	163624	43712.4–59043.5	77	5.953±0.012	6.078±0.012	6.167±0.017	0.125	0.089
HR 6690	163641	45105.5–60535.3	146	6.290±0.009	6.296±0.010	6.062±0.011	0.006	-0.234
93 Her	164349	44799.3–60535.4	356	4.680±0.009	5.923±0.009	7.141±0.010	1.243	1.219
HR 6719	164432	45105.5–60535.4	176	6.352±0.009	6.277±0.011	5.520±0.012	-0.075	-0.756

Table C.3: continued

Star name	HD or BD number	JDmin - JDmax -2400000	No. of obs.	<i>V</i> (mag.)	<i>B</i> (mag.)	<i>U</i> (mag.)	<i>B</i> - <i>V</i> (mag.)	<i>U</i> - <i>B</i> (mag.)
71 Oph	165760	45105.5–59793.4	106	4.663±0.008	5.615±0.009	6.356±0.011	0.952	0.741
102 Her	166182	44799.4–60535.4	491	4.359±0.008	4.189±0.010	3.392±0.011	-0.170	-0.797
101 Her	166230	46269.4–60531.4	343	5.115±0.008	5.278±0.009	5.458±0.010	0.162	0.180
15 Sgr	167264	41824.6–59027.5	32	5.315±0.018	5.388±0.018	4.524±0.020	0.073	-0.864
21 Sgr	169420	41824.6–59027.5	41	4.801±0.016	6.122±0.020	7.106±0.025	1.321	0.984
HR 6900	169578	44433.4–59044.5	271	6.732±0.010	6.758±0.011	6.561±0.013	0.026	-0.197
HR 6925	170137	44433.4–59044.5	145	6.003±0.012	7.659±0.012	9.520±0.019	1.656	1.860
HR 6928	170200	44433.4–59044.5	313	5.711±0.009	5.687±0.010	5.329±0.014	-0.024	-0.358
HR 6997	172044	49538.5–56899.4	58	5.413±0.006	5.319±0.009	4.805±0.014	-0.094	-0.514
HR 7028	172883	42993.5–59043.5	726	6.015±0.009	5.942±0.009	5.731±0.012	-0.072	-0.211
HR 7060	173664	42993.4–59051.5	891	6.207±0.009	6.282±0.009	6.434±0.013	0.074	0.153
ν2 Lyr	174602	49538.5–57973.4	333	5.240±0.008	5.338±0.011	5.438±0.011	0.098	0.100
HR 7123	175225	42998.4–59051.5	492	5.523±0.009	6.357±0.010	6.878±0.014	0.835	0.520
HD 175406	175406	55357.5–56541.4	292	8.133±0.008	8.395±0.008	8.480±0.011	0.261	0.086
HD 175469	175469	55357.5–56541.4	268	8.995±0.010	9.216±0.009	9.306±0.011	0.221	0.090
γ Lyr	176437	46969.4–59180.2	431	3.252±0.009	3.184±0.013	3.148±0.013	-0.068	-0.036
HR 7239	177817	53584.4–59098.3	75	6.012±0.010	5.993±0.010	5.648±0.010	-0.019	-0.345
51 Dra	178201	42994.4–56094.4	65	5.419±0.018	5.395±0.023	5.328±0.030	-0.024	-0.067
HD 180889	180889	46238.5–47374.4	157	6.907±0.008	7.078±0.010	7.239±0.015	0.172	0.161
HD 181751	181751	46238.5–47374.4	108	6.571±0.008	6.500±0.011	6.150±0.015	-0.070	-0.351
HR 7378	182645	53936.5–59098.3	46	5.716±0.010	5.753±0.012	5.424±0.011	0.037	-0.329
HR 7379	182678	54280.4–59098.3	45	6.719±0.009	6.766±0.008	6.695±0.011	0.047	-0.072
HR 7397	183227	44079.5–60575.4	1566	5.844±0.009	5.861±0.010	5.482±0.013	0.017	-0.379
HR 7404	183387	44079.5–60575.4	964	6.251±0.009	7.570±0.011	8.931±0.015	1.319	1.361
9 Vul	184606	46679.4–59025.5	103	5.008±0.009	4.909±0.010	4.499±0.012	-0.099	-0.410
HR 7438	184663	44079.5–60575.4	1137	6.373±0.009	6.782±0.010	6.748±0.012	0.409	-0.034
β Sge	185958	46238.5–58690.6	111	4.392±0.008	5.426±0.010	6.328±0.016	1.034	0.902
HD 185978	185978	54751.2–58402.4	102	7.892±0.011	8.398±0.014	8.493±0.016	0.506	0.095
HD 186239	186239	58324.5–58402.4	75	7.362±0.011	7.583±0.011	7.675±0.014	0.221	0.092
HR 7512	186568	45900.5–58696.5	597	6.077±0.009	6.003±0.009	5.713±0.011	-0.074	0.290
15 Cyg	186675	46679.4–60575.4	88	4.900±0.008	5.837±0.012	6.540±0.013	0.936	0.704
γ Aql	186791	46969.4–47061.3	20	2.717±0.010	4.231±0.013	5.945±0.020	1.515	1.713
17 Cyg	187013	57210.5–58696.5	81	5.007±0.010	5.469±0.012	5.471±0.013	0.462	0.001
HR 7550	187458	45900.5–58696.5	722	6.659±0.009	7.083±0.010	7.031±0.012	0.424	-0.052
HD 187664	187664	54280.5–59082.3	39	6.890±0.011	7.204±0.012	7.435±0.012	0.314	0.232
HD 188170	188170	43027.4–58682.6	104	7.352±0.013	7.275±0.015	6.900±0.017	-0.077	-0.375
13 Vul	188260	46665.5–59025.5	160	4.585±0.008	4.536±0.009	4.403±0.012	-0.049	-0.133
β Aql	188512	42654.3–57970.5	21	3.722±0.015	4.576±0.015	5.064±0.012	0.854	0.488
22 Cyg	188892	46238.5–60583.3	362	4.953±0.008	4.862±0.010	4.344±0.013	-0.090	-0.518
17 Vul	190993	44817.4–60583.3	225	5.082±0.010	4.908±0.011	4.228±0.013	-0.174	-0.680
18 Vul	191747	44432.5–60583.3	178	5.529±0.009	5.603±0.009	5.722±0.012	0.074	0.119
19 Vul	192004	44432.5–60583.3	118	5.492±0.012	6.907±0.012	8.406±0.016	1.415	1.499
33 Cyg	192696	46323.3–59101.4	59	4.289±0.010	4.398±0.012	4.501±0.014	0.109	0.103
36 Cyg	193369	46238.5–60583.3	273	5.593±0.009	5.633±0.009	5.663±0.013	0.040	0.030
HR 7815	194668	44433.5–59087.6	355	6.511±0.009	6.496±0.011	6.447±0.014	-0.015	-0.049
42 Cyg	195324	46680.4–59077.5	40	5.874±0.010	6.321±0.013	6.531±0.027	0.447	0.210
HD 197618	197618	53578.3–57964.5	127	6.995±0.009	7.154±0.009	7.241±0.011	0.159	0.087
η Cep	198149	41528.4–59082.5	296	3.426±0.010	4.337±0.011	4.953±0.015	0.911	0.616
HD 198679	198679	53686.2–57966.4	23	6.905±0.011	6.852±0.012	6.694±0.015	-0.053	-0.157
HD 198692	198692	51426.4–59101.4	65	6.660±0.011	7.672±0.010	8.483±0.017	1.012	0.811
HR 7996	198820	52165.4–59101.4	35	6.436±0.010	6.299±0.007	5.669±0.009	-0.138	-0.630
HD 199007	199007	51402.4–59101.4	154	7.958±0.012	7.907±0.009	7.587±0.011	-0.051	-0.320
HD 199311	199311	46269.5–60583.4	841	6.687±0.008	6.765±0.009	6.857±0.011	0.078	0.092
HD 199479	199479	46269.5–52094.5	135	6.845±0.010	6.804±0.009	6.587±0.013	-0.041	-0.217
HIP 103770	200270	52500.4–52549.4	163	7.768±0.010	8.227±0.012	8.171±0.013	0.459	-0.057
HIP 103874	200468	52500.4–52549.4	142	7.862±0.009	8.039±0.012	8.157±0.013	0.177	0.119
HR 8119	202214	45538.5–59101.4	130	5.617±0.007	5.737±0.008	4.982±0.010	0.120	-0.755
HD 202349	202349	44817.4–59082.5	217	7.362±0.010	7.195±0.009	6.222±0.012	-0.167	-0.974
HR 8161	203245	51067.3–60583.4	937	5.762±0.008	5.633±0.009	5.115±0.010	-0.128	-0.519
α Cep	203280	46988.4–52494.5	24	2.457±0.010	2.676±0.013	2.786±0.015	0.219	0.110

Table C.3: continued

Star name	HD or BD number	JDmin - JDmax -2400000	No. of obs.	<i>V</i> (mag.)	<i>B</i> (mag.)	<i>U</i> (mag.)	<i>B</i> - <i>V</i> (mag.)	<i>U</i> - <i>B</i> (mag.)
70 Cyg	204403	44817.4–59082.5	163	5.315±0.007	5.166±0.009	4.505±0.012	-0.149	-0.661
72 Cyg	205512	44817.4–60531.5	652	4.891±0.009	5.981±0.010	6.991±0.011	1.090	1.011
HD 206259	206259	45155.5–59097.4	32	7.534±0.010	7.596±0.011	7.032±0.014	0.062	-0.563
HD 206694	206694	57581.5–57996.5	157	8.804±0.012	9.319±0.011	9.393±0.014	0.515	0.074
π 2 Cyg	207330	42244.5–59097.4	83	4.244±0.008	4.116±0.011	3.404±0.015	-0.128	-0.713
12 Cep	207528	58740.4–59043.6	24	5.517±0.012	7.086±0.011	9.021±0.024	1.569	1.935
HR 8342	207636	57581.5–58006.5	168	6.475±0.009	6.466±0.011	6.437±0.012	-0.009	-0.029
HD 207793	207793	45155.5–59087.5	21	6.560±0.010	6.940±0.011	6.424±0.012	0.380	-0.516
HR 8473	210873	57581.5–58006.5	193	6.389±0.011	6.327±0.011	6.161±0.012	-0.063	-0.165
2 Lac	212120	41536.5–59180.2	88	4.550±0.011	4.445±0.013	3.916±0.014	-0.105	-0.529
β Lac	212496	45155.5–59097.4	40	4.448±0.010	5.458±0.012	6.249±0.016	1.009	0.791
4 Lac	212593	41536.5–58740.5	169	4.578±0.011	4.666±0.012	4.314±0.014	0.089	-0.352
6 Lac	213420	41929.5–59180.3	31	4.509±0.011	4.421±0.011	3.691±0.012	-0.088	-0.730
α Lac	213558	46280.5–50341.5	57	3.775±0.010	3.784±0.011	3.802±0.011	0.009	0.018
9 Lac	214454	42996.5–50341.5	44	4.641±0.011	4.887±0.010	5.005±0.012	0.246	0.118
15 Lac	216397	42993.5–46696.5	54	4.921±0.023	6.536±0.038	8.488±0.034	1.615	1.952
HR 8708	216608	46280.5–46696.5	25	5.771±0.009	6.060±0.013	6.170±0.016	0.290	0.110
HR 8733	217101	44432.5–60583.4	1455	6.175±0.009	6.028±0.009	5.220±0.011	-0.147	-0.808
2 And	217782	42993.5–60583.4	949	5.108±0.009	5.194±0.010	5.304±0.011	0.086	0.110
3 And	218031	46664.6–60189.5	263	4.662±0.008	5.718±0.010	6.618±0.012	1.056	0.899
1 Cas	218376	50854.2–51080.5	40	4.828±0.018	4.792±0.013	3.947±0.027	-0.035	-0.845
4 And	218452	43140.2–60583.4	892	5.301±0.011	6.724±0.011	8.443±0.015	1.423	1.720
5 And	218470	42266.5–60197.6	1203	5.686±0.009	6.116±0.010	6.100±0.012	0.430	-0.016
HR 8806	218525	43712.5–59077.6	25	6.524±0.011	6.692±0.010	6.892±0.010	0.168	0.200
7 And	219080	45561.5–60197.6	564	4.535±0.008	4.828±0.010	4.861±0.011	0.293	0.033
HD 219326	219326	53241.5–58006.5	318	8.361±0.010	8.462±0.011	8.575±0.012	0.101	0.114
HR 8870	219891	43712.5–59077.6	54	6.528±0.008	6.689±0.009	6.827±0.011	0.161	0.138
10 And	219981	46664.5–51066.6	25	5.788±0.012	7.321±0.015	9.185±0.019	1.533	1.865
HD 220073	220073	52136.6–58006.5	454	7.699±0.009	8.119±0.010	8.122±0.012	0.420	0.003
ι And	222173	42266.5–51372.4	25	4.304±0.016	4.205±0.013	3.886±0.021	-0.099	-0.319
κ And	222439	42266.5–60583.4	406	4.155±0.009	4.068±0.010	3.849±0.011	-0.086	-0.220
HR 9011	223229	45297.2–60583.4	395	6.085±0.009	5.957±0.008	5.289±0.010	-0.127	-0.668
HR 9057	224342	46287.6–58716.4	56	6.019±0.010	6.739±0.015	7.067±0.021	0.720	0.328
σ Cas	224572	50854.2–51080.5	38	4.880±0.013	4.805±0.010	4.006±0.016	-0.075	-0.799
HD 224890	224890	54754.3–55120.6	34	6.510±0.015	6.694±0.017	6.791±0.019	0.184	0.098
BD+52 2289	–	42994.4–54294.4	32	9.761±0.017	10.201±0.051	10.199±0.059	0.440	-0.002
BD+52 2288	–	42994.4–54294.4	45	9.029±0.018	9.490 ±.021	9.441±0.033	0.461	-0.048

Table C.4: The (less accurate) standard Johnson *UBV* magnitudes of less frequently observed comparison, check, and red standard stars used at Hvar.

Star name	HD or BD number	JDmin - JDmax -2400000	No. of obs.	<i>V</i> (mag.)	<i>B</i> (mag.)	<i>U</i> (mag.)	<i>B</i> - <i>V</i> (mag.)	<i>U</i> - <i>B</i> (mag.)
HR 1	3	46287.6–46290.6	9	6.718±0.008	6.783±0.011	6.858±0.014	0.065	0.075
HD 567	567	57634.5–58887.3	17	7.221±0.017	7.191±0.024	6.801±0.023	-0.029	-0.390
χ Peg	1013	42266.5–42278.5	3	4.866±0.011	6.504±0.019	8.350±0.017	1.638	1.846
HD 1687	1687	56092.5–56092.5	2	8.138±0.003	9.052±0.007	9.648±0.012	0.914	0.596
BD+81 13/A	3440	46689.6–46696.6	2	6.367±0.009	6.921±0.015	6.905±0.022	0.553	-0.016
ν And	4727	43136.2–59179.4	18	4.541±0.011	4.399±0.009	3.812±0.010	-0.142	-0.587
20 Cet	5112	43140.2–43152.3	2	4.738±0.059	6.351±0.023	8.287±0.030	1.613	1.936
ν 2 Cas	5395	52488.5–54021.5	16	4.639±0.007	5.597±0.008	6.266±0.012	0.958	0.669
BD+81 27/G	5817	46689.6–46689.6	1	8.429±0.000	9.019±0.000	9.015±0.000	0.590	-0.004
BD+81 29/F	5905	46689.6–46689.6	1	8.519±0.000	9.163±0.000	9.336±0.000	0.644	0.173
BD+81 30/E	6006	46689.6–46690.6	2	7.968±0.026	7.979±0.028	7.904±0.035	0.012	-0.075
80 Psc	6763	43140.2–43152.3	2	5.514±0.027	5.852±0.001	5.860±0.024	0.338	0.008
BD+80 35/C	7471	46689.6–46689.6	1	7.209±0.000	7.568±0.000	7.645±0.000	0.359	0.077
BD+80 36/B	7505	46689.6–46689.6	1	6.688±0.000	6.715±0.000	6.729±0.000	0.027	0.014
ξ And	8207	43136.3–43152.3	4	4.880±0.013	5.985±0.019	7.004±0.019	1.104	1.019
ψ Cas	8491	45216.5–45216.5	1	4.737±0.000	5.793±0.000	6.734±0.000	1.056	0.941
ν And	9826	46324.6–46324.6	3	4.094±0.002	4.623±0.002	4.691±0.003	0.529	0.068

Table C.4: continued

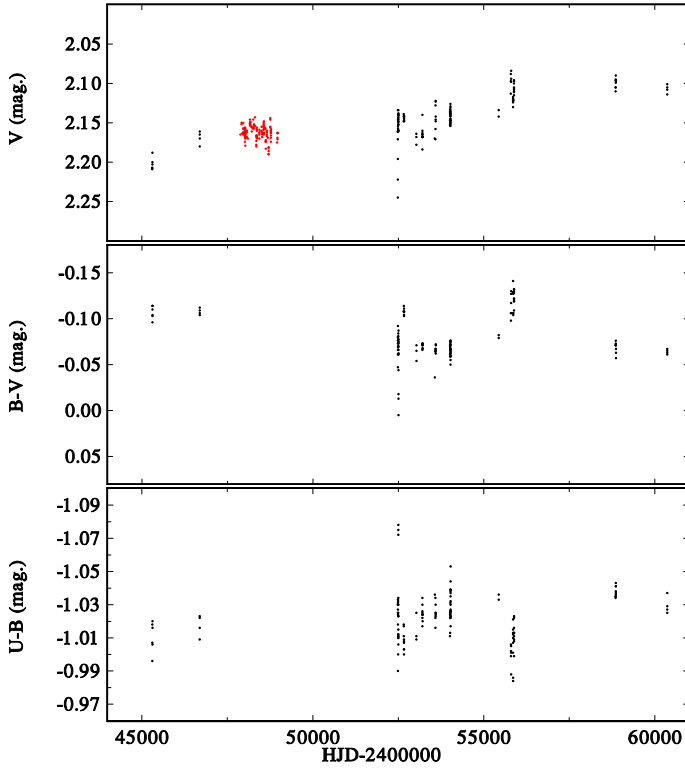
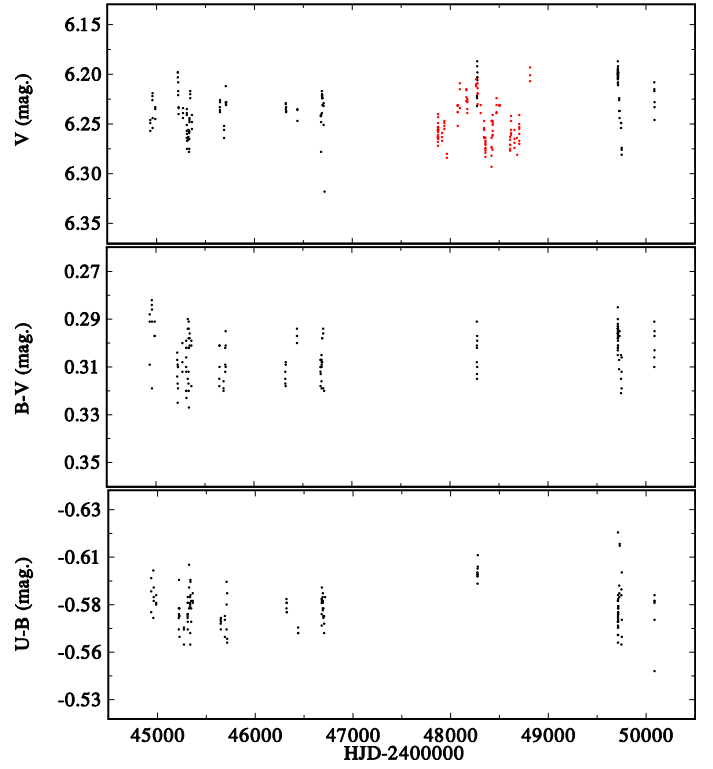
Star name	HD or BD number	JDmin - JDmax -2400000	No. of obs.	<i>V</i> (mag.)	<i>B</i> (mag.)	<i>U</i> (mag.)	<i>B</i> - <i>V</i> (mag.)	<i>U</i> - <i>B</i> (mag.)
τ And	10205	43136.3–43152.3	4	4.970±0.028	4.878±0.013	4.480±0.019	-0.091	-0.398
107 Psc	10476	46324.6–46324.6	3	5.267±0.007	6.097±0.009	6.604±0.019	0.830	0.507
HR 502	10857	51447.5–51928.3	9	6.256±0.008	6.323±0.006	6.406±0.008	0.067	0.083
HR 540	11408	51435.6–51928.3	12	6.449±0.005	6.638±0.006	6.751±0.012	0.188	0.113
HR 572	12005	56898.4–56898.4	2	6.056±0.004	7.195±0.003	8.033±0.006	1.140	0.837
50 Cas	12216	47371.6–47373.6	2	3.991±0.021	4.010±0.028	4.053±0.038	0.019	0.042
HD 13841	13841	46679.6–46680.6	7	7.365±0.014	7.606±0.009	6.977±0.009	0.242	-0.629
HD 14369	14369	54018.5–56095.4	19	8.097±0.012	8.499±0.015	8.440±0.016	0.402	-0.059
π Cet	17081	43136.4–43152.3	4	4.232±0.023	4.149±0.023	3.724±0.025	-0.083	-0.425
HR 975	20193	54026.5–54026.6	4	6.311±0.005	6.668±0.008	6.642±0.007	0.357	-0.025
α Per	20902	47049.5–52494.5	10	1.798±0.011	2.271±0.010	2.655±0.025	0.473	0.383
HR 1019	20995	54026.5–54026.6	4	5.795±0.009	5.780±0.006	5.623±0.004	-0.015	-0.157
HR 1041	21402	54026.5–54026.6	4	5.733±0.002	5.769±0.003	5.836±0.007	0.036	0.067
27 Tau	23850	52946.5–56508.6	11	3.642±0.008	3.548±0.014	3.196±0.011	-0.093	-0.352
HR 1188	23985	43140.3–43152.3	13	5.263±0.031	5.480±0.033	5.562±0.032	0.217	0.083
HR 1226	24843	52488.5–52488.5	2	6.302±0.005	7.368±0.001	8.273±0.008	1.066	0.905
HR 1234	25152	52502.5–55454.5	2	6.421±0.003	6.411±0.036	6.328±0.023	-0.010	-0.084
HD 25539	25539	55454.5–55454.5	8	6.872±0.017	6.916±0.030	6.323±0.034	0.044	-0.593
π 3 Ori	30652	56540.6–57996.6	15	3.186±0.009	3.631±0.014	3.625±0.014	0.446	-0.007
π 4 Ori	30836	56540.6–57634.6	10	3.682±0.011	3.513±0.018	2.704±0.010	-0.169	-0.809
HD 31617	31617	56002.3–56002.3	3	7.423±0.011	7.432±0.008	6.692±0.007	0.008	-0.740
HR 1617	32249	51445.6–51520.5	46	4.795±0.008	4.617±0.014	3.876±0.016	-0.178	-0.741
HR 1621	32309	43136.4–43152.3	4	4.902±0.018	4.858±0.032	4.726±0.026	-0.045	-0.131
HD 32328	32328	56002.3–56002.3	3	7.664±0.008	7.616±0.006	7.278±0.007	-0.049	-0.338
HR 1671	33224	51445.6–51520.5	25	5.820±0.015	5.735±0.015	5.344±0.017	-0.086	-0.391
HR 1697	33833	51445.6–51520.5	12	5.928±0.009	6.869±0.011	7.603±0.012	0.941	0.734
α Aur	34029	47049.5–47058.5	4	0.046±0.017	0.864±0.036	1.312±0.039	0.818	0.448
16 Cam	34787	45309.6–45697.4	7	5.260±0.007	5.239±0.015	5.195±0.013	-0.021	-0.044
β Tau	35497	47052.6–47058.5	2	1.660±0.015	1.516±0.003	1.027±0.004	-0.144	-0.489
HR 1833	36166	51943.3–53761.3	19	5.770±0.008	5.575±0.011	4.729±0.009	-0.195	-0.846
38 Ori	36777	51943.3–51943.4	3	5.340±0.011	5.397±0.010	5.448±0.013	0.057	0.051
φ 1 Ori	36822	53388.4–53388.4	3	4.388±0.007	4.246±0.002	3.301±0.007	-0.142	-0.945
σ Ori	37468	58499.4–58499.4	1	3.821±0.000	3.582±0.000	2.566±0.000	-0.239	-1.016
ξ Aur	39283	45308.5–55124.5	18	4.983±0.009	5.026±0.014	5.119±0.016	0.043	0.093
δ Aur	40035	45308.5–55124.5	12	3.758±0.009	4.755±0.016	5.587±0.014	0.997	0.832
HR 2224	43157	45359.3–45360.3	5	5.834±0.006	5.668±0.009	4.991±0.007	-0.166	-0.677
HR 2234	43319	45359.3–45360.3	5	6.009±0.013	6.092±0.009	6.172±0.008	0.084	0.080
HD 46149	46149	53388.5–53388.5	3	7.582±0.001	7.753±0.002	6.995±0.007	0.171	-0.758
ψ 2 Aur	47174	43140.5–43152.5	3	4.802±0.035	6.058±0.012	7.338±0.039	1.256	1.280
ν 3 CMa	47442	43140.5–43152.5	3	4.422±0.030	5.547±0.023	6.553±0.044	1.125	1.006
HD 50109	50109	54862.4–54862.4	4	9.085±0.019	9.079±0.011	8.983±0.017	-0.006	-0.096
HD 50169	50169	54862.4–54862.4	3	9.021±0.008	9.023±0.007	9.018±0.007	0.002	-0.005
HD 50346	50346	54862.4–54862.4	3	8.756±0.009	8.680±0.007	8.107±0.007	-0.076	-0.573
HD 50669	50669	54862.4–54862.4	3	8.929±0.011	9.625±0.013	9.915±0.008	0.696	0.290
HR 2572	50747	54862.4–54862.4	3	5.463±0.004	5.616±0.011	5.788±0.006	0.153	0.172
HD 53035	53035	52940.6–52940.6	13	7.897±0.016	7.827±0.005	7.311±0.037	-0.070	-0.515
λ Gem	56537	45065.3–50865.4	9	3.583±0.008	3.689±0.006	3.818±0.015	0.106	0.129
16 Pup	67797	43140.6–43152.5	3	4.395±0.005	4.249±0.007	3.653±0.017	-0.146	-0.596
9 Hya	74137	43140.6–43152.5	4	4.882±0.011	5.929±0.018	6.845±0.028	1.047	0.916
ι UMa	76644	43143.5–43143.5	1	3.141±0.000	3.351±0.000	3.411±0.000	0.210	0.060
κ UMa	77327	43140.6–43152.5	3	3.580±0.006	3.562±0.008	3.596±0.006	-0.017	0.034
ϑ Hya	79469	43143.5–43143.5	1	3.928±0.000	3.851±0.000	3.728±0.000	-0.077	-0.123
HR 3751	81817	56747.3–56747.4	4	4.278±0.008	5.756±0.007	7.470±0.005	1.479	1.714
21 LMi	87696	43143.6–43143.6	1	4.481±0.000	4.687±0.000	4.738±0.000	0.206	0.051
α Leo	87901	46095.5–58941.5	15	1.341±0.010	1.180±0.022	0.851±0.012	-0.161	-0.329
56 UMa	98839	41824.4–41828.3	2	4.997±0.018	5.970±0.033	6.746±0.014	0.972	0.776
γ Crt	99211	41824.4–41828.3	2	3.980±0.038	4.190±0.038	4.197±0.042	0.210	0.007
HD 100972	100972	41824.4–41828.4	2	6.842±0.002	6.838±0.015	6.843±0.002	-0.004	0.004
ζ Crt	102070	41824.4–41828.3	2	4.659±0.018	5.625±0.004	6.311±0.030	0.967	0.685
γ UMa	103287	43143.6–43143.6	1	2.452±0.000	2.465±0.000	2.475±0.000	0.013	0.010

Table C.4: continued

Star name	HD or BD number	JDmin - JDmax -2400000	No. of obs.	<i>V</i> (mag.)	<i>B</i> (mag.)	<i>U</i> (mag.)	<i>B</i> - <i>V</i> (mag.)	<i>U</i> - <i>B</i> (mag.)
HR 4561	103498	55357.4–55364.4	8	7.031±0.009	7.053±0.010	7.062±0.009	0.021	0.009
HR 4572	103799	55357.4–55364.4	6	6.613±0.009	7.096±0.011	7.082±0.011	0.483	-0.014
HD 103984	103984	55357.4–55364.4	6	6.931±0.009	7.334±0.008	7.319±0.009	0.403	-0.015
δ UMa	166205	46969.4–47006.3	6	3.312±0.006	3.388±0.013	3.445±0.017	0.076	0.057
η Vir	107259	41691.6–41696.6	4	3.861±0.019	3.867±0.027	3.910±0.040	0.006	0.043
6 Dra	109551	51376.4–51379.4	5	4.945±0.010	6.278±0.008	7.488±0.014	1.333	1.209
χ Vir	110014	41691.6–41696.6	4	4.607±0.024	5.794±0.023	7.166±0.042	1.188	1.371
β Com	114710	42646.3–42654.3	4	4.261±0.022	4.843±0.033	4.899±0.024	0.582	0.056
η UMa	120315	46969.4–47006.3	9	1.856±0.010	1.668±0.008	0.995±0.013	-0.189	-0.672
86 UMa	121409	41828.4–59025.4	18	5.740±0.009	5.701±0.012	5.629±0.011	-0.039	-0.072
ε Boo	129989	52494.4–52494.4	1	2.362±0.000	3.333±0.000	4.064±0.000	0.971	0.731
χ Boo	135502	52412.4–52500.4	12	5.294±0.007	5.347±0.007	5.418±0.006	0.053	0.071
γ CrB	140436	52412.4–52500.4	12	3.826±0.006	3.827±0.007	3.807±0.005	0.001	-0.020
θ Lib	142198	41824.4–58946.6	12	4.165±0.011	5.180±0.013	5.978±0.019	1.014	0.799
ν Sco AB	145502	41824.4–42929.4	7	3.998±0.008	4.047±0.009	3.389±0.012	0.049	-0.658
ψ Oph	147700	42241.4–42244.4	2	4.439±0.016	5.450±0.001	6.283±0.008	1.010	0.834
59 Her	154029	52068.3–55120.3	9	5.278±0.010	5.298±0.007	5.342±0.016	0.020	0.044
α Oph	159561	46969.4–47006.4	11	2.079±0.008	2.227±0.017	2.349±0.017	0.149	0.122
γ Dra	164058	46969.4–47061.3	22	2.227±0.008	3.762±0.010	5.620±0.016	1.535	1.858
HR 6757	165462	43712.4–43722.4	8	6.394±0.012	7.435±0.018	8.255±0.017	1.042	0.819
HD 166101	166101	57652.3–57652.4	4	8.793±0.027	9.574±0.016	9.798±0.042	0.780	0.224
δ UMi	166205	56858.5–56858.5	3	4.363±0.004	4.377±0.003	4.417±0.004	0.014	0.039
HD 166361	166361	57652.3–57652.4	3	7.454±0.018	9.292±0.015	11.089±0.153	1.839	1.796
HD 168443	168443	57652.3–57652.4	4	6.893±0.005	7.634±0.010	7.924±0.016	0.741	0.289
HR 6943	170650	55121.2–55121.3	13	5.877±0.009	5.788±0.015	5.270±0.016	-0.089	-0.518
HR 6966	171245	55121.2–55121.2	2	5.884±0.004	7.365±0.011	9.118±0.022	1.481	1.753
BD+24 3545	174369	55124.3–55124.3	2	6.750±0.014	6.833±0.001	6.898±0.005	0.083	0.066
ξ2 Sgr	175775	42241.4–53937.5	7	3.537±0.017	4.698±0.024	5.819±0.018	1.162	1.121
λ Lyr	176679	56491.4–56639.2	2	4.961±0.001	6.414±0.018	8.082±0.012	1.454	1.668
ζ Aql	177724	46969.4–47061.3	18	2.990±0.009	2.996±0.011	3.002±0.014	0.006	0.006
β1 Cyg	183912	46689.3–46689.4	2	3.067±0.003	4.189±0.001	4.864±0.007	1.123	0.674
κ Aql	184915	42647.3–42654.4	3	4.938±0.017	4.925±0.015	4.069±0.016	-0.013	-0.855
HD 187411	187411	57615.4–59082.4	13	8.105±0.009	8.471±0.010	8.601±0.013	0.366	0.130
23 Vul	192806	43027.4–50341.5	13	4.511±0.009	5.780±0.007	6.920±0.015	1.268	1.140
39 Cyg	194317	46688.4–46695.4	4	4.431±0.024	5.781±0.017	7.297±0.019	1.351	1.516
13 Cap	196348	43712.4–43722.5	2	6.791±0.011	8.017±0.008	9.292±0.012	1.227	1.274
71 Aql	196574	41528.4–59179.3	13	4.337±0.009	5.270±0.008	5.954±0.012	0.933	0.684
HR 7922	197226	47017.4–47022.4	7	6.521±0.006	6.396±0.008	5.907±0.017	-0.125	-0.489
ε Aqr	198001	41528.4–41528.4	2	3.775±0.022	3.779±0.011	3.790±0.037	0.003	0.012
HD 198424	198424	47017.4–47022.4	12	7.510±0.008	7.410±0.012	6.980±0.020	-0.100	-0.431
56 Cyg	198639	51715.4–51715.4	3	5.068±0.005	5.266±0.010	5.370±0.012	0.198	0.104
HD 198793	198793	53686.2–53686.2	3	7.141±0.003	7.058±0.005	6.592±0.007	-0.082	-0.466
HR 8029	199661	53686.2–53686.2	3	6.237±0.004	6.075±0.006	5.350±0.003	-0.162	-0.725
HD 199781	199781	51376.3–51380.5	5	8.335±0.026	8.789±0.041	8.778±0.075	0.453	-0.010
HD 199890	199890	51715.4–51715.4	3	7.518±0.001	7.422±0.007	7.044±0.012	-0.097	-0.378
HD 199986	199986	51377.4–58351.5	8	7.052±0.038	7.488±0.410	7.755±0.721	0.436	0.267
HR 8049	200205	46691.4–46691.4	2	5.537±0.004	6.964±0.004	8.562±0.007	1.427	1.599
θ Cap	200761	42607.5–43722.5	2	4.062±0.005	4.057±0.010	4.058±0.016	-0.005	0.001
HR 8107	201836	43027.4–43027.4	6	6.452±0.007	6.445±0.014	6.064±0.015	-0.007	-0.381
HR 8136	202654	43027.4–43027.4	5	6.445±0.014	6.308±0.009	5.626±0.011	-0.137	-0.682
1 Peg	203504	42237.4–42237.4	1	4.104±0.000	5.195±0.000	6.250±0.000	1.091	1.055
HR 8185	203644	51371.4–51371.5	4	5.688±0.005	6.787±0.015	7.825±0.019	1.099	1.038
κ Cap	206453	42607.6–43713.6	3	4.716±0.024	5.581±0.022	6.113±0.021	0.864	0.532
HD 209932	209932	55452.3–55460.5	52	6.522±0.012	6.490±0.015	6.350±0.016	-0.032	-0.140
BD+48 3613	210119	52940.2–52940.4	14	8.328±0.009	8.426±0.009	8.505±0.016	0.098	0.078
HD 210387	210387	55452.3–55460.5	33	6.799±0.013	6.761±0.014	6.486±0.016	-0.038	-0.275
35 Peg	212943	42266.4–42278.4	3	4.765±0.010	5.811±0.022	6.682±0.023	1.046	0.871
HR 8606	214240	43143.2–43326.6	7	6.276±0.016	6.227±0.012	5.664±0.010	-0.049	-0.563
11 Lac	214868	42607.6–42609.6	2	4.492±0.006	5.828±0.001	7.287±0.003	1.335	1.459
HR 8654	215359	58700.6–58700.6	3	5.921±0.008	7.442±0.004	9.139±0.015	1.521	1.698

Table C.4: continued

Star name	HD or BD number	JDmin - JDmax -2400000	No. of obs.	<i>V</i> (mag.)	<i>B</i> (mag.)	<i>U</i> (mag.)	<i>B</i> - <i>V</i> (mag.)	<i>U</i> - <i>B</i> (mag.)
α Peg	218045	46988.4–47061.3	23	2.482±0.009	2.441±0.011	2.389±0.014	-0.041	-0.052
HD 219430	219430	42278.5–42278.5	1	4.165±0.000	5.262±0.000	6.287±0.000	1.097	1.025
ψ 1 Aqr	219449	42237.6–42237.6	1	4.268±0.000	5.403±0.000	6.415±0.000	1.135	1.012
HR 8857	219668	43712.5–43722.5	5	6.505±0.006	7.547±0.016	8.539±0.014	1.042	0.991
72 Peg	221673	42237.6–42237.6	1	5.010±0.000	6.390±0.000	8.007±0.000	1.380	1.617
ω 2 Aqr	222661	42607.6–43713.6	3	4.454±0.022	4.385±0.024	4.248±0.032	-0.069	-0.137
BD+37 3873	228897	55121.3–55124.4	13	8.923±0.008	9.060±0.009	8.590±0.013	0.137	-0.470
HD 277197	277197	55851.5–55858.7	11	9.490±0.013	9.557±0.015	9.018±0.027	0.067	-0.539
HD 339764	339764	55454.4–55454.4	1	9.599±0.000	9.688±0.000	9.779±0.000	0.089	0.091
ADS 10347B	–	54275.4–54294.4	15	9.630±0.062	10.267±0.097	10.407±0.113	0.637	0.140
ADS 10347AB	–	54281.5–57948.4	15	6.334±0.033	6.581±0.068	6.702±0.131	0.247	0.121
BD+43 1166C	–	55596.4–56002.3	5	10.720±0.338	11.402±0.423	11.712±0.393	0.682	0.310
BD+67 248	–	55851.4–55858.6	11	9.024±0.012	9.752±0.013	10.463±0.012	0.728	0.711
BD+68 220	–	55858.6–55858.6	2	9.146±0.000	9.752±0.010	9.802±0.002	0.606	0.050
BD+43 1168	–	56002.3–56002.3	3	9.390±0.011	10.311±0.011	10.579±0.014	0.920	0.269

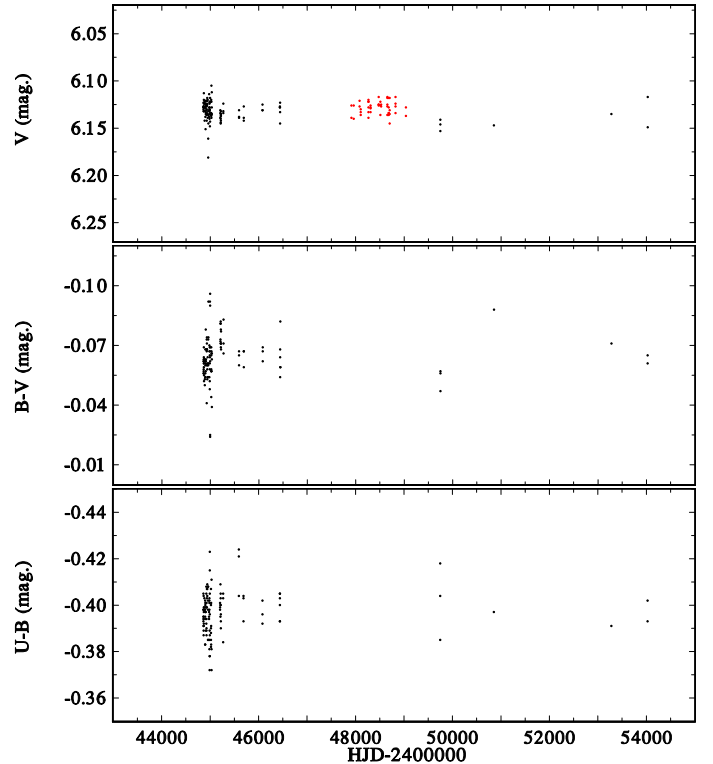

Fig. D.1: The *UBV* time variations of γ Cas.

Fig. D.2: The *UBV* time variations of V554 Per.

Appendix D: Brief discussion on the remaining more frequently observed hot emission-line stars

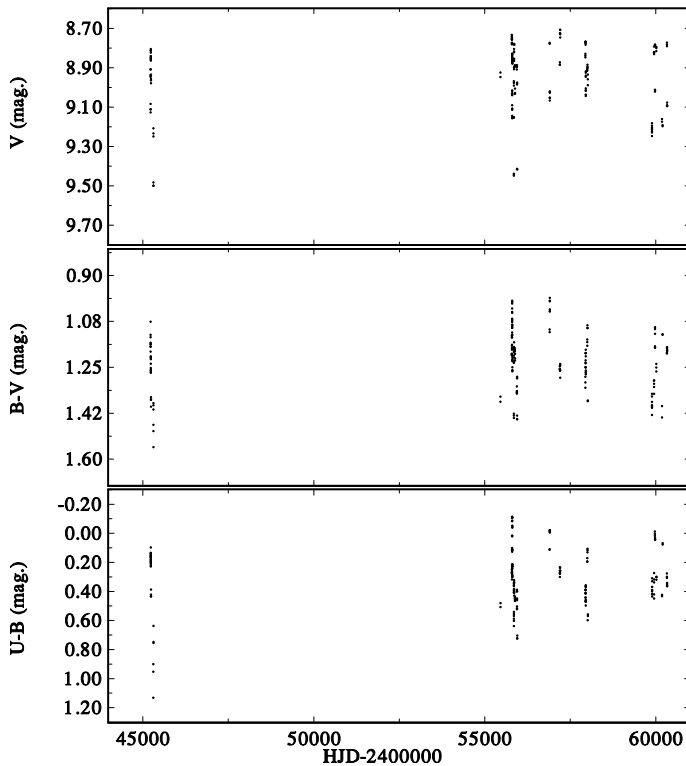
γ Cas = 27 Cas = HD 5394 This one of the brightest Be stars in the sky has been subject of more than 1100 studies. It is now known to be a spectroscopic binary with a 203^d52 orbital period (Harmanec et al. 2000; Nemravová et al. 2012; Borre et al. 2020, and references therein), with a low-mass companion, probably a white dwarf (Gies et al. 2023). Its light variations are characterised by long-term changes with positive correlation and rapid changes with periods 1^d216, and 0^d4033 (Harmanec 2002; Borre et al. 2020; Smith & Henry 2021, and references therein). Observations of this star at Hvar are not very numerous, mainly because of the fact that it was necessary to use a lower high voltage due to its brightness to avoid saturation. They are shown in Fig. D.1 and only complement the secular brightness changes documented in Harmanec (2002) and Smith & Henry (2021).

V554 Per = 10 Per = HD 14818 This object is classified as B2Ia but Weißmayer et al. (2022) observed its H α emission, reminiscent of a P Cyg profile. Its light variability was reported by Alvarez & Schuster (1981) and Pavlovski et al. (1997) but the variable-star name V554 Per was assigned to it only on the basis of Hipparcos photometry by Kazarovets et al. (1999). Hvar and Hipparcos photometry is shown in Fig. D.2. The brightness and colour variations are characterized by cyclic changes, with no obvious secular trend. A formal period analysis of combined Hvar and Hipparcos *V* photometry suggests a possible period of 237^d082, but with a large scatter around the mean phase curve.

HR 894 = HD 18552 Polidan (1976) tentatively suggested that this object is a B8V+gG9 binary, based on the calcium triplet emission in the infrared spectra. However, the presence


Fig. D.3: The *UBV* time variations of HR 894.

of a cool giant companion has never been confirmed. The object exhibits only mild variations of the H α emission over a long interval of spectral observations and Hvar photometry shows no significant light or colour changes (see Fig. D.3). We therefore did not continue to observe it.

Fig. D.4: The *UBV* time variations of RX Cas.

RX Cas = BD+67 244 This object is an interacting Be+G3III binary with a 32^d.3 period secularly increasing in time and with a cyclic brightness variation at light maxima on a scale of about 500 days (Struve 1944; Gaposchkin 1944; Kříž et al. 1980; Andersen et al. 1989). Mennickent et al. (2022) analysed more than a century of photometric observations, derived an improved quadratic ephemeris, and studied the long cycle of brightness variations at maximum light. To the best of our knowledge, there is no reliable RV curve of the Be primary hidden in the dense shell. The first part of Hvar photometry has already been used in Kříž et al. (1980) study. The complete set of Hvar observations is shown in Fig. D.4. In this case, we have not included Hipparcos photometry since the *B*–*V* index of the binary varies significantly with the binary orbital phase and with the long cycle and the transformation to Johnson *V* would deserve a more sophisticated treatment. Our new detailed study of the binary is under consideration and here we only show the phase coverage based on the complete set of Hvar data in Fig. D.5. The phase coverage is seen to be quite good. We note that the secondary minimum is absent in the *U* magnitude. However, a mild light decrease near orbital phase 0.8 is observed in all three passbands.

13 Tau = HD 23016 is a Be star that is only projected in the sky to the Pleiades cluster but is not its member. Barnsley & Steele (2013) provide some evidence of a mild change in the *H*α emission strength (equivalent range from 4.0 to 5.7 Å) over the time interval from JD 2451029 to 2455524. Hvar photometry shown in Fig. D.6 provides little evidence for a significant light variability over a time interval of nearly 10000 days.

V971 Tau = 23 Tau = HD 23480 For this bright Be star from the Pleiades cluster, also known as Merope, (McNamara

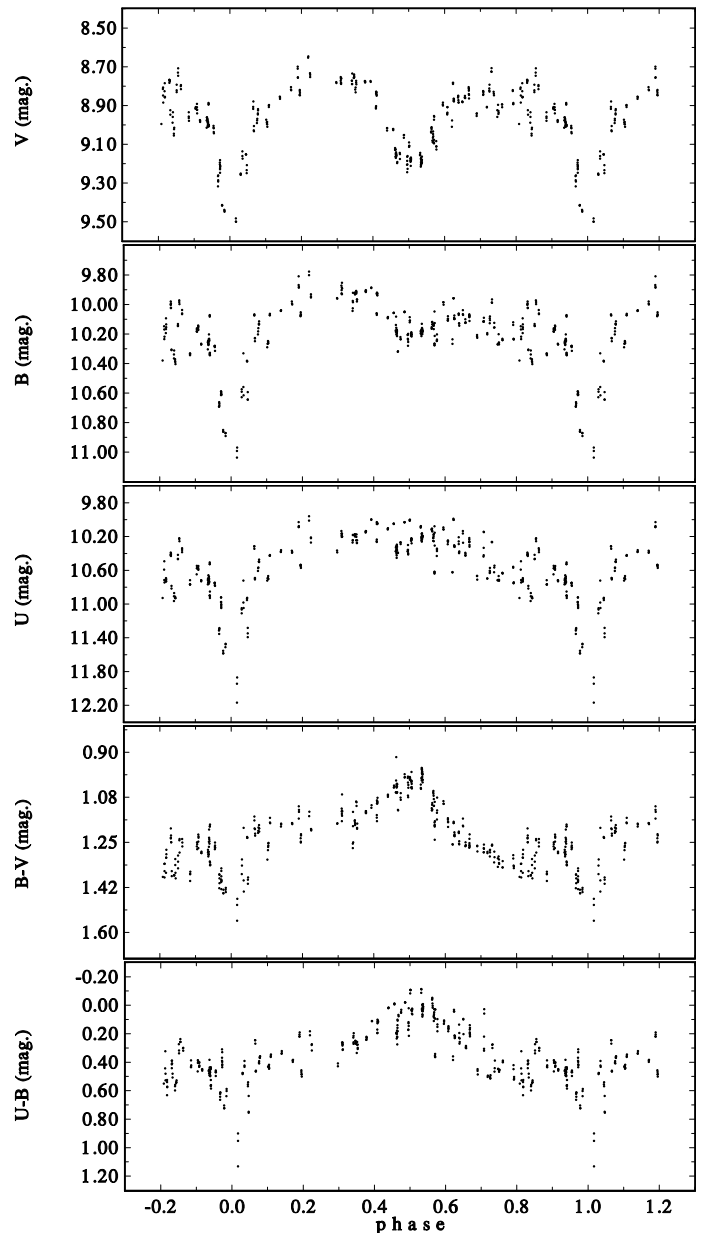
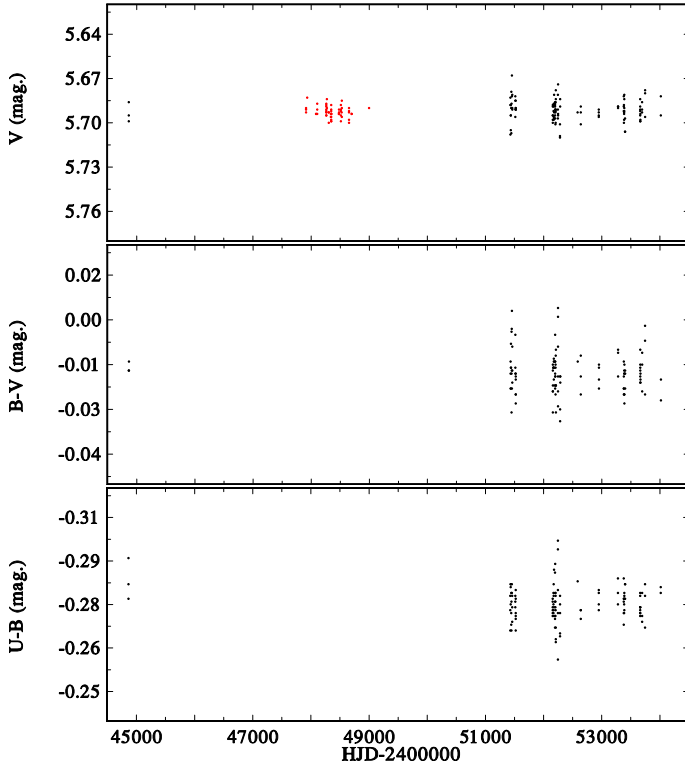
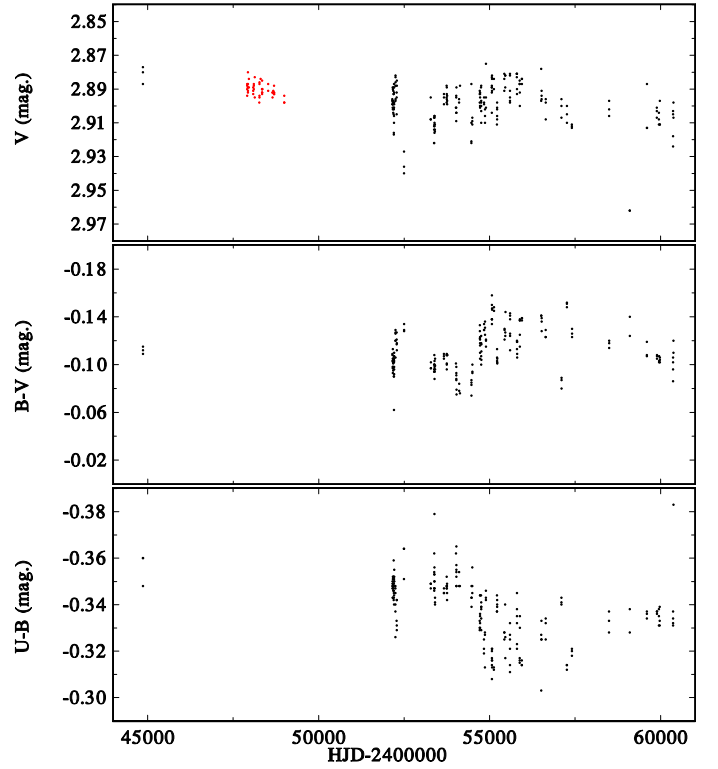
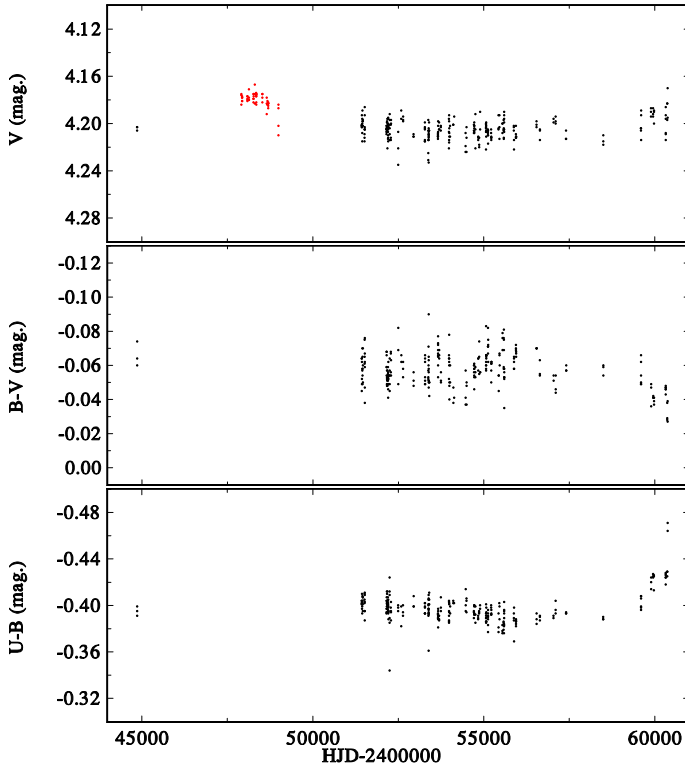


Fig. D.5: The magnitude and colour phase diagrams for RX Cas based on the quadratic ephemeris of Mennickent et al. (2022).

1985, 1987) found rapid variation with the 0^d.490 period and an amplitude of several thousands of magnitude. White et al. (2017) using data from the Kepler mission confirmed this periodicity and suggested the existence of several closely spaced periods. Despite a very small amplitude of rapid changes, the Hvar photometry is able to resolve periodic variations with the 0^d.490 period. The Hvar photometry presented in Fig. D.7 indicates that the small light variability is dominated by these rapid changes but also reveals mild long-term variations, best seen in the *U*–*B* index.

η Tau = 25 Tau = HD 23630 This brightest Be member of the Pleiades cluster, also known as Alcyone, is a visual multiple system WDS 03475+2406. Figure D.8 shows that mild brightness and colour variations on various time scales are probably present. A cyclic secular variation can best be seen in the *U*–*B* index. It is worth mentioning that Krelowski et al. (2019)

1570


Fig. D.6: The *UBV* time variations of 13 Tau.

Fig. D.8: The *UBV* time variations of η Tau.

Fig. D.7: The *UBV* time variations of V971 Tau.

studied the distances to the brightest stars in the Pleiades derived both from Gaia DR2 release and from interstellar Ca II lines and concluded that these stars do not form a compact cluster but are localized in front of the main Pleiades cluster at a distance close to what was derived from Hipparcos. They argued that the ob-

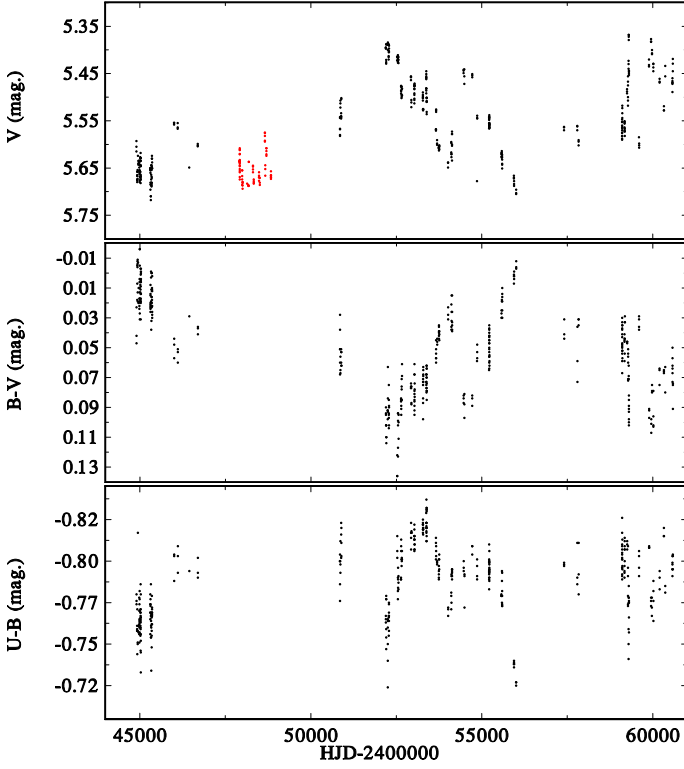
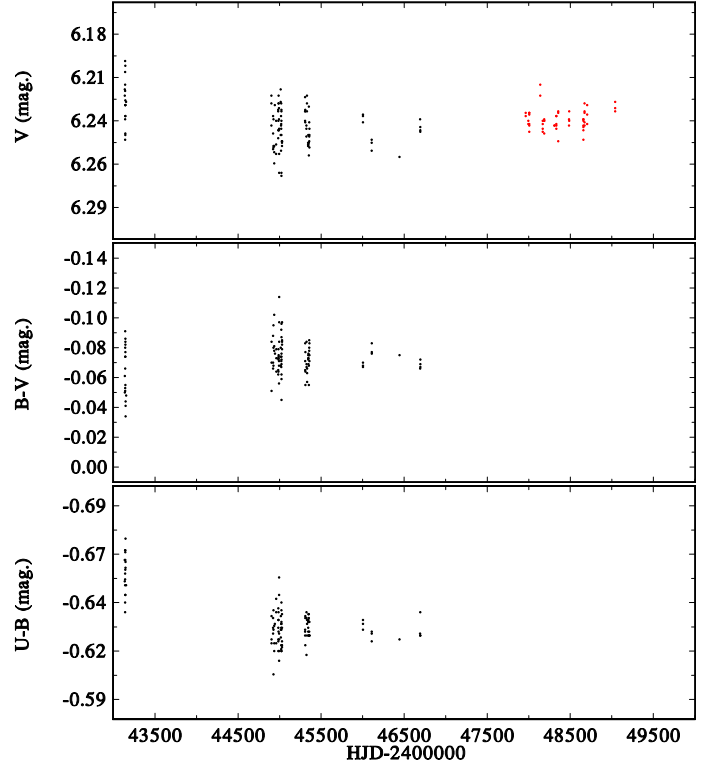
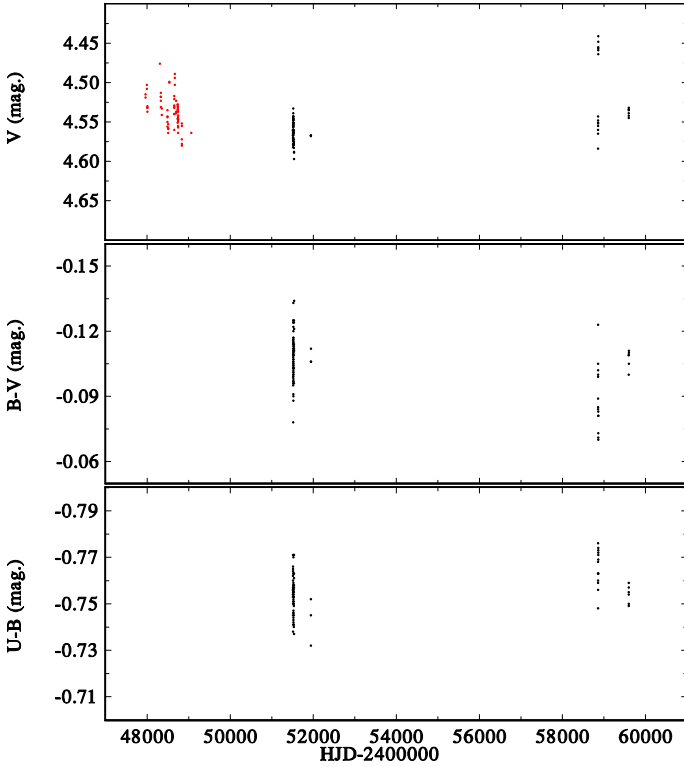
served spread in the individual distances of the stars in the core of the cluster could be explained by additional grey interstellar extinction due to the presence of larger dust grains in the cluster core.

V960 Tau = 120 Tau = HD 36576 The light variability of this star was discovered at Hvar and was first reported by Pavlovski & Božić (1982). As Fig. D.9 shows, the star was monitored quite systematically at Hvar and has complicated and seemingly irregular variations with a large range of 0^m.3 in *V*. Its detailed study, which will also include spectroscopic changes, is in preparation.

ω Ori = 47 Ori = HD 37490 Hvar photometry was obtained mainly as a part of a multisite campaign on the rapid line-profile and light variability, which resulted in the finding that both, line-profile and light changes are governed by a single 0^d.97 period (Balona et al. 2001). Several episodes of a rapid light increase have been reported (e.g. Guinan & Hayes 1984; Bergin et al. 1989) accompanied also by an increase of polarization so it is probable that this star has a positive correlation between the brightness and H α emission strength and might be similar to V442 And. Not very rich Hvar photometry can be seen in Fig. D.10. It seems that the variations of this star are dominated by rapid changes; no secular changes are seen.

V731 Tau = HD 37967 A limited set of Hvar observations seems to show only small and probably rapid changes - see Fig. D.11. Sigut & Ghafourian (2023) estimated the disk inclination of about 55° for this B4 star.

OT Gem = HD 58050 Hvar observations were already reported by Božić et al. (1982) who were unable to confirm earlier reports of rapid periodic changes, and by Božić et al. (1999)

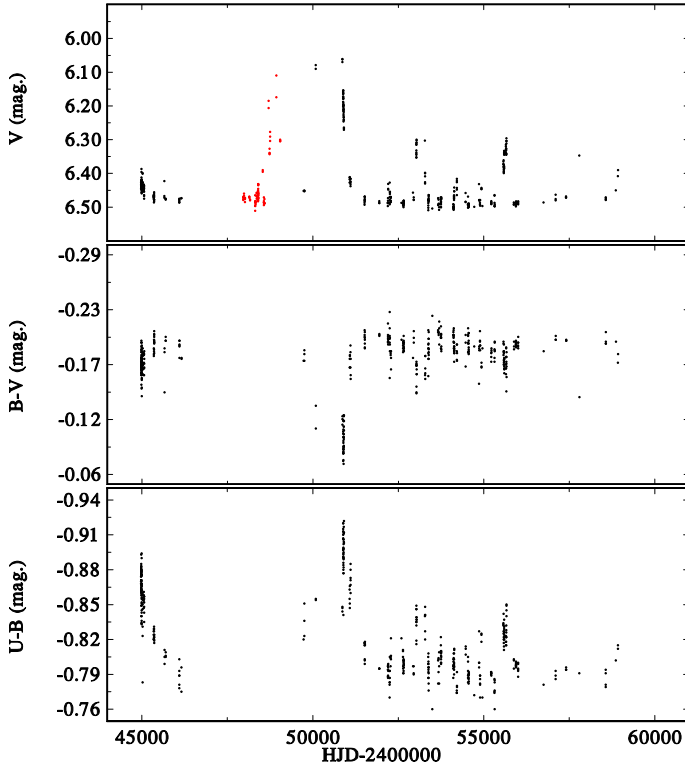
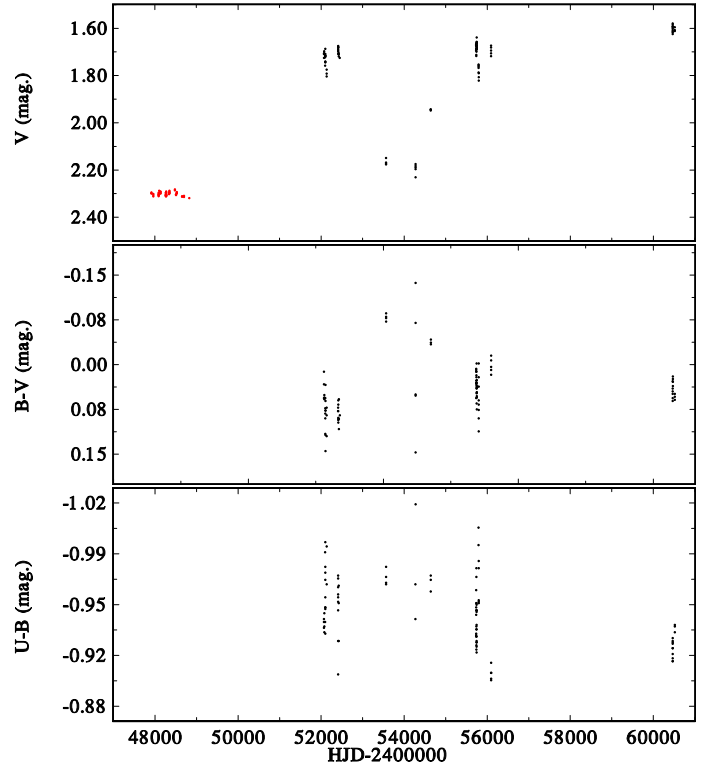
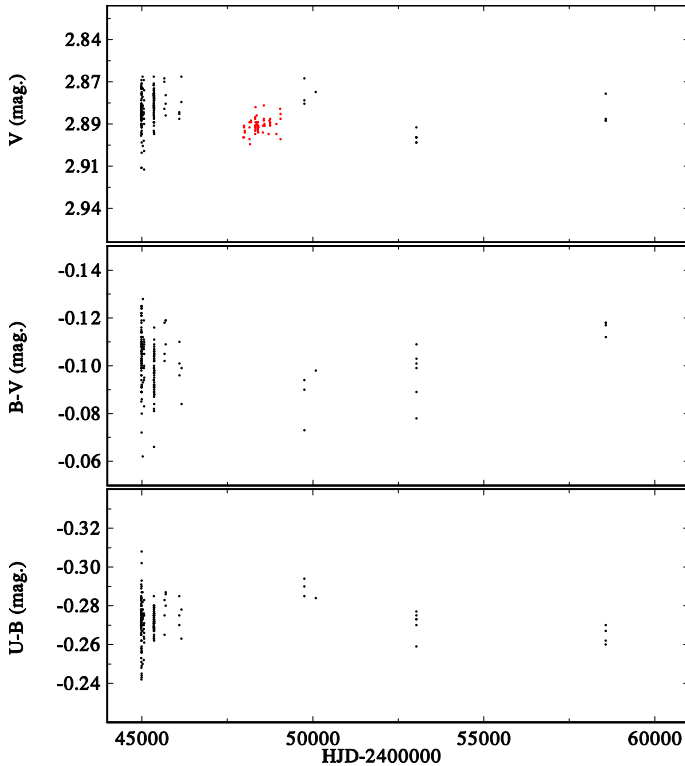

Fig. D.9: The *UB* time variations of V960 Tau.

Fig. D.11: The *UB* time variations of V731 Tau.

Fig. D.10: The *UB* time variations of ω Ori.

who found two episodes of light brightening and identified OT Gem as the object with a positive correlation. This agrees with the estimate of the inclination of about 20° to 30° by Sigut & Ghafourian (2023). Balona & Ozuyar (2021) analysed small-amplitude rapid light changes for a number of Be stars

using TESS observations. For OT Gem they found a period of 0^d4606 with a non-sinusoidal light curve. Labadie-Bartz et al. (2022) – investigating two sectors of TESS photometry – noted the light brightenings and changes on longer time scales but reported also two groups of short periodic changes near 0^d249 and 0^d472 . The complete Hvar photometry is shown in Fig. D.12 and shows frequent episodes of light brightenings, similar to V442 And.

β CMi = 58715 Dulaney et al. (2017) announced that the object is a single-line spectroscopic binary with a 170^d4 period and a semiamplitude of RV curve of 2.25 km s^{-1} . However, Harmanec et al. (2019) – measuring RVs in many high-dispersion spectra – were unable to confirm their result and also Klement et al. (2024) did not detect any secondary in their interferometry. Božić et al. (1982) were unable to find evidence of any rapid light variations, but Saio et al. (2007) detected very low light variations in the MOST satellite photometry, which they interpreted as g-mode non-radial pulsations. Using wavelet analysis, Harmanec et al. (2019) re-analysed the MOST photometry and found only one stable period of 0^d6169 , which they tentatively identified with the star rotational period. Balona & Ozuyar (2021) found a period of 0^d6207 with a non-sinusoidal light curve from TESS photometry. A rather limited set of Hvar photometry is shown in Fig. D.13. There is little evidence of any changes on longer time scales.

BR CMi = HD 61273 A detailed spectroscopic and photometric study, based largely on Hvar photometry, has been published by Harmanec et al. (2015). BR CMi was found to be a B9.5e + G8III semidetached binary in the late phase of mass transfer, having ellipsoidal light variations and a slowly increasing orbital period of 12^d919 . No secular or cyclic light changes were found.

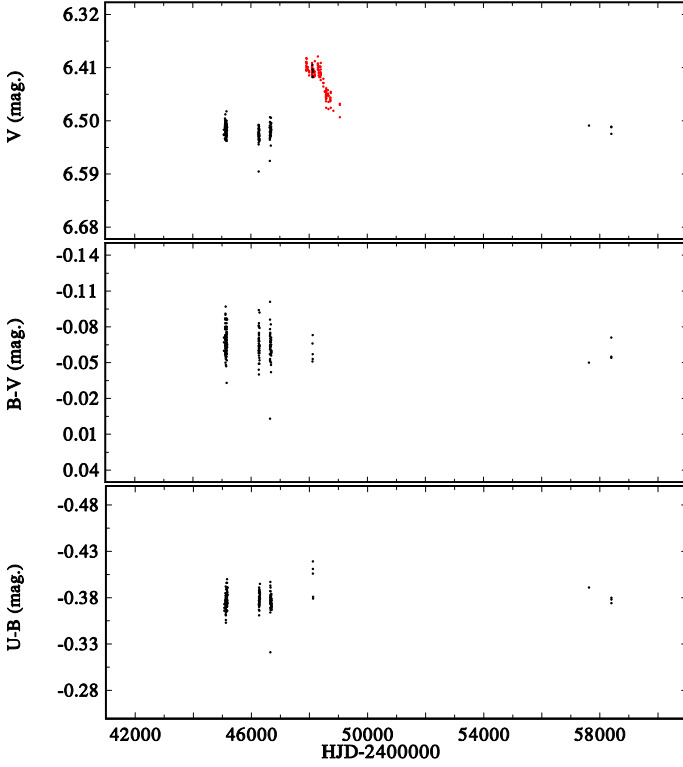
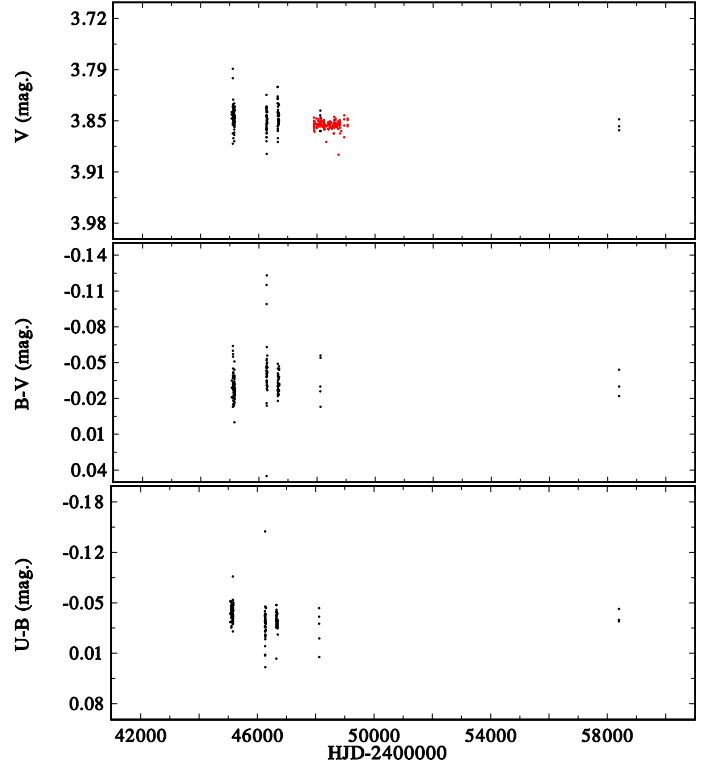

Fig. D.12: The *UBV* time variations of OT Gem.

Fig. D.14: The *UBV* time variations of δ Sco.

Fig. D.13: The *UBV* time variations of β CMi.

to slowly decrease over time at a rate of 0.26 s per year. In their discussion of W Ser class of binaries and double periodic variables, [Mennickent et al. \(2016\)](#) claimed that the period of UX Mon is constant.

HD 81357 = MWC 859 This object was found to be a semidetached binary in the late stage of mass exchange and an ellipsoidal variable. Its detailed study was published by [Koubský et al. \(2019\)](#) and profits from Hvar photometry. Neither secular nor cyclic light changes were found.

δ Sco = 7 Sco = HD 143275 This early B star was for a long time considered a non-variable object and was even recommended as a *uvby* β standard star. Carefully analysing previous records and using the MAPPIT optical interferometer, [Bedding \(1993\)](#) discovered that the object is a spectroscopic binary with a highly eccentric orbit and a 10.5 yr orbital period and estimated that the secondary is for $1^m5\pm0^m3$ fainter than the primary. This was then confirmed by several other studies. [Tycner et al. \(2011\)](#) published the revised orbit with a period of 10.817 yr, eccentricity of 0.9380, and orbital inclination of 32.9° . [Cote & van Kerkwijk \(1993\)](#) discovered the presence of $H\alpha$ emission, and since then the object has become a topic of many detailed studies. Large brightness and colour variations were observed, but no clear proof was found that the occurrence of $H\alpha$ emission was related to the periastron passages. In fact, a strong $H\alpha$ emission persisted for a long time. The evolution of the disk during three passages in the periastron was discussed by [Rast et al. \(2024\)](#), who also show the light and colour curve. It is rather surprising that all attempts to find the spectral lines of the secondary failed. Hvar observations are presented in Fig. D.14 and complement existing observations from other stations, for instance the *B*–*V* photometry by [Jones et al. \(2013\)](#). Note that the object was inevitably observed at large air masses from Hvar.

UX Mon = HD 65607 This binary was the subject of a very detailed spectroscopic and photometric study, based also on Hvar photometry ([Sudar et al. 2011](#)). It was found to be a rare binary system observed in the early stage of mass exchange, before the mass ratio reversal. Its 5^d9044 orbital period was found

Fig. D.15: The *UBV* time variations of V974 Her.Fig. D.16: The *UBV* time variations of *o* Her.

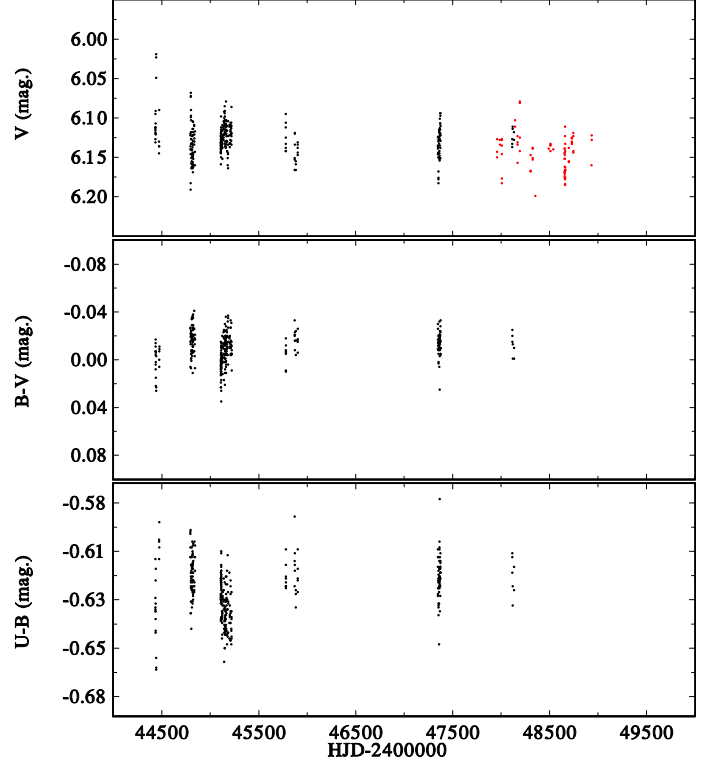
ζ Oph = 13 Oph = HD 149757 This star was used to be a photometric standard star in the past. However, several $H\alpha$ emission episodes were recorded in its spectra (see Ebbets 1981, and references therein). This very rapid rotator is also the first Be star for which rapid line profile variations were discovered by Walker et al. (1979). Harmanec (1989) and Harmanec (1999) interpreted the line-profile and small light changes as evidence of corotating structures revolving with a period of 0^d64 but many investigators understand these changes as evidence of non-radial pulsations. This was also the conclusion of a study based on MOST satellite photometry (Walker et al. 2005). Hvar photometry shows only small changes and no secular variations, but we warn that the star was always inevitably observed at large air masses at Hvar.

V974 Her = HD 164447 This is a relatively little studied B8e star. Hipparcos H_p photometry (Perryman & ESA 1997) shows a slow decrease in brightness over the whole interval of observations. Amateur spectra available in the BeSS database (Neiner et al. 2011),⁵ show that the star lost its Balmer emission in 2020. Hvar photometry shown in Fig. D.15 indicates a brightening characteristic for a positive correlation, which is rather rare for late type B stars.

o Her = HD 166014 This B9.5e star was proposed by Perry et al. (1987) as a bright *uvbyH β* photometric standard. All the $H\alpha$ spectra in the BeSS database (Neiner et al. 2011), covering the time interval from 2011 to 2024, show weak double $H\alpha$ emission not reaching the continuum level. A limited set of Hvar photometry shown in Fig. D.16 is indicative of small rapid changes and no secular variations.

NW Ser = HD 168797 The Hvar photometry of this B2e star was analysed together with photometry secured by

⁵ <http://basebe.obspm.fr/basebe/>

Fig. D.17: The *UBV* time variations of NW Ser.

John R. Percy in Toronto to document its rapid and possibly periodic light changes on time scales from 0^d4 to 5^d5 days (Percy et al. 1999). No more recent Hvar observations were secured since the publication of that study. Fig. D.17 shows the time plot of all available Hvar and transformed H_p observations.

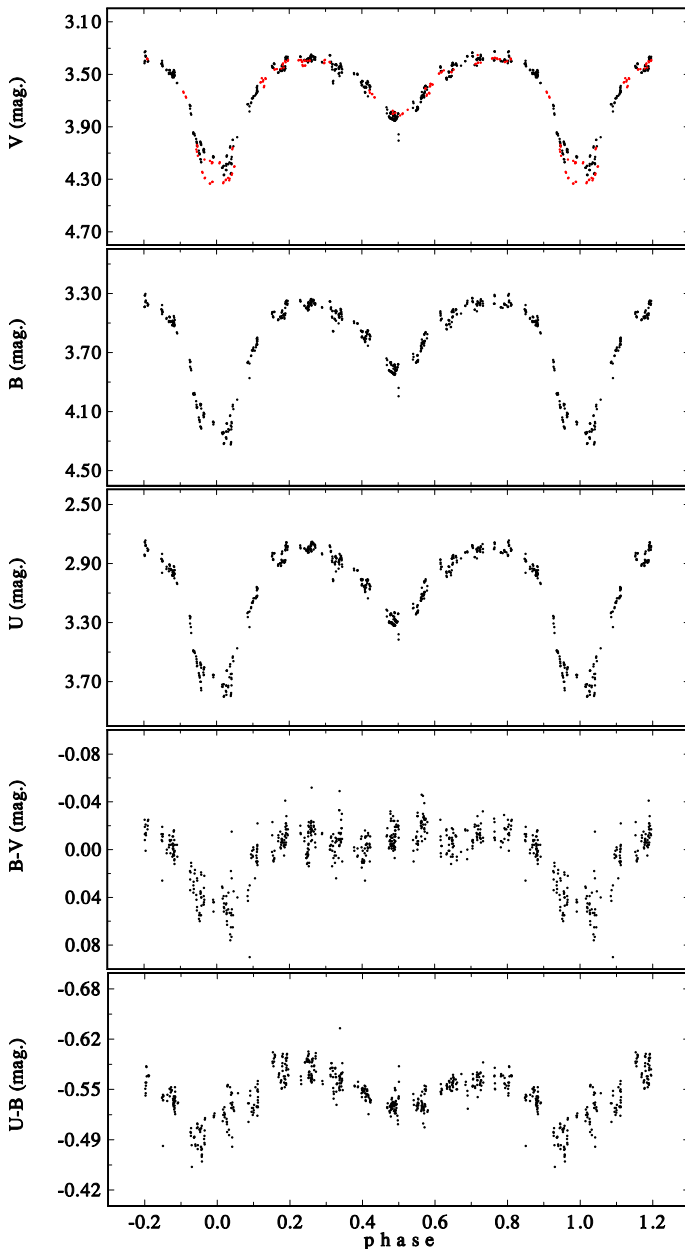


Fig. D.18: The orbital light curve of β Lyr.

β Lyr = 10 Lyr = HD 174638 This is one of two first discovered Be stars and a famous 12^d93 eclipsing and strongly interacting binary with a complicated structure of circumstellar matter comprising from a disk, scattering halo and bipolar jets and with a rapidly increasing orbital period (19 s per year). The history of its investigation was summarised by Harmanec (2002). Hvar observations (shown in a phase plot Fig. D.18) have been secured in support of several large studies, which also provide summaries of more recent studies: Harmanec et al. (1996); Ak et al. (2007); Mourard et al. (2018); Brož et al. (2021). For a long time known cycle-to-cycle variations inside the binary eclipses are seen there. There is, however, no secular trend in either the brightness in *V* passband or in the colour indices.

V1507 Cyg = HD 187399 This object was known to have H α emission since 1921 and was found to be a peculiar binary with an eccentric orbit and a 27^d97 orbital period (Merrill 1949). Hutchings & Redman (1973) interpreted the object as a binary

in the phase before the onset of a large scale mass exchange and also discussed a very peculiar orbital light curve, which was later published in detail by Hill et al. (1976). The peculiar shape of the light curve was confirmed by our Hvar observations (Pavlovski et al. 1979). Hutchings & Redman (1973) interpreted the light-curve minima as evidence of shallow eclipses. Davidge (2023) published a very detailed study of the binary and also summarized all other published studies. Measuring weak emission wings of the Si II 6347 and 6371 Å lines, similarly as several investigators did for β Lyr, he obtained a RV curve of the secondary and estimated the component masses. He argued that the brighter primary, whose spectrum is closely reminiscent of the spectra of bright supergiants such as β Ori, is now the less massive star of the system, which lost its mass toward the secondary during the earlier rapid phase of the mass transfer. He correctly pointed out that the orbital period of 27^d9705 (Hutchings & Redman 1973) has remained constant within the limits of the accuracy of its determination since the study Merrill (1949), implying that the system must now be in the stage of terminal, slow mass transfer. He also speculated about the possibility that the unusually eccentric ($e=0.388$) orbit could be the consequence of perturbation by a third star in the system or fly-by. Koenigsberger & Estrella-Trujillo (2024) investigated the role of the tidal share energy dissipation for stars undergoing light brightenings during periastron passage and modelled such a effect. The orbital light curve for the combined Hvar and Hipparcos H_p observations transformed to Johnson *V* is shown in Fig. D.19. No secular light changes were found.

20 Vul = HD 192044 This is a little studied B8 star. Copeland & Heard (1963) reported broad nebulous H I and He I lines and double H β and H γ emission lines with variable intensity and *V/R* changes for their photographic spectra from the years 1938 to 1961 but no details were given. We are not aware of any systematic study devoted to this object. The available Hvar photometry is shown in Fig. D.20.

QR Vul = HR 192685 This object is the brighter component of a visual binary ADS 13589, the component B located only 0^h7 from it and being for 2^m7 fainter. **Its photometric variability was discovered at Hvar and it was then identified as a Be star** (see Pavlovski et al. 1983, and references therein). Balona & Ozuyar (2021) analysed the TESS observations and suggested that the light variations can be phased with a 0^d7918 period with a non-sinusoidal shape, which they identified with the period of rotation. The limited Hvar photometry shown in Fig. D.21 is indicative of rapid changes and occasional light brightenings.

P Cyg = 34 Cyg = HD 93237

The brightness variations of this famous luminous blue variable have been monitored for 5 years with the BRITE satellites, and the results are presented by Elliott et al. (2022). These authors were unable to find any consistent periodicities and concluded that the variations are stochastic in nature. Our limited Hvar observations are shown in Fig. D.22. The first part of them had already been reported, along with data from other stations, by Percy et al. (1988), who were unable to find any strict periodicity. The Hvar data can complement the existing observations. We note that the variations in the *U*–*B* index are larger than those in *B*–*V*.

25 Vul = HD 193911 Balona & Ozuyar (2021) concluded from the TESS photometry that the small light changes

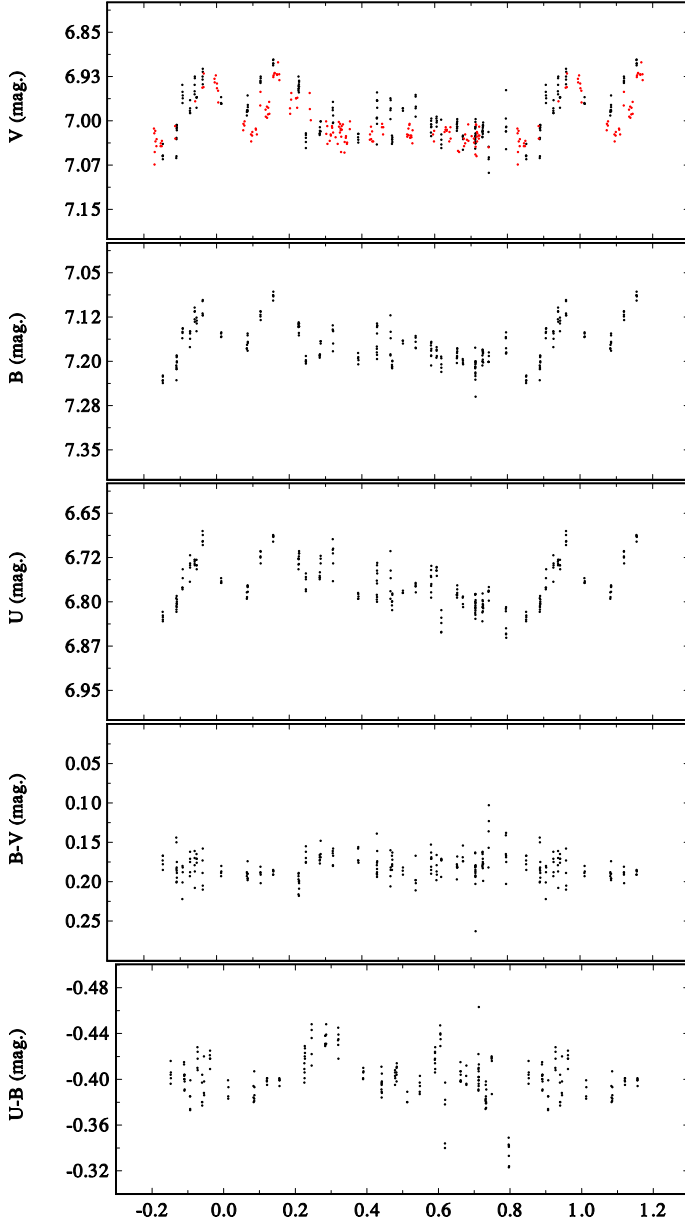


Fig. D.19: The 27^d9705 orbital light curve of V1507 Cyg based on Hvar (black) and transformed Hipparcos H_p (red) observations.

can be reconciled with a 1^d890 period with a non-sinusoidal light curve. They identified it with the star rotational period. Limited Hvar photometry shown in Fig. D.23 is indicative of small-amplitude rapid changes, with possibly some secular evolution in the $U-B$ index.

V2119 Cyg = HD 194335 Klement et al. (2024) obtained an interferometric circular orbit with a period of 63^d1475 and summarised the previous studies of this Be binary with a hot compact companion. Unfortunately, no optical RV curve is available. Hvar photometry is shown in Fig. D.24. A plot of combined Hvar V magnitude and the transformed H_p magnitude versus the orbital phase does not show a convincing light curve.

V1661 Cyg = 55 Cyg = HD 198478 This star is classified as a B3-4Ia supergiant. It was a subject of almost 500 studies, so we only refer the readers to the paper of Kraus et al.

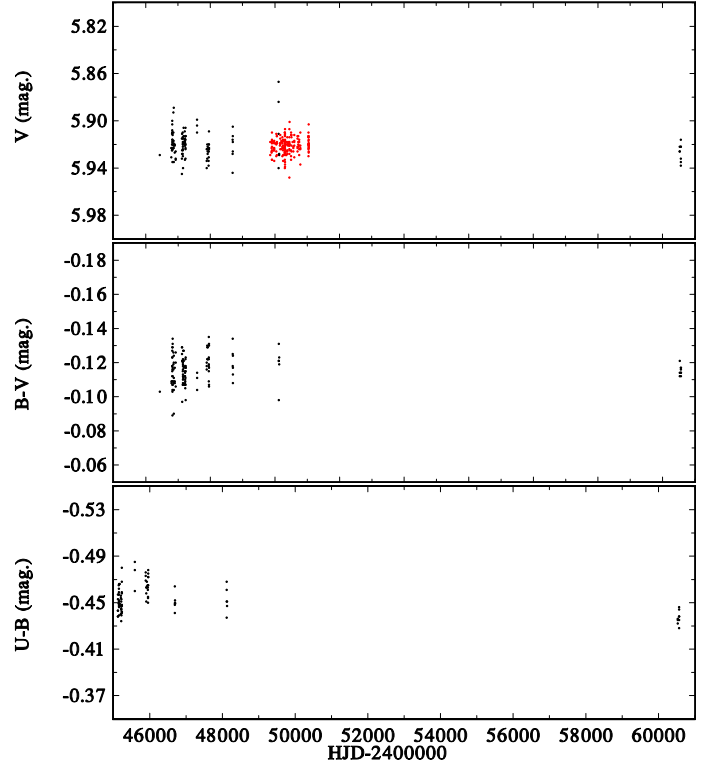


Fig. D.20: The UBV time variations of 20 Vul.

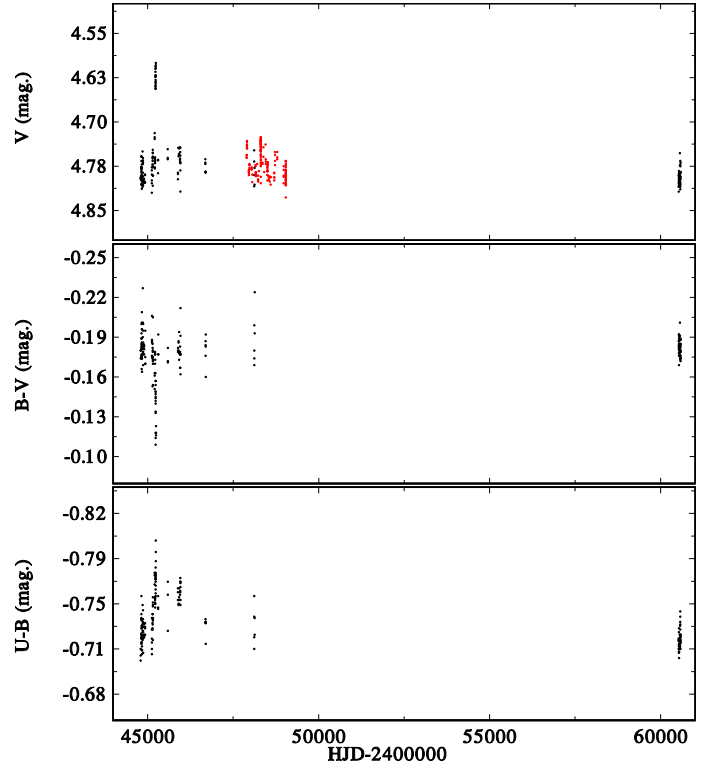
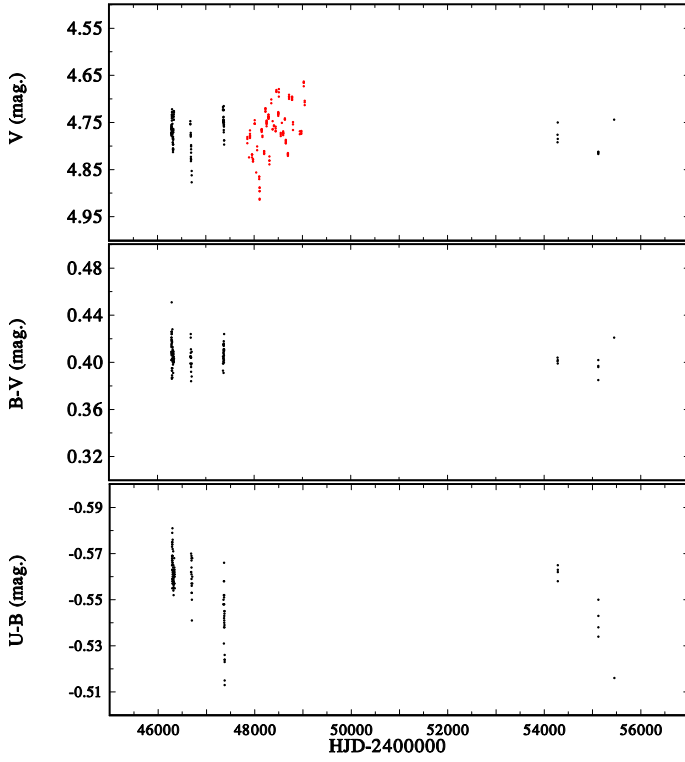
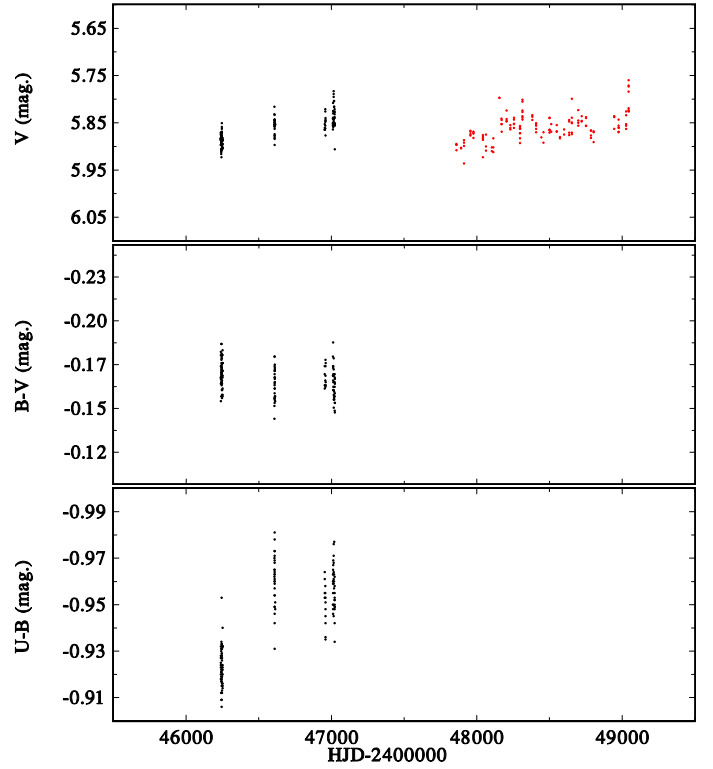
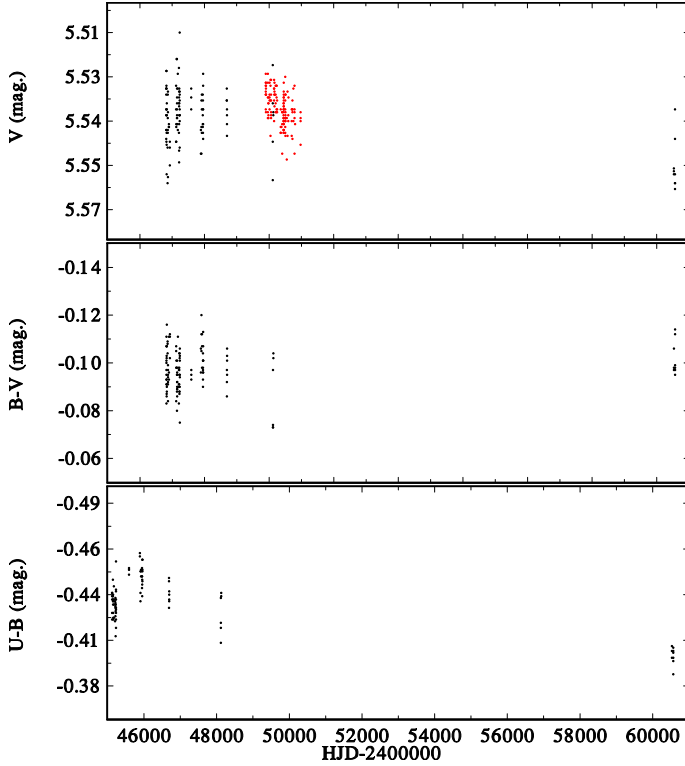
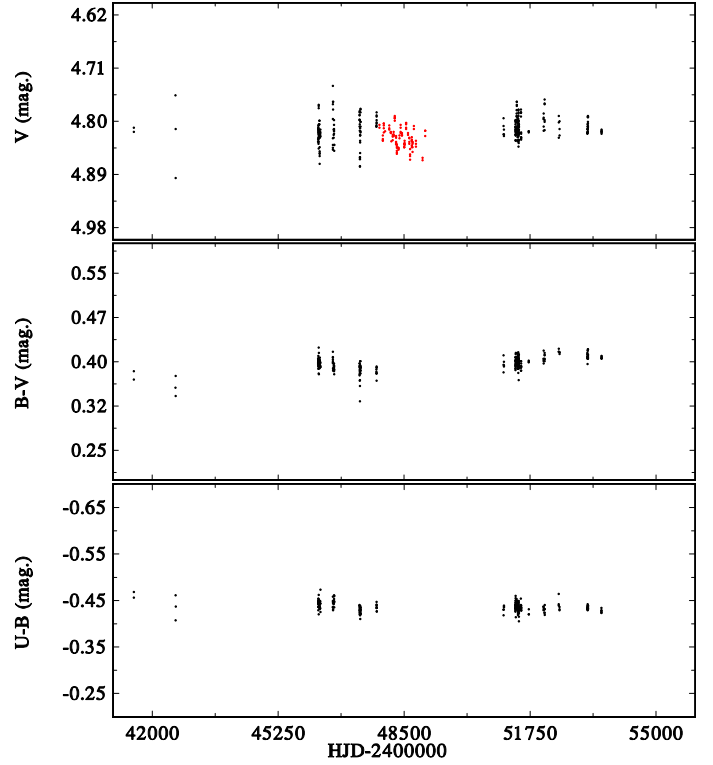


Fig. D.21: The UBV time variations of QR Vul.

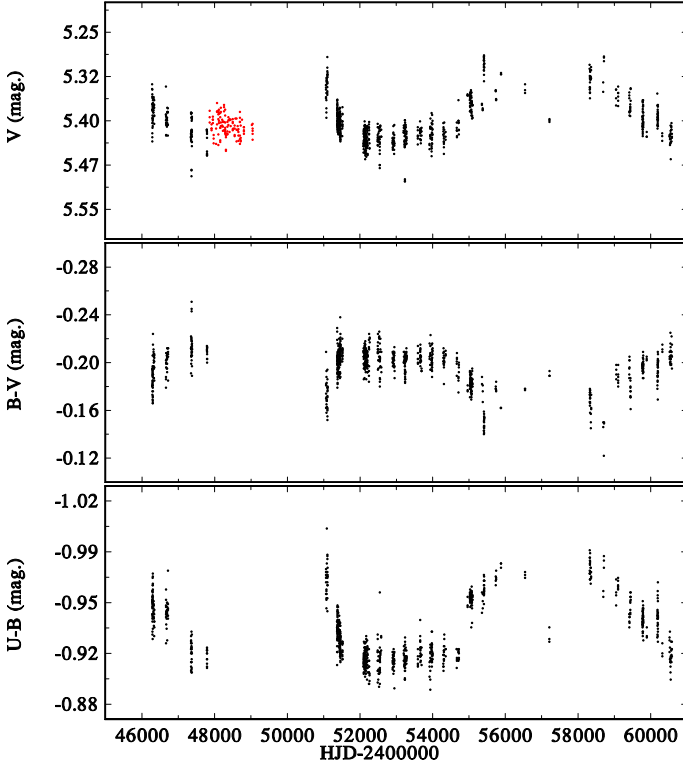
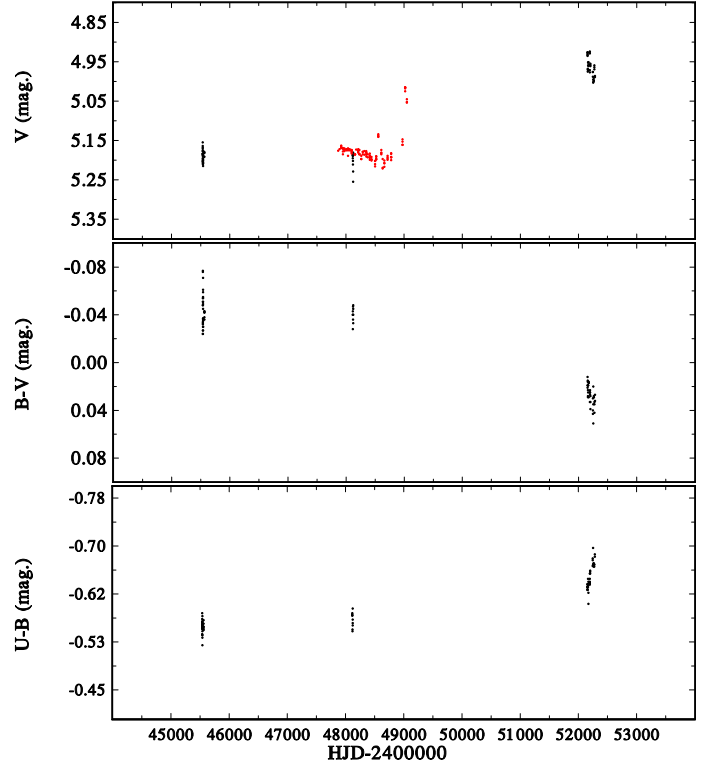
(2015), where the studies of spectral and photometric variability of V1661 Cyg are summarised. These authors tried to study an interplay between the mass loss and pulsations and decomposed the observed variations in several observables into a number of periods ranging from 2.7 hours to 22^d5. Our limited set of Hvar


Fig. D.22: The *UBV* time variations of P Cyg.

Fig. D.24: The *UBV* time variations of V2119 Cyg.

Fig. D.23: The *UBV* time variations of 25 Vul.

Fig. D.25: The *UBV* time variations of V1661 Cyg.

observations is shown in Fig. D.25. It shows some variability in *V* and *B−V* colour but, notably, no variability in the *U−B* index.

V1931 Cyg = 60 Cyg = HD 200310 This object is the brighter component of a visual binary WDS J21012+4609. Koubský et al. (2000) discovered that the object is also a spec-

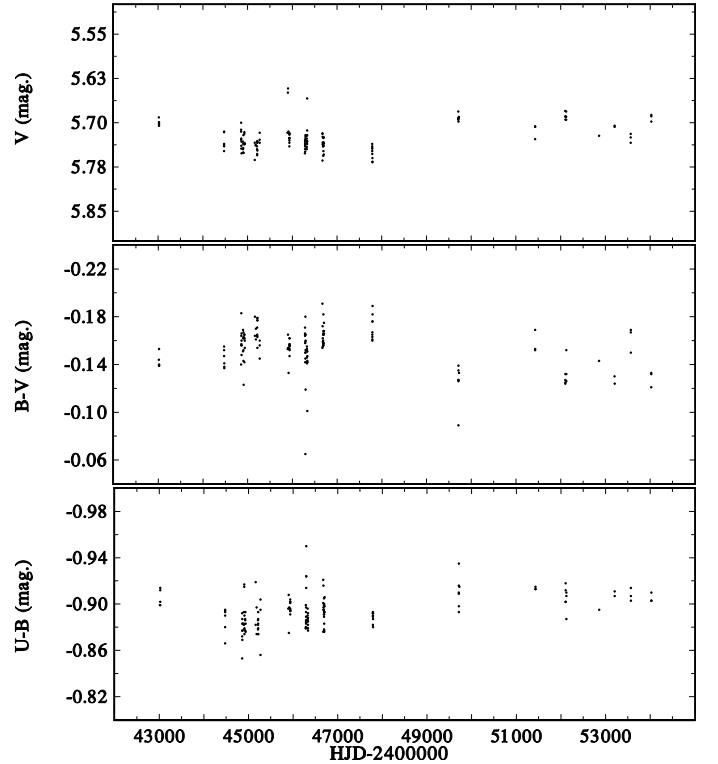
troscopic binary with a 146^d6 period and analysing photometry including Hvar observations, they reported large cyclic changes and several possible rapid periods near 1 d. For comparison, Balona & Ozuyar (2021) reported a rotational period of 0^d6109 with a double-wave light curve from TESS photometry. The bi-


Fig. D.26: The UB time variations of V1931 Cyg.

Fig. D.27: The UB time variations of V382 Cep.

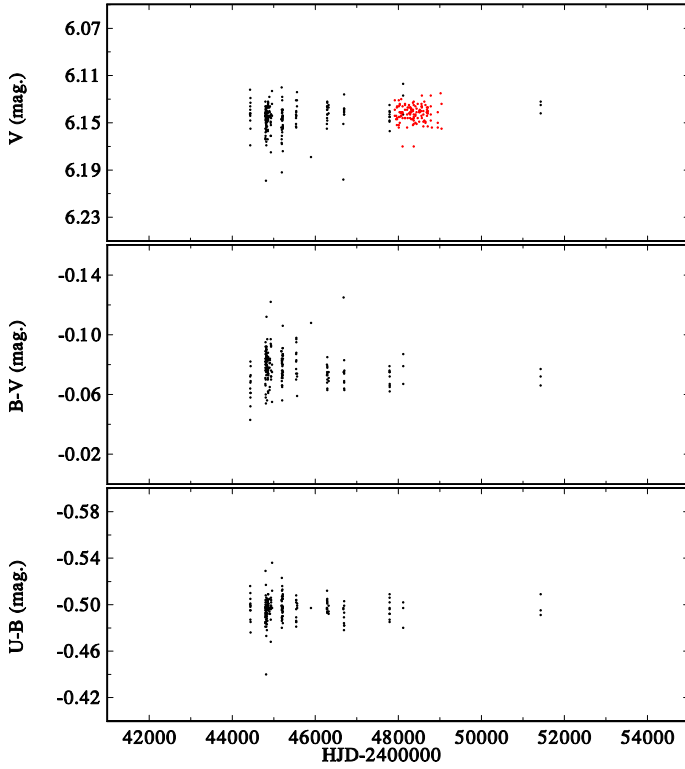
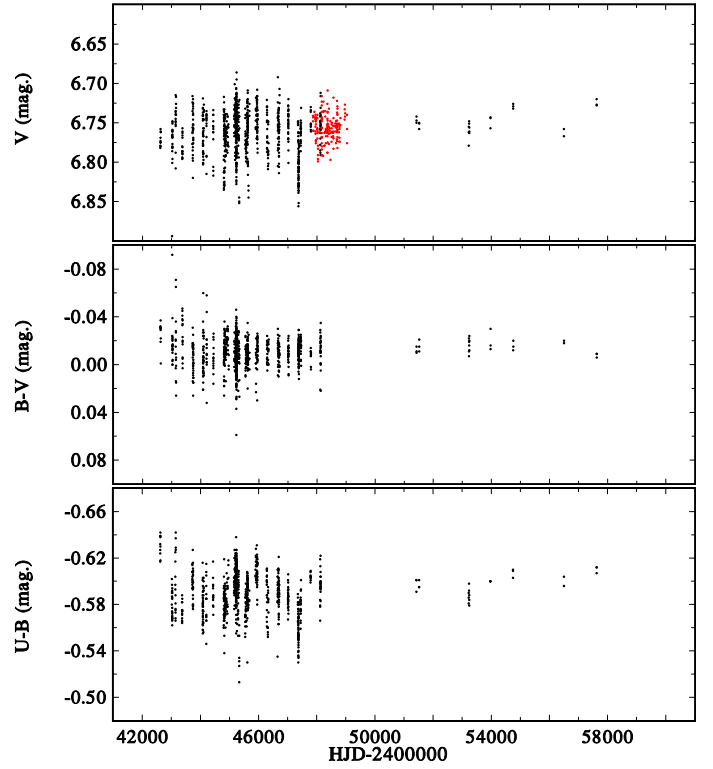
nary was resolved interferometrically and the combined spectroscopic and astrometric solution gave an improved period of $147^{\text{d}}617$, an eccentric orbit with $e = 0.20$, and the orbital inclination of $84.^{\circ}6$ (Klement et al. 2024). Hvar photometry plotted in Fig. D.26 shows the pronounced cyclic light and colour changes on a time scale of years. Surprisingly, it shows a clear positive correlation in the $U-B$ vs. $B-V$ diagram. Is the circumstellar disk tilted with respect to the binary orbit?

V382 Cep = 6 Cep = HD 203467 Krajčeva & Koubský (1983) analyzed two sets of RVs from photographic spectra and suggested that the object could be a close spectroscopic binary with periods of either $2^{\text{d}}4389$ or $0^{\text{d}}7085$. Balona & Ozuyar (2021) found a photometric period of $1^{\text{d}}658$, which they identified with the star rotational period. Limited Hvar observations are shown in Fig. D.27. They show some secular changes but little can be said about their character.

8 Lac A = HD 214168 = HIP 111546 8 Lac is a multiple system WDS J22359+3938 composed of components Aa, Ab, B, C, D, E, F, G, H, I, and J. Component B is also an early B star with $V = 6^{\text{m}}48$ according to a few Hvar observations, in agreement with the HD catalog. We note that the SIMBAD bibliography gives incorrectly $V = 5^{\text{m}}67$ for 8 Lac B. Regrettably, there are no Hipparcos H_p observations with error flags 0 or 1 in the Hipparcos catalogue for either 8 Lac A or 8 Lac B. Balona & Ozuyar (2021) classify the star as β Cep and rotational variable from TESS photometry and give a rotation period of $0^{\text{d}}4277$. Klement et al. (2024) were unable to resolve the binary in a consistent way from their interferometric observations. Hvar photometry is shown in Fig. D.28. It indicates mild rapid and secular cyclic changes but little can be concluded about their character.


Fig. D.28: The UB time variations of 8 Lac A.

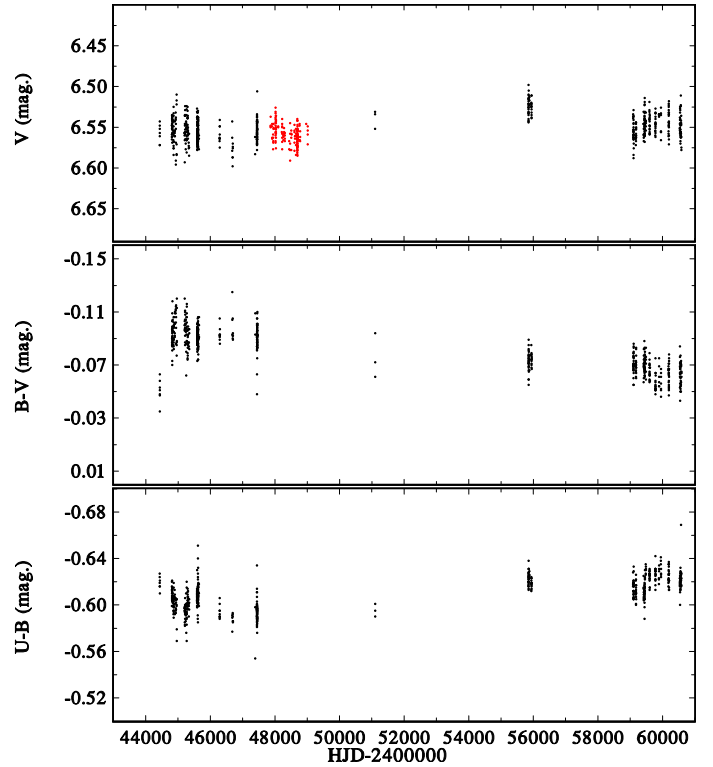
HR 8682 = HD 216057 This B8 star has no variable-star name and the BeSS spectra since 2001 to 2024 show no or only marginal $H\alpha$ emission (Neiner et al. 2011). A limited set of Hvar photometry is in Fig. D.29. No clear evidence of variability was found.


Fig. D.29: The *UBV* time variations of HR 8682.

Fig. D.30: The *UBV* time variations of KY And.

V360 Lac = HD 216200 This object was found to be a semi-detached Be+F binary with a critically rotating secondary and an orbital period of $10^d.085$ (Hill et al. 1997; Linnell et al. 2006). There are also mild cyclic brightness and colour changes but no slow changes on the LTCV time scale. Since no new Hvar photometry was obtained since the publication of Linnell et al. (2006), we refer readers to the two cited papers, where also other studies of this object are summarised.

KY And = HD 218674 Analysing Sept.1982 Hvar photometry, Pavlovski & Ružić (1988) found a dominant period of $0^d.751$ in their data. Stagg et al. (1988) published the results of an international observing spectral and photometric campaign on five Be stars including KY And. Hvar photometry represented a significant contribution. While rapid light variations were undoubtedly found for KY And, determination of a consistent period or a combination of several periods was not convincing. The most promising period of $0^d.753$ was detectable only in a part of the data. Complete Hvar photometry is in Fig. D.30. It is obvious that the rapid changes dominate, no secular trends are seen.

LQ And = HD 224559 This is one of the first Be stars for which the presence of small-amplitude periodic light variations was found (Percy 1983). A very detailed period analysis of numerous photometric observations, including numerous observations from Hvar by Harmanec et al. (1991) led to the conclusion that that light variations follow a $0^d.61904$ period with a double-wave light curve, which was tentatively identified with the star rotation period. Matthews et al. (1991) analyzed a series of electronic spectra and reported that the object could be a single-line spectroscopic binary with a $7^d.413$ orbital period. The RV residuals from the orbital solution as well as line intensities and equivalent widths were found to vary with the photometric $0^d.61904$ period. It is necessary to add that the binary


Fig. D.31: The *UBV* time variations of LQ And.

period was not confirmed in any of the follow-up studies. The unpublished $H\alpha$ spectra and spectra from the BeSS database indicate that during the past 20 years the star had a strong emission reaching up to 4 times the continuum level. Hvar photometry is shown in Fig. D.31.